UNIVERSITY OF CALIFORNIA, SAN DIEGO

Human Cytomegalovirus Subverts and Utilizes Components of the Ubiquitin-Proteasome System in Facilitating a Productive Infection

A Dissertation submitted in partial satisfaction of the requirements for the degree

Doctor of Philosophy

in

Molecular Pathology

by

Karen Tran

Committee in Charge:

Professor Deborah H. Spector, Chair
Professor Michael David
Professor Dan Donoghue
Professor Steve Dowdy
Professor John Guatelli
Professor David Rose

2009

The dissertation of Karen Tran is approved, and it is acceptable in quality and form for publication on microfilm:

_____

_____

_____

_____

_____

_____

Chair

University of California, San Diego

2009

DEDICATION

To my family: Mom, Dad, & Bai Kiet.

For all of your love and support.

TABLE OF CONTENTS

LIST OF FIGURES

ACKNOWLEDGEMENTS

The text of Chapter 2 is a reprint of the material as it appears in *Journal of Virology*, 82(1): 529–537, 2008. Tran, K., J.A. Mahr, J. Choi, J.G. Teodoro, M.R. Green, and D.H. Spector. Accumulation of substrates of the anaphase-promoting complex (APC) during human cytomegalovirus infection is associated with the phosphorylation of Cdh1 and dissociation and relocalization of APC subunits. The dissertation author was the primary investigator and author of this paper.

The text of Chapter 4, in part, is a reprint of the material as it was submitted to *Journal of Virology*. Tran, K., J.A. Mahr, and D.H. Spector. Proteasome subunits relocalized during human cytomegalovirus infection and proteasome activity is necessary for efficient viral gene transcription and DNA replication. The dissertation author was the primary investigator and author of this paper.

VITA

1998–2001	Undergraduate Research Assistant, Institute of Behavioral Genetics
2001–2002	Intern, Ribozymes Pharmaceuticals, Inc.
2002	Bachelor of Arts, University of Colorado, Boulder
2002–2003	Research Assistant, National Jewish Research and Medical Center
2003-2009	Graduate Student Research Assistant, University of California, San Diego
2009	Doctor of Philosophy, University of California, San Diego

PUBLICATIONS

Tran, K., J. A. Mahr, and D. H. Spector. Proteasome subunits relocalize during human cytomegalovirus infection and proteasome activity is necessary for efficient viral gene transcription and DNA replication (Submitted: J Virol. Oct 2009).

Kapasi A.J., C. L. Clark, K. Tran, and D. H. Spector. 2009. Recruitment of cdk9 to the Immediate-Early Viral Transcriptosomes during Human Cytomegalovirus Infection Requires Efficient Binding to Cyclin T1, a Threshold Level of IE2 86, and Active Transcription. J Virol 83:5904-5917.

Tran, K., J. A. Mahr, J. Choi, J. Teodoro, M. Green, and D. H. Spector. 2008. Accumultion of substrates of the anaphase-promoting complex (APC) during human cytomegalovirus infection is associated with the phosphorylation of Cdh1 and the dissociation and relocalization of APC Subunits. J Virol 82:5904-5917.

Regan, E., J. Flannelly, R. Bowler, K. Tran, M. Nicks, B.D. Carbone, D. Glueck, H. Heijnen, R. Mason, and J. Crapo. 2005. Extracellular superoxide dismutase and oxidant damage in osteoarthritis. Arthritis Rheum 52:33479-3491.

Bowler, R. P., M. Nicks, K. Tran, G. Tanner, L.-Y. Chang, S. K. Young, and G. S. Worthen. 2004. Extracellular superoxide dismutase attenuates lipopolysaccharide-induced neutrophilic inflammation. Am J Respir Cell Mol Biol 31:432–439.

Bowler, R. P., M. C. Ellison, B. Duda, K. Tran, M. Nicks, C. Cool, K. Greene, and J.D. Crapo. 2004. Lung inflammation with direct injection of agarose: a technique for simultaneous molecular and morphometric measurements. Exp Lung Res 30:673–686.

FIELD OF STUDY

Major Field: Molecular Pathology
Studies in Molecular Virology
Professor Deborah H. Spector

ABSTRACT OF THE DISSERTATION

Human Cytomegalovirus Subverts and Utilizes Components of the Ubiquitin-Proteasome System in Facilitating a Productive Infection

by

Karen Tran

Doctor of Philosophy in Molecular Pathology

University of California, San Diego, 2009

Professor Deborah H. Spector, Chair

This dissertation further explores some of the many facets by which human cytomegalovirus (HCMV) subverts and utilizes components of the ubiquitin-proteasome system in facilitating a productive infection. HCMV infection causes severe cell cycle

deregulation and arrest, mediated in part by the deactivation of the anaphase-promoting complex (APC), one of the main E3 ubiquitin ligases involved in cell cycle regulation. By characterizing the effects on the APC subunits and its co-activator Cdh1 during the infection, I have further delineated the mechanism(s) by which APC^{Cdh1} is disabled during the infection. Cdh1 becomes abnormally phosphorylated early in the infection in a Cdk-independent manner, which may inhibit its ability to bind and activate the APC. UL97 is identified as the viral protein kinase involved in mediating Cdh1 phosphorylation. Analysis of the APC core subunits reveals that the complex dissociates during the infection with the TPR subunits relocalizing to the cytoplasm while APC1 remains nuclear, which is caused by the proteasome-mediated degradation of APC5 and APC4. Studies utilizing a UL97-deletion virus indicate that Cdh1 phosphorylation and APC dissociation occur independently despite similar kinetics. The possible redundancy of these mechanisms underlies the importance of deactivating the APC during the infection. The targeting of an intermediate component in the ubiquitin-proteasome pathway is necessary as inhibition of the proteasome is also found to be detrimental to viral replication. Proteasome inhibition assays show that proteasome activity is required at all stages of the infection. Moreover, proteasome activity increases as the infection progresses, and proteasome subunits relocalize in and around viral replication centers. Characterization of the peri-replication center region shows it to be proteolytically and transcriptionally active. Taken together, these results suggest that proteasomes (or specific subunits) may play a direct role in facilitating viral DNA replication and transcription.

CHAPTER 1

INTRODUCTION

HUMAN CYTOMEGALOVIRUS

Human cytomegalovirus (HCMV) is a β-herpesvirus endemic within the human population, affecting 50–90% of the general adult population worldwide, that establishes a lifelong latent infection. While the virus usually remains asymptomatic following primary infection or reactivation in a healthy host with a functional immune system, it is an opportunistic pathogen that can cause serious disease in immunocompromised individuals or those lacking a mature immune system (for review, see (13, 110). HCMV is the leading infectious cause of birth defects, with 30–50% transmission to the fetus if the primary infection of the mother occurs during pregnancy. About 10–15% of the babies will develop birth defects, including hearing and vision loss and mental retardation, and in some infants may result in death. HCMV also continues to be a significant pathogen in adults given the rise in AIDS and organ transplantation, with complications including retinitis, encephalitis, pneumonia, graft rejection, and death. Chronic infection with the virus has also been associated with atherosclerosis, rheumatologic disorders, and vascular disease. Current drug treatments have produced a significant clinical improvement, but have a low

potency and dose-limiting toxicities. Moreover, there is a developing resistance to the drugs (for review, see (76). Thus, HCMV remains an important pathogen of study; understanding the molecular basis of infection will help identify new potential therapeutic targets as well as the clinical manifestations of the infection.

ß-herpesviruses are species-specific, have a relatively long replication cycle, and are among the largest of the herpesvirus subfamilies. HCMV can infect a broad range of cell types, including epithelial, endothelial, fibroblasts, and smooth muscle cells. HCMV is a double-stranded DNA virus with a 260 Kbp linear genome, encoding over 230 ORFs (103). The genome of the virion is housed in an icosahedral protein capsid that is surrounded by a proteinaceous tegument layer and enclosed by a phospholipid envelope. Viral encoded glycoproteins on the envelope mediate viral entry through membrane fusion, which releases the capsids and tegument into the cell. The tegument contains a large mixture of both viral and cellular proteins and RNA molecules (64) (156). Nearly 60 different viral proteins have been identified (4) (156), but activities for less than half have been reported, which include viral replication, evasion of the host immune response, inhibition of apoptosis, capsid transport to the nucleus, and virus assembly and egress (64).

Viral replication. During a productive infection and replication cycle, viral gene expression is regulated into 3 different kinetic classes: immediate early (IE), early, and late (for review, see (101). If infection occurs during G_0 or G_1 phases of the cell cycle, IE genes are immediately expressed after viral entry and do not require de novo viral or cellular protein synthesis. Expression of early genes is dependent on the expression of functional IE products, late gene expression requires viral DNA

synthesis. IE gene expression, which begins within one-hour post infection (h p.i.), is mainly from the MIE locus and gives rise to the major regulatory proteins of viral replication, IE1 and IE2, but also includes other proteins involved in regulation, inhibition of apoptosis, and immune evasion. Early genes (expressed beginning 12–14 hpi) are mainly involved in viral DNA replication (begins 16–24 hpi), while late gene products (expressed beginning 24–36 hpi) are more structural and maturation proteins involved in virion packaging and egress with peak release of progeny occurring 72–96 hpi.

For a productive infection, the virus must be able to create a cellular environment conducive for viral replication, affecting various signaling pathways and cell systems, while inhibiting the host's immune surveillance and apoptosis pathways (for review, see (17, 133)). Many of these pathways and systems are also regulated by the host's ubiquitin-proteasome system (UPS). Much of the work in the Spector lab and the general focus of this thesis has been to better understand the interplay between the virus and the UPS, especially with regard to the severe cell cycle dysregulation and arrest that occurs after infection.

THE UBIQUITIN-PROTEASOME SYSTEM

The UPS is a highly regulated process in which a protein becomes ubiquitinated and then degraded by the proteasome (for review, see (33, 40, 158)). Proteins become ubiquitinated through a multi-step process involving the E1 (ubiquitin activating enzyme), E2 (ubiquitin conjugating enzyme), and E3 (ubiquitin

ligase) enzymes (114). E1 adenylates the C-terminal glycine of ubiquitin and then forms a thioester bond between the glycine and cysteine on the E1 catalytic site. E2 then forms a similar bond between its active site cysteine and the activated ubiquitin through a transthioesterification reaction. E3 facilitates the transfer of the activated ubiquitin to its recruited substrate. The amino group of a lysine on the substrate attacks the thioester bond between ubiquitin and the E2, thereby forming an isopeptide bond between itself and ubiquitin. The process is repeated wherein a newly activated ubiquitin is then conjugated to an internal lysine (usually lysine 48) of the previously conjugated ubiquitin to form a polyubiquitin chain, which serves as the major targeting signal to the proteasome. The ubiquitin is then removed and recycled by deubiquitinating enzymes (DUBs) as the protein is processed by the proteasome.

Substrate specification and regulation of the UPS is controlled through the hierarchal organization of the E1, E2, and E3 enzymes as well as the balance of their activities with DUBs. In humans, there is one E1, dozens of E2s, and hundreds of E3s, with more still being discovered. Substrate specificity is conferred at the level of E3s. Each E3 targets a specific set of substrates and can interact with one or more E2s. Each protein may also be recognized by multiple E3s, which may interact with different E2s, giving rise to further complexity and points of regulation.

Beyond proteasome-mediated degradation, other forms of ubiquitination, including monoubiquitin, multiubiquitin, or ubiquitination on alternative lysine residues, can regulate protein function in various other cellular processes, including endocytosis, membrane transport, and transcription regulation (53). Ubiquitin-independent proteasome mediated degradation can also occur. Other ubiquitin-like

modifications that can also target proteins to the proteasome include SUMO, Nedd8, and ISG15.

The Proteasome. The mammalian 26S proteasome is a large (~2.5 MDa) multi-subunit complex, which normally consists of a 19S regulatory complex on either end of the 20S catalytic core (for a comprehensive review, see reference (33). The 19S can be further divided into a base component, composed of a hexameric ring of AAA ATPase subunits (Rpt1–Rpt6) and three non-ATPase subunits (i.e. Rpn1, Rpn2, and Rpn10), and a lid component consisting of nine non-ATPases (i.e. Rpn3, Rpn5, Rpn6, Rpn7, Rpn8, Rpn9, Rpn11, Rpn12, and Rpn15). A fourth potential non-ATPase base component has recently been identified as Rpn13/ADRM1, which binds ubiquitin and the proteasome-associated DUB, UCH37, but may only be dynamically associated with the proteasome (43, 63, 120, 161, 171). The 19S regulatory functions include: polyubiquitin recognition, deubiquitination, protein unfolding through ATP hydrolysis, gate opening of the 20S α ring, and translocation of proteins into the 20S for degradation. The 20S catalytic core is composed of four stacked hexameric rings of α and ß subunits (α_{1-7}–$ß_{1-7}$–$ß_{1-7}$–α_{1-7}). Subunits ß1, ß2, and ß5 contain proteolytic active sites, with caspase-like (i.e. cleavage on the C-terminal side of acidic residues), trypsin-like, and chymotrypsin-like (i.e. cleavage after hydrophobic residues) site specificities, respectively (9).

A heterogeneous population of proteasomes is present in the cell as various species of proteasomes can be formed. The proteolytically active ß subunits are substituted by ß1i, ß2i, and ß5i, respectively, in forming the immunoproteasomes. Other regulators of the proteasome (i.e. REGγ, PA28/11S, and PA200/Blm10) can

bind the 20S themselves or in combination with the 19S in forming chimeric proteasomes. REGγ/PA28γ has no ATPase activity but can open the 20S channel gate and facilitate ubiquitin-independent degradation. A study done with HeLa cell extracts determined the proteasome pool to contain: 40% free 20S, 25% 19S-20S-PA28, 20% PA28-20S or PA28-20S-PA28, and only 15% 19S-20S or 19S-20S-19S (146).

The diversity of the proteasome and the UPS in general facilitates regulation of a multitude of different cellular processes in a proteolytic or nonproteolytic fashion. It is the major extralysosomal protein degradation pathway in the cell and is involved in antigen processing, cell cycle regulation, apoptosis, signal transduction, transcription regulation, DNA repair, and chromatin remodeling (23, 40). However, this diversity also lends itself susceptible to misregulation and targeting by pathogens, often manifest as different forms of disease (38, 137).

HCMV PROTEINS ASSOCIATED WITH THE UPS

Immunoevasins. One of the first indications that HCMV exploits the UPS occurred with the discovery of the viral-encoded immunoevasins (for review, see (86, 116). US11 is an ER resident type I transmembrane glycoprotein that dislocates newly synthesized MHC class I molecules from the ER to the cytosol, where they are then degraded by the UPS, thereby preventing antigen presentation to CD8+ T lymphocytes (168). US2 mediates the degradation of MHC class II as well as MHC class I heavy chain (62). US2 and US11 both require a functional UPS, although ubiquitination of

the MHC class I heavy chain is only required during US2-mediated degradation and not US11 (46).

pp71. The multi-functional tegument protein pp71 (UL82) has been shown to target proteins for proteasome-mediated degradation independent of ubiquitin. It is delivered to the nucleus after viral entry and facilitates viral mRNA accumulation, IE gene expression, and viral replication (11). It prevents cell surface expression of MHC class I (153). pp71 mediates the ubiquitin-independent proteasome-mediated degradation of Daxx, thereby alleviating its repression on IE gene expression (57, 129), as well as that of Rb, p107, p130, thereby allowing E2F activation of S-phase genes and accelerating cell cycle progression (65, 66).

UL48. UL48 is a tegument protein with DUB activity, which appears to facilitate virion release (160).

EFFECTS OF HCMV INFECTION ON THE HOST CELL CYCLE

Proper cell cycle progression is intimately coupled with the UPS, which ensures the timely expression and degradation of different cell cycle regulators, including the various cyclins and associated cyclin dependent kinases (cyclin/cdk). Quiescent cells can be induced from G_0 into the cell cycle through various growth factors or serum stimulation. Subsequent phosphorylation of substrates through the activation of cyclin D/cdk4 and cyclin D/cdk6 facilitates passage of the cell through G_1. During G_1, the cell prepares for DNA replication through the induction of transcription factors and genes encoding proteins necessary for nucleotide metabolism

and DNA replication. A prereplication/licensing complex is formed at the origins of DNA replication with the binding of ORC to the DNA followed by cdc6 and Cdt1, which in turn recruits and facilitates the binding of MCM proteins (91, 106, 127). Cyclin E/cdk2 is induced and mediates the transition into S. In S phase, DNA replication is mediated through cyclin A/cdk2. Cdt1 is released from the replication complex and its binding to ORC is further prevented with the accumulation of geminin to ensure a single firing of the origin. In G_2, regulators of mitosis (M) begin to accumulate, including cyclin B. As cells transition into M, cdc25 phosphatase dephosphorylates cdk1, allowing cyclin B/cdk1 and cyclinA/cdk1 complexes to be active and phosphorylate the many substrates involved in cell division. Mitotic exit is facilitated through the inactivation of cdk1 and degradation of cyclins A and B.

HCMV infection causes severe cell cycle dysregulation and arrests cells in a pseudo-G_1/S phase (10, 19, 28, 51, 61, 87, 130, 133, 165, 166). Cells infected in G_0/G_1 are induced towards S. Progression through G_1 allows for the stimulation of the host's biochemical pathways in generating DNA precursors and resources that would be necessary for DNA replication as the cell prepares to enter S; however, entry into S and cellular DNA replication are blocked, as the virus utilizes the cellular resources for its own DNA replication. Normal cyclin/cdk expression is dysregulated, as cyclin D1 and cyclin A expression are inhibited (10, 61, 130, 166), while cyclin E and cyclin B1 are highly expressed along with their associated kinase activities (61, 131, 166). The effects on cyclins D1, A, and E are at the transcriptional level, while that of cyclin B1 appears to be due to increased protein stability (130, 131). Licensing of the cellular origins of DNA replication is inhibited with the abnormal accumulation of

geminin in G_1, which prevents proper loading of the MCMs (7, 167). Several other cell cycle regulators (e.g. Aurora A, PTTG/securin, cdc6, etc.) also abnormally accumulate early after the infection (7, 164). p53 is also stabilized but sequestered in viral replication centers and cannot activate target promoters (10, 22, 35, 102). Rb is hyperphosphorylated early after infection, thereby allowing the induction of E2F responsive genes, many of which encode for proteins required for DNA replication (30). Infection of cells in G_0/G_1 also appears to be necessary for the initiation of viral gene expression, as viral genes are not expressed if cells are infected near or in S phase until the cell completes the cell cycle and reaches the next G_1 (34, 130). Interestingly, this blockade during S-phase infection was relieved upon addition of a proteasome inhibitor (34).

The main E3s involved in cell cycle regulation are the SCF (Skp1-Cullin-F-box) and the APC (Anaphase-Promoting Complex). The SCF remains active throughout the cell cycle, while the APC functions mostly in mitosis through G_1. SCF substrates in general do not appear to be affected during HCMV infection; however, many of the abnormally accumulated cell cycle regulators are substrates of the APC (i.e. cyclin B1, cdc6, geminin, securin, and Aurora A). This observation led to the initial hypothesis that APC activity is downregulated during the infection (7, 131).

The APC is a large multi-subunit E3 active from mitosis through G_1, most notable in ensuring proper cell division and sister chromatid separation (for review, see (113, 155). The APC core contains 12 subunits. APC 2 and APC 11 form the catalytic core, which binds the E2 (i.e. UbcH5, UbcH10, E2-25K, and E2S) and allows transfer of ubiquitin. The TPR subcomplex consists of APC3, APC6, APC7, and

APC8, each of which contains multiple copies of the TPR (tetratricopeptide peptide repeat) protein-protein interaction motifs as well as most of the APC phosphorylation sites. The catalytic core and the TPR subcomplex are associated through APC1, APC4, and APC5. APC activation and regulation is achieved through interactions with its co-activator proteins Cdc20 or Cdh1, which bind to APC3 and APC2. APC phosphorylation in mitosis allows interaction with Cdc20, which recognizes APC substrates containing destruction boxes (D boxes). The spindle assembly checkpoint inhibits APC^{Cdc20} in a substrate-specific manner, preventing the degradation of securin and cyclin B until sister chromatids are properly separated; meanwhile, other substrates like cyclin A are targeted by APC^{Cdc20} for degradation. The mechanisms by which these processes occur remain unclear. Subsequent degradation of securin, cyclin B, and others after spindle assembly allows for sister chromatid separation and the completion of mitosis. During late anaphase, cdk inactivation along with the phosphatase cdc25 relieves the inhibitory phosphorylation of the second co-activator Cdh1, which is now able to bind and activate the APC. Cdh1 recognizes D box substrates along with those containing KEN boxes. Cdc20 is targeted for degradation by APC^{Cdh1}, which remains active through G_1 in regulating the levels of cyclins A and B along with S phase regulators (e.g. Orc1, cdc6, geminin, etc.). As cells enter S phase, APC^{Cdh1} is inactivated through the phosphorylation of Cdh1 and its subsequent dissociation from the APC. APC inactivation through G_2 is aided by Emi1, which has been shown to inhibit both APC^{Cdc20} and APC^{Cdh1}, possibly by binding to Cdc20 and Cdh1 to prevent their interaction with the APC and/or targeting them for ubiquitination through the SCF complex.

Given the complex regulation of the UPS and of the APC itself, inactivation of the APC could potentially be mediated at several different levels: the APC core complex and any one of its subunits, the APC co-activators and inhibitors, the E1 or E2s, DUBs, or the proteasome itself. Based on initial studies done in the Spector lab, an inactivation due to an overexpression of the APC inhibitor Emi1 or a lack of E2 expression (i.e. UbcH5 or UbcH10) seemed unlikely, as Emi1 expression in HCMV-infected cells was less than in mock during the infection, while E2 expression was fairly comparable (unpublished). Moreover, there was a high-level accumulation of the co-activator Cdh1 that did not appear to be associated with the APC. Since several of the misregulated cell cycle proteins are substrates of APC^{Cdh1}, the activation of the APC by Cdh1 is likely prevented. A study published during the course of this dissertation further corroborated these initial observations (164). Although the previous studies have helped pinpoint that the accumulation of APC substrates and cell cycle dysregulation are likely due to the lack of APC^{Cdh1} activation, the mechanism by which HCMV is effecting this inactivation remained unclear. An inactivation of the proteasome itself also seemed unlikely, given the continued proteasome-mediated degradation observed for several different cellular proteins during these initial stages of the infection (e.g. MHC class I, wee-1, Daxx, etc.), although the possibility had not yet been specifically addressed. Interestingly, a study using proteasome inhibitors suggested that proteasome activity is necessary for a productive infection; however, whether proteasome activity is necessary through all stages of the infection or only at the onset was not clear (119).

GOAL OF THIS WORK

The aim of the studies in this dissertation is to further understand how HCMV manipulates the UPS in facilitating a productive infection, specifically with regards to the APC and the proteasome. The means by which APC inactivation occurs during HCMV infection is explored (Chapter 2). Initial studies identified Cdh1 to be phosphorylated early during the infection, which may account for the lack of its binding and activation of the APC. Surprisingly, these studies also revealed that the APC core complex dissociates during the infection, which would also explain the disabling of the APC. These mechanisms and their relative contribution to the inactivation of the APC are further delineated (Chapter 3). These studies identified the viral protein kinase UL97 to be responsible for phosphorylating Cdh1 during the infection as well as the loss of APC5 as the key in mediating the dissociation of the APC. Moreover, these two events are further determined to occur independently. A model for the events mediating the inactivation of the APC during HCMV infection is presented. Proteasome inhibitor studies were used to address whether proteasome activity is necessary through all stages of the infection (Chapter 4). Interestingly, proteasome activity is required throughout the infection and may facilitate viral transcription. The results and significance of this work are summarized at the end of the dissertation (Chapter 5).

CHAPTER 2

ACCUMULATION OF SUBSTRATES OF THE ANAPHASE-PROMOTING COMPLEX (APC) DURING HUMAN CYTOMEGALOVIRUS INFECTION IS ASSOCIATED WITH THE PHOSPHORYLATION OF CDH1 AND THE DISSOCIATION AND RELOCALIZATION OF THE APC SUBUNITS

ABSTRACT

Cell cycle dysregulation upon human cytomegalovirus (HCMV) infection of human fibroblasts is associated with the inactivation of the Anaphase-Promoting Complex (APC), a multi-subunit E3 ubiquitin ligase, and accumulation of its substrates. Here, we have further elucidated the mechanism(s) by which HCMV-induced inactivation of the APC occurs. Our results show that Cdh1 accumulates in a phosphorylated form that may prevent its association with and activation of the APC. The accumulation of Cdh1, but not its phosphorylation, appears to be CDK-dependent. Lack of association of exogenously added Cdh1 with the APC from infected cells indicates that the core APC may also be impaired. This is further supported by the examination of the localization and composition of the APC. Co-immunoprecipitation studies show that both Cdh1 and the subunit APC1 become dissociated from the complex. In addition, immunofluorescence analysis demonstrates that as the infection progresses, several subunits redistribute to the cytoplasm, while APC1 remains nuclear. Dissociation of the core complex itself would account for not only the

observed inactivity, but also its inability to bind to Cdh1. Taken together, these results illustrate that HCMV has adopted multiple mechanisms to inactivate the APC, which underscores its importance for a productive infection.

INTRODUCTION

Human cytomegalovirus (HCMV) infection is the leading viral cause of birth defects and results in severe disease in immunocompromised individuals (for review, see (109)). The replication of this virus is temporally regulated and involves an intricate set of interactions between the virus and the host cell machinery that optimize the cellular environment for viral replication and assembly. Similar to DNA tumor viruses that can infect quiescent cells, HCMV induces cells towards S phase such that the cellular DNA machinery is activated and available for viral DNA replication. Subsequent dysregulation of multiple cellular factors involved in the cell cycle causes the infected cell to arrest in a pseudo-G_1/S state (7, 10, 28, 61, 87, 130, 131, 165-167). The Rb family pocket proteins that regulate transcription in complex with E2Fs in a cell cycle-dependent manner become phosphorylated and accumulate, while the tumor suppressor protein, p53, is stabilized (35, 61, 96, 102). Cyclin A mRNA synthesis is blocked, and only low levels of cyclin A protein and its associated kinase activity can be detected (61, 130). In contrast, cyclins E and B, as well as their associated kinase activities, are upregulated (61, 96, 130).

Cyclin expression, along with other cell cycle proteins, is partially regulated by the ubiquitin-proteasome pathway, in which a protein becomes ubiquitinated and then degraded by the proteasome (40, 41). Ubiquitination occurs through a multi-step mechanism involving the E1 (ubiquitin activating enzyme), E2 (ubiquitin conjugating enzyme), and E3 (ubiquitin ligase) enzymes. Target specificity is determined at the

level of E3s, where each E3 interacts with specific E2s and protein substrates. The main E3s involved in cell cycle regulation are the SCF (Skp1-Cullin-F-box) complex and the APC (Anaphase- Promoting Complex).

The APC, also known as the cyclosome, is a large multi-subunit complex that is evolutionarily conserved from yeasts to plants to mammals (for review, see (18, 113)). It is active from mitosis through G_1 to ensure proper cell cycle progression, in particular for anaphase entry and exit from mitosis. Cryo-negative staining electron microscopy, biochemical reconstitution assays, and labeling experiments have been used to delineate the architecture of the APC (29, 39, 111, 149). Vertebrate APC contains at least 12 subunits, which can be further divided into two separable subcomplexes (149). Subunits APC2 and APC11 (catalytic core), along with APC10, form the platform, which binds the E2 (UbcH5 or UbcH10) and allows transfer of ubiquitin. APC3 (Cdc27), APC6, APC7, and APC8, all of which contain tetratricopeptide repeats (TPR), form the arc lamp that functions mainly in binding the activator proteins. APC1, APC4, and APC5 serve as a scaffold, bridging the two subcomplexes together. APC activation and regulation is achieved through interactions with its co-activator proteins Cdc20 or Cdh1, which bind to APC3. APC2 and APC7 have also been shown to facilitate the interaction between Cdh1 and the APC (150, 157). Phosphorylation of the APC upon entry into mitosis mediates binding of Cdc20, thus forming an active complex that initiates mitotic cyclin degradation (81, 140, 172). During late anaphase, inactivation of cyclin dependent kinases (CDKs) relieves the inhibitory phosphorylation of Cdh1, which is now able to bind and

activate the APC. APC^{Cdh1} remains active through G_1 and prevents the premature accumulation of cyclin A, cyclin B, and S phase regulators (e.g. Cdc6 and geminin). As cells enter S phase, rising cyclin A/Cdk2 activity results in the phosphorylation of Cdh1, which blocks the binding of Cdh1 to the APC and shuts off ubiquitylation of the APC substrates. Cell cycle specific expression of trans-acting factors such as Emi1, RASSF1A, and the mitotic spindle checkpoint proteins also modulate APC activity.

Initial studies from our lab and others showing that several substrates of the APC (e.g. cyclin B, Cdc6, and geminin) abnormally accumulate early in the HCMV infection led to the hypothesis that APC activity is downregulated during the infection (7, 61, 131, 164, 167). Subsequently, Wiebusch et al. (164) reported that the APC isolated from HCMV-infected cells had significantly reduced to no activity, as measured by in vitro ubiquitination assays. This decrease in APC activity did not appear to be due to an overexpression of APC inhibitor Emi1 or a lack of E2 expression (i.e. UbcH5 or UbcH10). It was also noted that Cdh1 protein expression was significantly upregulated during the infection, while mRNA levels remained unchanged. However, immunoprecipitation assays using an antibody to APC3 indicated that little to no Cdh1 was associated with this subunit as the infection progressed, although it was not determined whether other APC subunits remained in a complex with APC3. Based on these results, it was proposed that the decreased APC activity during HCMV infection is due to the lack of Cdh1 binding and activation of the complex. However, questions regarding the mechanism by which this occurs were not addressed.

In this report, we have further investigated the mechanism(s) by which the APC becomes inactivated during the HCMV infection. Importantly, we show that Cdh1 is phosphorylated during the infection in a CDK-independent manner and that the APC becomes destabilized, as evidenced by the dissociation of not only Cdh1, but also APC1, the largest subunit of the APC. In contrast, subunits that contain the TPR motif (APC3, APC7, and APC8) remain in a complex. We also show that this dissociation coincides with the retention of APC1 in the nucleus and redistribution of the TPR subunits to the cytoplasm. Thus, it appears that multiple mechanisms are involved in mediating the inhibition of APC activity during the infection.

MATERIALS AND METHODS

Cells and Virus. Human foreskin fibroblasts (HFFs) were obtained from the University of California, San Diego, Medical Center and cultured in minimum essential medium with Earle's salts supplemented with 10% heat-inactivated fetal bovine serum, 1.5 μg/ml amphotericin B, 2 mM L-glutamine, 200 U/ml penicillin, and 200 μg/ml streptomycin. All cell culture media were from Gibco-BRL. Cells were kept in incubators maintained at 37°C and 7% CO_2. The Towne strain of HCMV was obtained from the American Type Culture Collection (VR 977) and propagated as previously described (144).

Cell Synchronization and Infection. All experiments were performed under G_0 synchronization conditions (130). Cells were trypsinized 3 days after the monolayer became confluent and replated at a lower density to induce progression into the cell cycle. At the time of replating, cells were either infected with HCMV at a multiplicity of infection (MOI) of 5 or mock infected with tissue culture supernatants as described (130). Stock solutions of MG132 (Calbiochem) and Roscovitine (Calbiochem) were made in DMSO. Cell cultures were incubated with 2.5 μM MG132, 20 μM Roscovitine, or an equivalent volume of DMSO as a control at the times shown. Cells were harvested at the indicated times post infection (p.i.) and processed as described for each experiment. All experiments were performed at least twice.

Western Blot Analysis. Cells were lysed in Laemmli reducing sample buffer (62.5 mM Tris pH 6.8, 2% SDS, 10% glycerol, 5% β-mercaptoethanol) supplemented with a protease inhibitor cocktail (Roche) and phosphatase inhibitors (50 mM sodium fluoride, 1 mM sodium orthovanadate, 10 mM β-glycerophosphate). The lysate was sonicated, boiled for 5 min, and clarified by centrifugation for 10 min at 16,000 x g. Equal amounts of lysate (i.e. by cell number) were loaded onto SDS-polyacrylamide gels (SDS-PAGE) unless otherwise stated. Following electrophoresis, the proteins were transferred to nitrocellulose (Schleicher & Schuell), and then Western blot analyses were performed using appropriate antibodies. The Supersignal West pico and West femto chemiluminescent detection methods (Pierce) were used to visualize the proteins according to the manufacturer's instructions.

Phosphatase Assays. Cell samples were lysed in buffer A (50 mM Tris-HCl pH 7.5, 10 mM KCl, 1 mM $MgCl_2$, 10% glycerol, 300 mM NaCl, 0.1% NP-40, protease inhibitor cocktail) or in buffer B (buffer A plus phosphatase inhibitors: 50 mM sodium fluoride, 1 mM sodium orthovanadate, 10 mM β-glycerophosphate). After incubation on ice for 5 min, cells were subjected to three cycles of freeze-thaw. The lysate was then centrifuged at 16,000 x g for 10 min; the supernatant was collected and analyzed for protein concentration using the Bio-Rad protein assay. For λ-protein phosphatase treatment, buffer A lysates were incubated with 1 X λ-protein phosphatase buffer (New England Biolabs), 2 mM $MnCl_2$ and λ-protein phosphatase (New England Biolabs) at 5 units/ug protein for 30 min at 30^{o}C. Buffer B lysates were incubated in parallel without λ-protein phosphatase. Reactions were terminated

with addition of 2X Laemmli reducing sample buffer. Samples were then boiled and analyzed by Western blot.

Immunoprecipitations. Cell pellets were lysed in extraction buffer (20 mM Tris-HCl pH 7.5, 150 mM NaCl, 5 mM $MgCl_2$, 0.2% NP-40, 10% glycerol, 1mM DTT; supplemented with 1X protease inhibitor cocktail, 50 mM sodium fluoride, 10 mM β-glycerophosphate, and 1 mM ATP) using an end-over-end rotator at 4ºC. Lysates were centrifuged at 16,000 x g for 10 min and supernatants collected. For APC3 co-immunoprecipitation assays, lysates were first pre-cleared by Protein G beads (Santa Cruz Biotechnology) coupled to mouse immunoglobulin (IgG) (Jackson ImmunoResearch), and then incubated with Protein G beads coupled with an anti-APC3 monoclonal antibody (BD Biosciences). Beads were washed with TBS-T (0.01% Tween-20) between incubations and eluted in Laemmli reducing sample buffer by boiling for 5 min. Pre and post-immunoprecipitation (IP) samples were also collected and boiled in reducing sample buffer. Samples were analyzed by Western blot. Pre and post-IP (PIP) lanes were loaded with the same cell equivalents, whereas IP lanes were loaded with 5–10 times more. All incubations and washes were performed at 4ºC.

In Vitro Binding Assay. Rabbit reticulocyte lysate (T7-Quick Couple TNT Kit; Promega) was first immunodepleted of APC with an anti-APC3 antibody before being used to generate ^{35}S-labeled Cdh1 via an in vitro transcription/translation (TNT) reaction. Human Cdh1 (gift from Dr. Jan-Michael Peters) was cloned into pcDNA3 (Invitrogen) under the T7 promoter. TNT reactions using pcDNA3 vector alone were used as a negative control. Mock- or HMCV-infected cells were harvested at 8 and 16

h p.i. and lysed in extraction buffer. ^{35}S-Cdh1 or ^{35}S-pcDNA3 was pre-incubated with cell lysates at room temperature for 1 hr. The pre-incubation mixture was then immunoprecipitated for APC3. Immunoprecipitations using mouse IgG coupled beads were performed in parallel as a negative control. Following SDS-PAGE, the gel was divided in half such that the upper portion was used to detect APC3 by Western blot, and ^{35}S-Cdh1 was detected by autoradiography using the lower portion. IP lanes were loaded with 20 times cell equivalents compared to pre and post-IP lanes.

Immunofluorescence Assays. Cells were seeded onto glass coverslips at the time of infection. At the indicated times p.i., cells were washed in phosphate buffered saline (PBS) and fixed with 4% paraformaldehyde for 20 min. Cells were then permeabilized with 0.2% Triton X-100 for 5 min and washed in PBS prior to immunofluorescence staining. Normal goat serum (10% in PBS) (Jackson ImmunoResearch) was used as a blocking solution and to dilute the primary and secondary antibodies. A mouse monoclonal antibody to APC3 and rabbit antibodies against APC 1, 7, 8, and 10 were used. Mouse or rabbit IgG (Jackson ImmunoResearch) served as negative controls. Following primary antibody incubation and subsequent washes in PBS, coverslips were incubated with appropriate FITC- or TRITC-conjugated secondary antibody (Jackson ImmunoResearch) plus Hoescht stain. Coverslips were treated with SlowFade Gold, an anti-photobleaching reagent (Molecular Probes), and mounted onto a slide for imaging. Co-stained samples were analyzed by a DeltaVision deconvolution microscopy system (Applied Precision) using a 100x oil immersion objective lens with SoftWoRx software (Applied Precision) on a Silicon Graphics O2 workstation. Images were taken at 0.2 μm

increments along the z-axis with pixel intensities maintained in the linear range by a Photometrics CCD camera mounted on the fluorescence/dic microscope. The fluorescent data sets were deconvolved and analyzed by DeltaVision SoftWoRx programs. Adobe Photoshop 7.0 was used to prepare images for the figures.

Antibodies. The sources of antibodies used are as follows: Cdh1 (Ab-2, Calbiochem); Rb (Ab-1, IF8, Neomarkers); Cdc6 (180.2, Santa Cruz Biotechnology); geminin (FL-209, Santa Cruz Biotechnology); actin (AC-15, Sigma); GAPDH (6c5, Fitzgerald); IE1/IE2 (Ch16.0, Virusys). APC antibodies: APC1 (gift from Dr. Michael Green; ref. (49, 148)); APC3 (clone 35, BD Biosciences) and (AF3.1, Santa Cruz Biotechnology); APC7 (poly6113, Biolegend) and (H-300, Santa Cruz Biotechnology); APC8 (poly6114, Biolegend) and (H-300, Santa Cruz Biotechnology); APC10 (poly6115, Biolegend); APC11 (poly6116, Biolegend).

RESULTS

Cdh1 becomes phosphorylated during the infection. A previous report by Wiebusch et al. (164) suggested that APC inactivity during HCMV infection is due to the lack of Cdh1 binding. In accord with their study, we have also observed the dissociation of Cdh1 from the APC despite a significant upregulation in expression beginning 8–12 h p.i. (data not shown). However, by Western blot analysis, the Cdh1 from infected cells appeared to migrate slower on the gel, suggesting that the association of Cdh1 with the APC might be inhibited due to a modification of Cdh1 during the infection. Because Cdh1 phosphorylation normally prevents its association with the APC (83, 174), phosphatase assays were used to determine whether Cdh1 becomes phosphorylated. Lysates from mock-infected or HCMV-infected HFFs harvested at 24 h p.i. were treated with or without λ-protein phosphatase (λpp) and analyzed by Western blot. As a control, samples were blotted for Rb, which becomes hyperphosphorylated upon HCMV infection (61). As shown in Figure 2.1, more hyperphosphorylated Rb (*) was present in the infected cells. Subsequent treatment with phosphatase reduced the hyperphosphorylated Rb in both the mock and virus-infected samples. The lysates were also tested for viral IE1-72 and IE2-86 expression and phosphorylation status. Consistent with previous studies (45), IE2-86 is phosphorylated (*), as treatment with phosphatase resulted in a lower molecular weight form, whereas IE1-72 was unaffected. In the case of Cdh1, no mobility changes were observed with the mock cell samples upon phosphatase treatment, indicating that Cdh1 is not phosphorylated at this time point. Phosphatase treatment of

the infected sample, however, resulted in a mobility shift such that the Cdh1 band co-migrated with the unphosphorylated form found in the uninfected cell. These results illustrate that Cdh1 is phosphorylated upon HCMV infection.

Cdh1 is normally phosphorylated by CDKs in late G1 to inactivate the APC. To assess whether the observed Cdh1 phosphorylation is due to the activation of the several CDKs upon HCMV infection, HFFs were either infected with virus or mock-infected in the presence or absence of Roscovitine, an inhibitor of CDKs 1, 2, 5, 7, and 9 (26, 31, 98, 136, 159). Three different periods of drug treatment were used, from 0–24, 4–24, and 8–24 h p.i. The choice of these time intervals was based on our previous studies that showed that addition of Roscovitine at the beginning of the infection altered viral IE and early gene expression, while a delay in the addition of the drug until 4 to 8 h p.i. allowed the infection to progress normally until late times (132). Cells were harvested at 24 h p.i. and processed for Western blot analysis. Again, Rb and IE expression were used as controls. Roscovitine should inhibit CDK-mediated phosphorylation of Rb. As expected, significantly more phosphorylated (*) Rb was present in the virus-infected cells than in the mock cells, and treatment with the drug reduced the amount of hyperphosphorylated Rb in all cases (Figure 2.2A). The incomplete inhibition in the infected cells is likely due to phosphorylation of Rb by kinases that are not affected by Roscovitine. Addition of the drug from 0–24 h p.i. favored IE2 expression over IE1, an effect of the drug that has been previously characterized (132). For Cdh1, the Roscovitine treatment from 0–24 h p.i. was most effective in inhibiting its accumulation in the virus-infected cells, whereas no significant differences were observed in the mock-infected cells. Interestingly,

increasingly more phosphorylated (*) Cdh1 accumulated as the drug was administered later during the infection. To further confirm that Cdh1 is phosphorylated, phosphatase assays were performed as previously described. As shown in Figure 2.2B, the subsequent mobility shift in the infected sample upon phosphatase treatment indicates that Cdh1 was phosphorylated in the presence of Roscovitine. Similar to Rb, the lack of inhibition of Cdh1 phosphorylation by Roscovitine suggests that other kinases may be responsible for its phosphorylation in the infected cell.

Since Cdh1 remained phosphorylated in the infected cells treated with Roscovitine, we also assessed accumulation of the APC substrates Cdc6 and geminin by Western blot to help determine whether the APC still remained inactive. In general, treatment of both the mock and HCMV-infected cells with Roscovitine resulted in lower levels of Cdc6 and geminin relative to the corresponding untreated cells at all time periods (Figure 2.2A). In the infected cells, the difference was most notable for both proteins when the drug was administered at the beginning of the infection, whereas the effect was greater for geminin than Cdc6 when the drug was added at the later times. However, significantly more Cdc6 and geminin accumulated in the infected cells when the inhibitor was added after 4 h p.i. than in the uninfected cells in the absence of the inhibitor, suggesting that APC activity was downregulated. Taken together, these results suggest that the increased accumulation of the APC substrates and Cdh1, but not Cdh1 phosphorylation, is at least partly CDK-dependent during the infection.

The APC becomes destabilized upon HCMV infection. Although CDK-mediated phosphorylation of Cdh1 during late G1 has been shown to inhibit its

association with the APC (74, 89), we could not conclude that the induced phosphorylated state of Cdh1 upon HCMV infection impeded its association since phosphorylation of other sites on Cdh1 or other modifications may affect its physical structure differently. On the other hand, an alteration in the APC itself might also inhibit binding to Cdh1. To this end, in vitro binding assays were used to determine whether the ability of the APC to bind exogenous Cdh1 is also affected during the infection. ^{35}S-labeled Cdh1 was synthesized in an in vitro transcription/translation (TNT) reaction using rabbit reticulocyte lysate. The reticulocyte lysate was first immunodepleted of endogenous APC (141, 173) and assayed for endogenous Cdh1 expression, which was not detected by Western blot, before being used for the TNT reactions. Excess ^{35}S-Cdh1 was incubated with cell lysate from mock or virus-infected HFFs harvested at 8 and 16 h p.i., and the complexes were then immunoprecipitated with antibody against APC3. Negative controls included a vector alone TNT reaction (p3) and immunoprecipitation using beads coupled with mouse IgG. Samples were analyzed for immunoprecipitated APC3 by Western blot and for co-precipitated ^{35}S-Cdh1 by autoradiography. ^{35}S-Cdh1 was detected as a doublet (Figure 2.3), which may be due to an alternative start site within the coding region or a small amount of degradation. It should also be noted that the proteins in the IP lanes appeared to migrate slightly slower, a phenomenon we have often observed with our IP gels. As shown in the APC3 Western blot (short exposure), the amount of precipitated APC3 was comparable between the samples. APC3 was also immunodepleted in these samples, as evidenced by its absence in the post-IP lanes (longer exposure). ^{35}S-Cdh1 co-precipitated with APC3 in the lysate from the HCMV-infected cells at 8 h p.i.,

although the amount was less than that from the mock-infected cells. In contrast, at 16 h p.i., very little ^{35}S-Cdh1 was found in the co-precipitate from the infected cells, whereas the level of ^{35}S-Cdh1 in the co-precipitate from the mock samples was comparable to that observed at the 8 h time point. These results suggest that the APC binding capacity for exogenous Cdh1 is also affected during the infection, which could contribute to the loss in endogenous Cdh1 binding.

To further investigate whether the APC core complex is altered upon HCMV infection, Western blotting was first used to assess the steady state levels of the APC subunits during the infection. Individual subunits could be degraded or modified such that the complex is not properly formed. Protein levels for APC3, APC7, and APC11 remained comparable between infected and mock samples through 48 h p.i. (Figure 2.4), which is consistent with a previous report that APC2 and 3 levels remained unchanged (164). A modest increase in protein expression was observed for APC1, beginning at 24 h p.i., and APC8 and APC10, beginning at 36 h p.i. Although not all APC subunits have been tested, the loss in activity does not appear to be due to decreased subunit expression.

Co-immunoprecipitation experiments using an antibody to APC3 coupled with Western blot analysis of the co-precipitated proteins were then utilized to determine complex stability in infected cells between 8 and 16 h p.i. We first assessed whether APC7 and APC8, which are TPR subunits normally in a subcomplex with APC3, were present (149). GAPDH was used as a negative control. As shown in Figure 2.5, the amount of APC7 and APC8 that co-immunoprecipitated with APC3 (lane labeled IP) was comparable between infected and mock cells throughout the time course. Both

subunits also remained in complex with APC3, as evidenced by the depletion of the proteins in the post-IP (lane labeled PIP), although a small amount of APC7 was present in the post-IP of the lysate from infected cells at 16 h p.i. In striking contrast, a significant decrease in associated APC1, a scaffolding protein, was observed in the infected cells. While APC1 levels in the complex were similar for both mock and infected cells at 8 h p.i., a slight decrease was observed at 12 h p.i. in the infected cells, and no APC1 was detected in the complex by 16 h p.i. In the mock-infected cells, the amount of APC1 co-precipitated with APC3 remained comparable at all time points, although not all APC1 was in complex since some protein was still seen in the post-IP sample. The presence of Cdh1 was also checked as a positive control for association with APC3. As expected, Cdh1 remained in complex with APC3 throughout the time course in the uninfected samples, but was lost from the APC as the infection progressed. Taken together, these results suggest that the APC becomes destabilized upon HCMV infection, as evidenced by the dissociation of at least two subunits.

APC subunits relocalize to the cytoplasm of HCMV-infected cells. Given that APC1 protein levels are not affected between 8 and 16 h p.i., the loss of APC1 from the complex may be associated with altered localization of either APC1 or other APC subunits. Immunofluorescence assays (IFA) were used to further examine the localization pattern of various APC subunits during an infection time course. Samples were co-stained for APC3 (mouse monoclonal antibody) along with APC1, APC7, APC8, or APC10 (rabbit polyclonal antibodies) and analyzed by deconvolution microscopy. Hoescht dye was added to visualize the nuclei of the cells. Mouse or

rabbit IgG, which were used as respective negative controls, gave minimal background staining (Figure 2.6). As expected, the APC subunits all showed a predominantly nuclear staining pattern in mock-infected cells, which remained unchanged between 8 and 16 h p.i. At 8 h p.i., both APC1 and APC7 remained relatively co-localized with APC3 in the nuclei of the infected cells. However, as the infection progressed, APC3 and APC7 showed a more cytoplasmic staining pattern whereas APC1 remained primarily nuclear. A similar cytoplasmic redistribution in HCMV-infected cells was also observed for APC8 and APC10 (data not shown). These results provide additional evidence that APC1 becomes dissociated from the complex during the infection. We could not determine if the other APC subunits showed a similar cytoplasmic pattern of localization due to lack of antibodies that were suitable for immunostaining. Taken together, however, these studies suggest that both destabilization of the complex and altered localization could account for the loss in APC activity and accumulation of its substrates, which are primarily nuclear proteins.

DISCUSSION

The APC plays a key role in cell cycle regulation by targeting the degradation of specific cell cycle proteins in a timely manner. Not surprisingly, viruses target the APC as they manipulate the host cell cycle to facilitate their own replication (48). Adenovirus E4orf4 has been implicated in targeting phosphatase PP2A to APC6 to inactivate the complex through dephosphorylation (73). The chicken anemia virus apoptin protein has also been shown to target, and perhaps sequester, APC1, causing complex destabilization and G_2/M arrest (49, 148). Similarly, HCMV appears to specifically inhibit the APC in the process of creating a cellular environment more conducive for viral replication. Previous work indicated that Cdh1 no longer binds to APC3 as the infection progresses, suggesting that the loss in APC function is due to the lack of activation by Cdh1 (164). Our studies show that this is only one of the multiple effects of the infection on the APC that could be responsible for its inactivation.

We find that Cdh1 becomes phosphorylated early upon HCMV infection. In normal uninfected cells, Cdh1 phosphorylation and its subsequent dissociation from the complex is a key mechanism in mediating APC inactivation as the cells transition from G_0/G_1 to S phase. The phosphorylation of Cdh1 in the infected cells would not be surprising given the heightened state of CDK activity during the infection. However, treatment with the CDK inhibitor, Roscovitine, did not inhibit Cdh1 phosphorylation, although it did affect its accumulation. This would imply that other kinases are involved in phosphorylating Cdh1 in infected cells. Alternatively, these results could

be attributed to the indirect effects the drug has on the infection. We also noted that addition of Roscovitine at the beginning of the infection prevented the accumulation of not only Cdh1, but also two other APC substrates, geminin and Cdc6. Roscovitine had less effect on the accumulation of these proteins when administered at 4 or 8 h p.i. There are several explanations for this result, and they are not mutually exclusive. As our lab and others have shown, Roscovitine severely reduces viral replication (12, 132, 134). Addition of the drug at the time of infection alters IE gene expression such that IE2-86 expression is enhanced while IE1-72 is reduced. Early viral gene expression and viral DNA replication are also inhibited. However, if the drug is added at 6 h p.i., it no longer affects IE1-72 expression, and early gene expression along with viral DNA replication are restored (132). Thus, some viral early gene expression may be necessary for inactivation of the APC. The kinetics of stabilization of the APC substrates (beginning around 8 h p.i.) provides support for this (7, 61, 131, 164, 167). Alternatively, CDK activity may be required for the accumulation of some APC substrates due to direct effects on phosphorylation of other APC subunits or other proteins involved in the ubiquitin-proteasome degradation pathway. It is also possible that the drug affects the levels of RNA. These latter two possibilities may apply to both infected and uninfected cells, as the levels of geminin were also lower in the uninfected cells treated with the drug during all of the intervals. A small decrease in Cdc6 was also observed in the treated uninfected cells, although the levels were at the limit of detection in both the treated and untreated cells. Taken together, the results show that the phosphorylation of Cdh1 in infected cells is not CDK dependent, but the

accumulation of the APC substrates may be partially affected, either directly or indirectly, by the inhibition of CDK activity.

While phosphorylation of Cdh1 in infected cells may contribute to its lack of association with the APC, we also found that exogenous TNT-synthesized Cdh1 had decreased binding affinity for APC3 in lysates obtained from infected cells as the infection progressed from 8 to 16 h p.i.; yet there was little change in binding to APC3 in uninfected cell lysates at any time point. APC3 from the uninfected cell lysates was still able to bind more ^{35}S-Cdh1 despite potentially competing cellular Cdh1, whereas this would not have been a factor in the infected cells at 16 h p.i. based on the APC3 co-immunoprecipitation data. These results indicate that the core APC in infected cells is no longer capable of associating with the activator as the infection progresses. While unlikely, we cannot exclude the possibility that the ^{35}S-Cdh1 was modified by a factor in the infected-cell lysate.

In accord with the in vitro binding experiments using exogenous Cdh1, we demonstrate by co-immunoprecipitation assays that APC1 becomes dissociated from the TPR subunits with similar kinetics in the infected cells. Recent studies have further defined the intricate architecture of the APC (29, 39, 111, 149). The complex is composed of two main subcomplexes, one containing the catalytic core (i.e. APC2 and APC11) and the other containing the TPR subunits (i.e. APC3, APC6, APC7, and APC8), that are bridged by APC1, APC4, and APC5 (150) (see Figure 2.7A for model). The binding between APC1, APC4, APC5, and the TPR subunit APC8, is also interdependent, in that each subunit is required for the association of the other three (149). Without APC1, the overall structure of the APC would be greatly affected, as

the two subcomplexes would likely be separated. Since full binding of Cdh1 to the APC is dependent on both APC3 and APC2 (149), the dissociation of the core complex could therefore also account for the inability of Cdh1 to bind the complex and for the lack of APC activity. Interestingly, previous studies have suggested that the APC contains multiple copies of the TPR subunits (29, 111) and that these TPR subunits remain assembled even in the absence of APC1 (149). This then correlates with our finding that APC3, APC7, and APC8 still remained in complex together despite the dissociation of APC1 upon HCMV infection.

We further showed by IFA that several APC subunits relocalized to the cytoplasm as the infection progressed, while APC1 remained nuclear. It is unclear whether the dissociation of APC1 causes the other subunits to disperse into the cytoplasm, or whether it is the TPR subcomplex that is dissociating from the rest of the APC.

An important question raised by these studies is why does HCMV destabilize the APC? There are at least three different possibilities. First, to inhibit host cell functions or promote viral replication, the virus may require high levels of cellular proteins that normally would be ubiquitinated by the APC and degraded by the proteasome. An example might be the premature accumulation of geminin, which inhibits the licensing of cellular origins of DNA replication. A second possibility is that there may be essential viral proteins that would be targeted for degradation by a functional APC. Finally, one or more of the individual APC subunits may need to be recruited for a specific role in the viral infection. Studies are currently in progress to

address this question and to further elucidate the molecular mechanisms by which the APC is destabilized.

In summary, multiple mechanisms appear to be involved in inactivating the APC upon HCMV infection, including dissociation of the core APC and the relocalization of some subunits to the cytoplasm of the infected cells, beginning 8–12 h p.i. This time frame also correlates with the observed accumulation of APC substrates (7, 61, 131, 164, 167) and loss of APC activity (164). Although it is unknown at this time whether these events are interdependent or represent redundant pathways, they underscore the importance of disabling the APC during the infection.

ACKNOWLEDGEMENTS

We appreciate the gift of the Cdh1 clone from Dr. Jan-Michael Peters and the use of the Deltavision microscope and SoftWorx software at the UCSD Cancer Center Digital Imaging Shared Resource. We would like to thank Anokhi Kapasi and Rebecca Sanders for their helpful discussions and comments on the manuscript. This work was supported by NIH grants CA073490 and CA034729 to D.H.S.

The text of this chapter is a reprint of the material as it appears in *Journal of Virology*, 82(1): 529–537, 2008. Tran, K., J.A. Mahr, J. Choi, J.G. Teodoro, M.R. Green, and D.H. Spector. Accumulation of substrates of the anaphase-promoting complex (APC) during human cytomegalovirus infection is associated with the phosphorylation of Cdh1 and dissociation and relocalization of APC subunits. The dissertation author was the primary investigator and author of this paper.

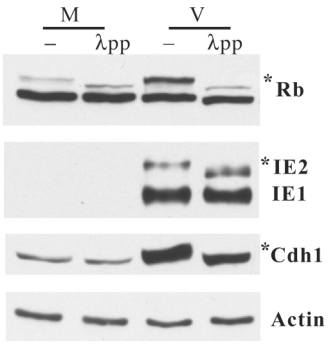

Figure 2.1 Cdh1 becomes phosphorylated during HCMV infection. HFFs infected with HCMV Towne at MOI 5 (V) or incubated with conditioned media (M) were harvested at 24 h p.i. Cell lysates were incubated with or without **(–)** λ-protein phosphatase (λpp) and analyzed by Western blot with antibodies to Rb, IE2, IE1, and Cdh1. Actin served as a control for protein loading. For Rb, IE2, and Cdh1, the phosphorylated (*****) forms are shown as indicated.

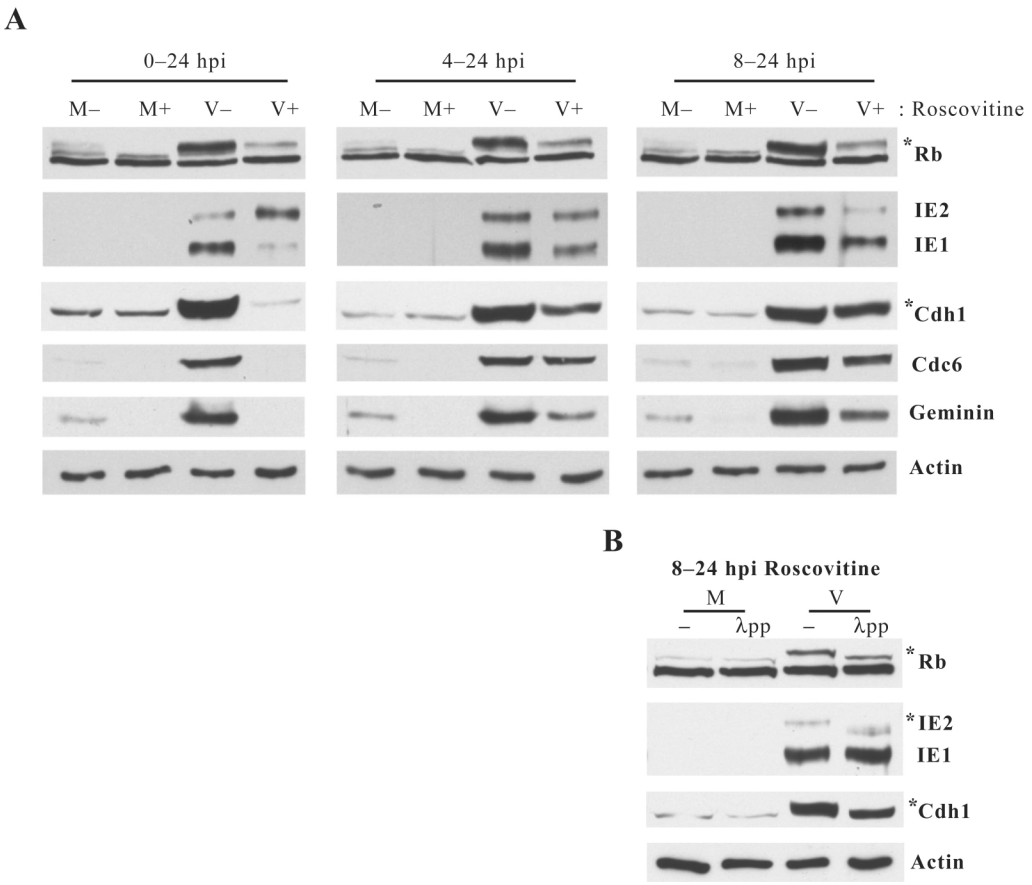

Figure 2.2 Roscovitine treatment at early times of the infection inhibits Cdh1 accumulation but not phosphorylation. A) DMSO **(–)** or 20 μM Roscovitine **(+)** was added at 0, 4, or 8 h p.i. to mock (M) or HCMV (V) infected cells. Cells were harvested at 24 h p.i. for Western blot analysis with antibodies to Rb, IE2, IE1, Cdh1, Cdc6, and geminin. Actin served as a loading control. For Rb and Cdh1, the phosphorylated (*) forms are shown as indicated. The Cdh1 blot for the 0–24 h p.i. samples is slightly overexposed to show the presence of phosphorylated Cdh1 in the infected cells plus Roscovitine treatment. **B)** Mock (M) or HCMV (V) infected cells were treated with 20 μM Roscovitine from 8–24 h p.i., harvested at 24 h p.i., incubated with or without (–) λ-protein phosphatase (λpp), and analyzed by Western blot as previously described.

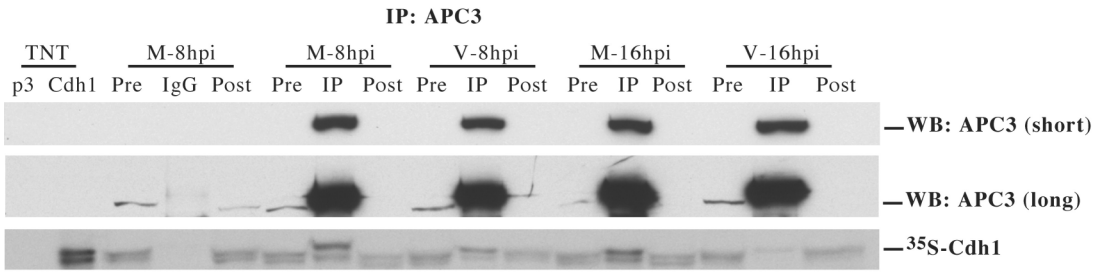

Figure 2.3 Exogenous Cdh1 binding to APC3 from HCMV infected cells is reduced as the infection progresses. Mock (M) or HCMV (V) infected HFFs harvested at 8 and 16 h p.i. were lysed and incubated with TNT-synthesized ^{35}S-Cdh1 using APC-depleted reticulocyte lysate. Complexes were immunoprecipitated with antibody against APC3. Samples were assayed for APC3 by Western blot and co-precipitating ^{35}S-Cdh1 by autoradiography. A short and longer exposure of the APC3 blot is shown. Empty vector pcDNA3 (p3) and immunoprecipitation using mouse IgG were used as negative controls. Pre = input lysate; IgG = IgG IP; IP = APC3 IP; Post = post-IP.

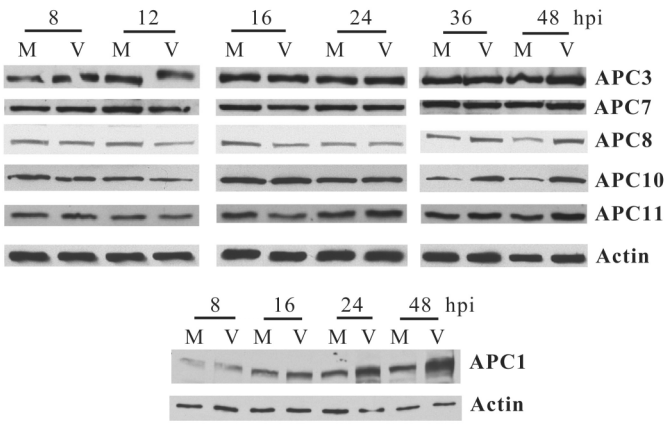

Figure 2.4 Levels of some APC core subunits increase during HCMV infection. Mock (M) or HCMV (V) infected HFFs were harvested at the times indicated and processed by Western blot analysis with antibodies to APC3, APC7, APC8, APC10, APC11 and APC1. Actin was used as a loading control.

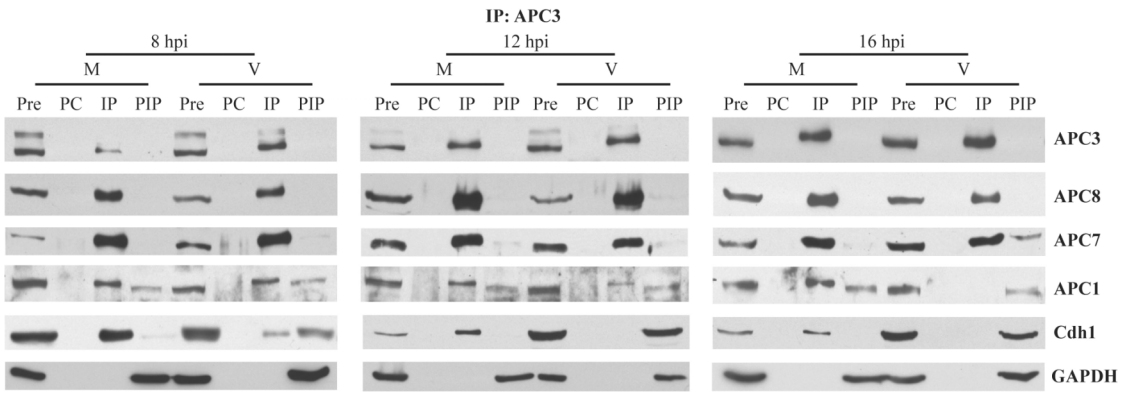

Figure 2.5 The APC becomes destabilized during the course of HCMV infection. Mock (M) or HCMV (V) infected HFFs were harvested at the times shown and immunoprecipitated for APC3. Western blots were used to identify co-precipitating APC subunits with antibodies to APC1, APC3, APC8, APC7, and Cdh1. The Cdh1 blot for the 8 h time point is slightly overexposed to show the presence of co-precipitating Cdh1 in the infected cells. GAPDH is shown as a negative control. Pre = input lysate; PC = IgG IP; IP = APC3 IP; PIP = post-IP.

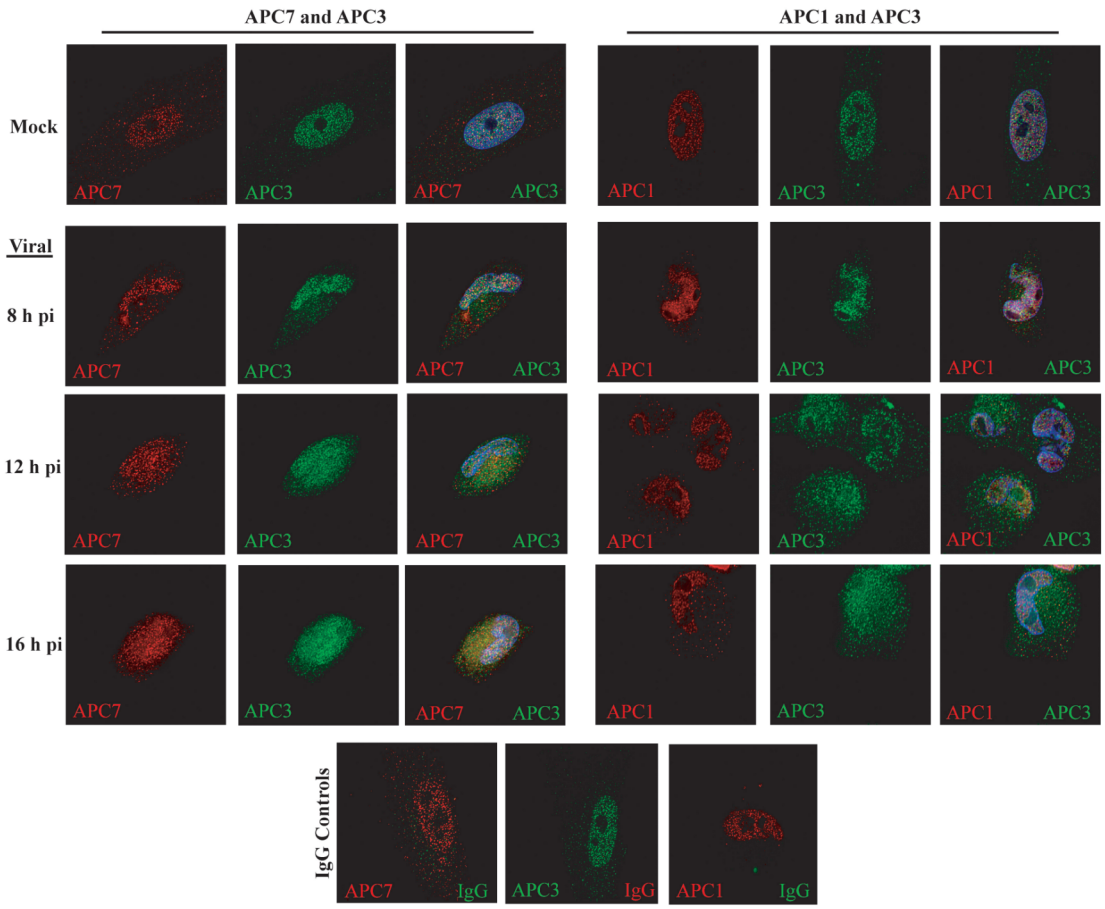

Figure 2.6 Several APC subunits are relocalized to the cytoplasm of HCMV infected cells. Mock or HCMV-infected HFFs at 8, 12 and 16 h p.i. were fixed and assayed by immunostaining for APC1, APC3, and APC7. Mouse and rabbit IgG were used as negative controls on HCMV infected cells from the 8 h p.i. time point. Samples were analyzed by deconvolution microscopy using a 100x oil immersion lens with pictures taken at 0.2 um sections along the z-axis. A midsectional plane of representative cells is presented. Images are separated to show the staining of each individual subunit; merged images are also shown with Hoescht staining in blue.

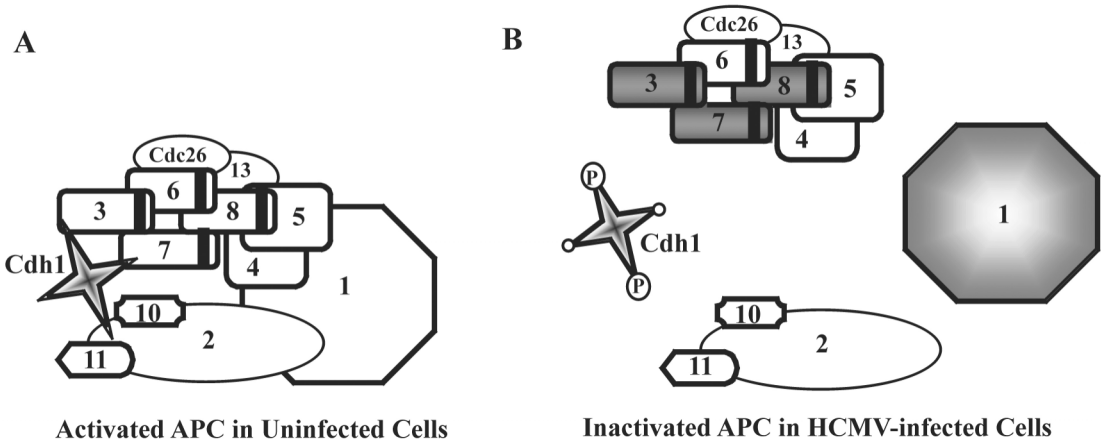

Figure 2.7 The APC is inactivated through multiple mechanisms upon HCMV infection. A) Schematic diagram of activated APC. Subunits are numbered accordingly. Unphosphorylated Cdh1 associates with and activates the complex, allowing ubiquitination of the recruited substrate in concert with E1 and E2 ubiquitination enzymes. The relative location of the subunits is based on the model presented by Thornton et al. (38). **B)** Model of APC upon HCMV infection. Cdh1 is phosphorylated (P) and no longer associates with the complex. APC1 becomes dissociated from the complex. It is unclear whether the other subunits remain in complex together other than APC3, APC7, and APC8 (shaded).

CHAPTER 3

INACTIVATION OF THE ANAPHASE-PROMOTING COMPLEX DURING HCMV INFECTION IS CAUSED BY THE DEGRADATION OF THE APC5 AND APC4 SUBUNITS INDEPENDENT OF THE VIRAL-MEDIATED PHOSPHORYLATION OF CDH1

ABSTRACT

We had previously identified multiple mechanisms by which the anaphase-promoting complex (APC) is disabled during human cytomegalovirus (HCMV) infection (152). Namely, the co-activator, Cdh1, is phosphorylated during the infection and can no longer bind to and activate the APC, while the APC core complex also dissociates. In the present study, the primary mechanism by which APC inactivation occurs is further delineated. UL97 is identified as the viral kinase responsible for phosphorylating Cdh1 during the infection; however, studies using a UL97 deletion virus still showed APC dissociation occurring with similar kinetics as with wild type virus, suggesting that the phosphorylation of Cdh1 is independent of the complex dissociation. The dissociation of the complex is further determined to be due to the loss of the APC5 and APC4 subunits that occurs early in the infection and is dependent on viral early gene expression.

INTRODUCTION

Human cytomegalovirus (HCMV), a highly prevalent ß-herpesvirus, can cause serious birth defects and disease in immunocompromised individuals, and it may be associated with cancer and cardiovascular disease (101). The virus has adopted different strategies in altering the cellular environment to be more conducive for a productive infection, including the stimulation of the host's DNA replication pathways, cell cycle deregulation and arrest, immune evasion, and inhibition of apoptosis. Infection of quiescent cells induces passage of the cells toward S phase such that the cellular DNA replication machinery can then be used for viral DNA replication, while host DNA synthesis is inhibited as the cell cycle is arrested in G_1/S. The Rb family pocket proteins become phosphorylated and accumulate, cyclins E and B and their associated kinase activities are upregulated, while that of cyclin A is inhibited, and p53 is stabilized (35, 61, 96, 102, 130).

Proper cell cycle regulation is partly governed by the APC (Anaphase-Promoting Complex), an E3 ubiquitin ligase that targets the timely degradation of various cell cycle regulators and mitotic cyclins in mediating cycle progression from mitosis through G_1 to S ((113, 155)). The APC is a large multi-subunit complex containing 11–13 subunits. The APC2, APC11, and APC10 subunits form the catalytic core. Each of the APC3, APC8, APC6, and APC7 subunits contain multiple copies of the tetratricopeptide repeat (TPR) motif and together make up the TPR subcomplex, which provides a platform of various protein interaction surfaces including the binding

to the co-activators Cdh1 (through APC3) and Cdc20. These two subcomplexes are bridged by the large scaffolding subunit APC1, with the TPR subcomplex tethered by APC4 and APC5. The binding between APC1, APC4, APC5, and APC8 is also interdependent such that the loss of one subunit decreases the association of the other three. The abnormal accumulation of APC substrates (e.g. cyclin B, Cdc6, and geminin) early during HCMV infection led to the hypothesis that APC activity is downregulated during the infection (7, 131, 164, 167). We have subsequently reported that this inactivation is mediated through multiple mechanisms (152). Cdh1, the co-activator of the APC responsible for regulating APC activity from mitotic exit through G_1, becomes phosphorylated during the infection in a CDK-independent manner and no longer binds to the complex through APC3. Importantly, we also showed that the APC core complex dissociates during the infection, with the TPR subunits (i.e. APC3, APC7, APC8) and APC10 becoming more cytoplasmic while the APC1 remains nuclear. Interestingly, both the phosphorylation of Cdh1 and the dissociation of the APC occurred with similar kinetics. Although either of these mechanisms can render the APC inactive, it was unclear whether these events are linked or represent independent (or redundant) pathways.

I have continued our studies of the mechanism(s) leading to HCMV-mediated inactivation of the APC and the potential viral components that may be involved. A likely candidate is the viral protein kinase UL97. Conserved among herpesviruses, UL97 functions in replication of the viral genome (6, 92, 170), regulating cellular factors involved in transcription and translation (2), and in nuclear egress of viral

capsids (75). Although best known for its ability to phosphorylate nucleoside analogs (i.e. ganciclovir) (143), recent studies have further characterized it as a CDK mimic, with structural similarity to Cdk2 (95) and common substrates. UL97 has been shown to phosphorylate nuclear lamin A/C in vitro on sites targeted by Cdc2/Cdk1 (44), the carboxyl-terminal domain of RNA polymerase II (2), the translation elongation factor 1δ (70), and Rb (56, 118). Given that cyclin A-Cdk2 and cyclin B1-Cdk1 complexes normally phosphorylate Cdh1 in regulating its activity and preventing its association with the APC, it was hypothesized that UL97 is involved in the phosphorylation of Cdh1 during HCMV infection.

In accord with this hypothesis, the experiments presented in this report indicate that Cdh1 phosphorylation is mediated by UL97 during the infection. The mechanism leading to the dissociation of the APC core complex is further determined to be due to the loss of the APC5 and APC4 subunits. Importantly, studies using a UL97 deletion virus still show dissociation of the APC with similar kinetics as in a wild type virus infection, suggesting that these are two independent mechanisms. Although UL97-mediated phosphorylation of Cdh1 may provide a small kinetic advantage in inactivating the APC slightly faster, the primary mechanism of inactivation appears to be the dissociation of the complex mediated by the targeted degradation of APC5 and APC4.

MATERIALS AND METHODS

Cells and Virus. Human foreskin fibroblasts (HFFs), obtained from the University of California, San Diego, Medical Center, were cultured in minimum essential medium with Earle's salts supplemented with 10% heat-inactivated fetal bovine serum, 1.5 μg/ml amphotericin B, 2 mM L-glutamine, 200 U/ml penicillin, and 200 μg/ml streptomycin. All cell culture media were from Gibco-BRL. Cells were kept in incubators maintained at 37°C and 7% CO_2. The Towne and AD169 strains of HCMV were obtained from the American Type Culture Collection and propagated as previously described (144). The UL97 deletion virus RCΔ97.08 (ΔUL97) was a generous gift from Dr. Mark Prichard (117).

Infections and Drug Treatments. Experiments were done under G_0 synchronization conditions unless otherwise noted. Cells were trypsinized 3 days after the monolayer reached confluency and either infected with virus at the indicated multiplicity of infection (MOI) or mock infected with tissue culture supernatants as described (130). The cells were then replated at a lower density to induce cell cycle progression. For the confluent culture infections, virus or mock tissue culture supernatants were added to the monolayer three days after reaching confluency. Infections with the ΔUL97 virus were done at MOI 3 with AD169 as the wild-type control. UV-inactivated virus was prepared by subjecting virus or mock tissue culture supernatants to UV irradiation via a Stratalinker UV Crosslinker (Stratagene). HFFs were infected at an MOI 2 equivalent and sodium pyruvate was added to a final

concentration of 5 mM to scavenge free radicals. The absence of viral IE or early gene expression was confirmed by Western blot analysis.

For proteasome inhibition assays, mock or Towne-infected HFFs (MOI 2) were treated with DMSO (vehicle control), 2.5 μM MG132 (Calbiochem), or 100 nM salinosporamide A (Sal A; gift from B. Moore) at the times indicated and harvested at the end of treatment. Similarly, 20 μM actinomycin D (ActD; Calbiochem) or 100 μg/ml cyclohexamide (CHX; Sigma) were added at the time of infection or as indicated for viral gene expression assays. For the inhibitor release experiments, cell cultures were rinsed twice in PBS and then recovered in fresh media.

Western Blot Analysis. Cells were lysed in Laemmli reducing sample buffer (62.5 mM Tris pH 6.8, 2% SDS, 10% glycerol, 5% β-mercaptoethanol) supplemented with a protease inhibitor cocktail (Roche) and phosphatase inhibitors (50 mM sodium fluoride, 10 mM β-glycerophosphate, 1 mM sodium orthovanadate), sonicated, and boiled. Equal amounts of lysate (i.e. by cell number) were run on SDS-polyacrylamide gels unless otherwise stated. Following electrophoresis, proteins were transferred to nitrocellulose (Schleicher & Schuell), and Western blot analyses were performed using appropriate antibodies. The Supersignal West pico and West femto chemiluminescent detection methods (Pierce) were used to visualize the proteins according to the manufacturer's instructions.

Phosphatase Assay. Cell lysates were prepared in buffer A (50 mM Tris-HCl pH 7.5, 10 mM KCl, 1 mM $MgCl_2$, 10% glycerol, 300 mM NaCl, 0.1% NP-40,

protease inhibitor cocktail) or buffer B (buffer A plus phosphatase inhibitors: 50 mM sodium fluoride, 1 mM sodium orthovanadate, 10 mM β-glycerophosphate) as previously described (152) with protein concentrations determined by Bradford assay (Biorad). Lysates were incubated with 1 X λ-phosphatase buffer (New England Biolabs), 2 mM $MnCl_2$ and λ-phosphatase (New England Biolabs) at 5 units/ug protein for 30 min at 30°C. Reactions were terminated with addition of 2X Laemmli reducing sample buffer. Samples were then boiled and analyzed by Western blot.

Immunoprecipitation. Cells were harvested and lysed directly in extraction buffer (20 mM Tris-HCl pH 8, 150 mM NaCl, 5 mM $MgCl_2$, 0.2% NP40, 10% glycerol; supplemented with 1X protease inhibitor cocktail, 50 mM sodium fluoride, 10 mM β-glycerophosphate, 1 mM ATP, and 1 mM DTT) using an end-over-end rotator at 4º. Lysates were clarified by centrifugation at 16,000 x g. For APC3 co-immunoprecipitation (co-IP) assays, lysates were incubated with Protein G PLUS-Agarose beads (Santa Cruz Biotechnology) coupled with an anti-APC3 monoclonal antibody (AF3.1, Santa Cruz Biotechnology) or with beads coupled with mouse immunoglobulin (IgG) (Jackson ImmunoResearch) as a negative control. Beads were washed with TBS-T pH 8 (0.01% Tween-20, supplemented with protease and phosphatase inhibitors and 1 mM ATP) and proteins were eluted in Laemmli reducing sample buffer by boiling for 5 min. All IP steps were performed at 4ºC. Pre and post-IP (PIP) samples were also collected and boiled in reducing sample buffer. Samples were analyzed by Western blot with same cell equivalents loaded for Pre and PIP lanes, while IP lanes were loaded with 5 times more.

Quantitative RT-PCR. Total RNA from mock or HCMV-infected cells was isolated using a NucleoSpin RNA II prep kit (Machery-Nagel). Eluates were subjected to a second DNase treatment using TURBO DNA-*free*™ DNase (Ambion) to ensure complete DNA removal. RNA concentrations were determined by UV spectrophotometry. Quantitative RT-PCR (qRT-PCR) was performed with the ABI Prism 7000 sequence detection system (Applied Biosystems) using the TaqMan One-Step RT-PCR Master Mix Reagents kit (Applied Biosystems) with 50 ng RNA, oligonucleotide primers and TaqMan dual-labeled (5' 6-carboxyfluorescein, 3' black hole quencher-1) probes (Integrated DNA Technologies). Standard curves were generated using RNA isolated from cells harvested at 24 h p.i. Values were normalized to G6PD as a control for input RNA. The primers and probes used were as follows: APC4 forward (5'- ATTCTCGTCCTTGGAGGAAGCTCT -3'), APC4 reverse (5'- TTCTGGCCATCCGAGTTACTTCAG -3'), APC4 probe (5'-AATTGCTCGAGTCACAGGGATTGCTGGT -3'); APC5 forward (5'-GTGCCATGTTCTTAGTGGCCAAGT -3'), APC5 reverse (5'-GATGCGCTCTTTGCAGTCAACCTT -3), APC5 probe (5'-AAGAAAGCAGAAGCTCTGGAGGCTGCCA -3'); G6PD forward (5'-TCTACCGCATCGACCACTACC -3'), G6PD reverse (5'-GCGATGTTGTCCCGGTTC -3'), G6PD probe (5' ATGGTGCTGAGATTTGCCAACAGGA -3')

Antibodies. Antibodies to HCMV proteins IE1/IE2 (CH16.0), UL57, UL44, and UL99 were from Virusys. Other antibodies used include: Cdh1 (Ab-2, Calbiochem); geminin (Santa Cruz Biotechnology; Rb (Ab-1, IF8) and cdc6 (Ab-1, DCS-180) from LabVision Thermo Scientific; APC4 (A301-176A), APC5 (A301-026A), and APC6 (A301-165A) from Bethyl Laboratories; APC7 (poly6113) and APC8 (poly6114) from Biolegend; APC1 (gift from Dr. Michael Green); actin (AC-15, Sigma); and GAPDH (6c5, Fitzgerald).

RESULTS

Phosphorylation of Cdh1 during HCMV infection is UL97-dependent. We had previously shown that Cdh1 becomes phosphorylated during HCMV infection, beginning 8 to 12 h p.i. and that this phosphorylation still occurs in the presence of the CDK inhibitor roscovitine (152). Based on recent studies characterizing the HCMV early protein kinase UL97 as a CDK mimic and involved in the hyperphosphorylation of Rb during the infection (56, 118), it emerged as the leading viral candidate involved in the phosphorylation of Cdh1.

A UL97 deletion virus was utilized in testing this hypothesis. The UL97 deletion virus RCΔ97.08 (ΔUL97) has over 70% of its ORF deleted, including homologous subdomains to other protein kinases, and replaced by selectable genetic markers *gpt* and *lacZ* (117). Replication of the virus in primary fibroblasts is impaired with 2 to 3-fold lower titers (117). While an early replication defect reduces DNA accumulation by 4 to 6-fold, a late capsid maturation defect appears to be primarily responsible for the decrease in viral titer (170). Expression kinetics of viral genes and various cell cycle regulators were first analyzed by Western blot and qRT-PCR in comparison to wild type virus AD169 during an infection time course. Confluent G_0-synchronized cells were trypsinized and replated at a lower density to induce cell cycle progression. Cells were infected with virus at the time of replating and harvested at various times p.i. In accord with previous studies by Prichard et al (117), viral gene expression in the ΔUL97 infection is slightly delayed compared to wild type infection (Figure 3.1A). While no change is observed in IE expression, both early proteins

UL44 and UL57 as well as the late protein UL99 are expressed at lower levels at 48 h p.i. compared to wild type, but recover by 72 h p.i. Geminin levels were also assessed to determine whether the protein is stabilized during the ΔUL97 infection as in indication of APC activity. While geminin accumulated to levels comparable to those in the AD169 cells by 48 h p.i., it was difficult to determine whether the modest accumulation observed in the ΔUL97 infected cells at 16 and 24 h p.i. was due to stabilization or normal cell cycle progression as indicated by the mock-infected cells at 24 h p.i.

To help mitigate induced protein expression due to normal cell cycle progression, infections were done in G_0-synchronized cells maintained at confluency through the course of the infection. Cells were harvested at various times p.i. and protein expression was analyzed by Western blot (Figure 3.1B). The kinetics of viral gene expression was similar to those observed with the G_0 release infection (Figure 3.1A) as indicated by IE2, IE1, UL57, and UL44 expression. Various other cell cycle proteins that are alo APC substrates (i.e. Cdh1, cyclin B, Cdc6, and securin) were analyzed along with geminin. In general, the cell cycle proteins remained at low or undetectable levels through the time course in the mock-infected cells as expected. Increased protein expression of the different APC substrates was observed in the ΔUL97-infected cells compared to mock, albeit with a slight delay or at slightly lower levels compared to AD169. These results indicate that cell cycle deregulation still occurs in the ΔUL97 infection and that the APC may still be inactivated.

Although the increase in Cdh1 expression was slightly delayed compared to the wild type infection, it was interesting to note that the migration pattern remained

comparable to that observed in the mock-infected samples through the time course, while Cdh1 in the wild type virus infected cells migrated slightly slower, suggesting that Cdh1 may not be modified in the ΔUL97 infection. Phosphatase assays were used to verify whether Cdh1 is phosphorylated during the ΔUL97 infection. HFFs infected with ΔUL97, AD169, or mock-infected were harvested at 16 h p.i. and treated with lambda protein phosphatase (λpp) (Figure 3.1C). While phosphatase treatment shifted the migration pattern of Cdh1 from the AD169 infected cells to a faster migrating form comparable to that seen in the uninfected cells, no change was observed in the ΔUL97 infection sample after phosphatase treatment, suggesting that Cdh1 is not phosphorylated. Given that the progression of the ΔUL97 infection is slightly delayed, samples were also checked at late times during the infection time course but no differences were seen (data not shown). Rb is shown as a positive control for the phosphatase assay and actin as a loading and negative control. Although Rb would not be phosphorylated by UL97 in the deletion virus infection, it would still be subject to CDK phosphorylation.

To confirm whether Cdh1 is a direct substrate of UL97, in vitro kinase assays were performed using purified Cdh1 and GST-UL97 by Jeremy Kamil in collaboration with Don Coen's laboratory. Initial results point toward Cdh1 as being a direct substrate of UL97.

APC dissociation during HCMV infection is independent of UL97-mediated phosphorylation of Cdh1. Since the viral mediated phosphorylation of Cdh1 is prevented in the ΔUL97 infection, we next determined whether Cdh1 is still able to bind and activate the APC. APC3 co-IP assays were done with mock, ΔUL97,

or AD169 infected HFFs at 8, 16, and 24 h p.i. As shown in Figure 3.2, the APC subunits APC7, APC8, and APC1 as well as Cdh1 remained in complex with APC3 in the mock and virus infected samples. By 16 h p.i., however, APC1 is dissociated from APC3 in the ΔUL97 sample, similar to the wild-type infection. Cdh1 association with APC3 was also severely diminished in the ΔUL97 sample by 16 h p.i., as in the wild type infection, and was no longer detected at 24 h p.i. Although the phosphatase assays indicated that Cdh1 is not phosphorylated at that time, it was still unable to bind to the APC as the dissociation of the complex was still occurring. As a complement to the co-IP experiments, we also performed localization studies of the APC subunits by IFA. Similar to the wild type virus, the TPR subunits APC3, APC7, and APC8 showed a more cytoplasmic distribution as the ΔUL97 infection progressed, while APC1 remained nuclear (data not shown). Although Cdh1 phosphorylation by UL97 could potentially account for the lack of binding to the APC and resulting inactivation of the APC, the dissociation of the complex still occurs in the ΔUL97 infection with the same kinetics as the wild type infection and appears to be independent of the viral-mediated phosphorylation of Cdh1.

APC4 and APC5 protein expression are decreased during HCMV infection. To further delineate the mechanism behind the dissociation of the APC, we reexamined the structure of the core complex. Our studies in both wild type and the ΔUL97 viruses have consistently shown the separation of the TPR subcomplex (i.e. APC3, APC7, and APC8) from APC1. As previous structural studies of the APC have reported (149), the TPR subcomplex (via APC8) is associated to APC1 via APC4 and APC5. Moreover, the association between APC1, APC4, APC5, and APC8 is

interconnected such that each subunit is necessary for the others to bind effectively. Thus, APC4 and APC5 might also be targets in the disrupted association between the TPR subunits and APC1 during the infection.

We had previously reported that all APC subunits tested exhibited stable protein expression through the infection time course (152); however, we were unable to confirm the expression of APC4, APC5, and APC6 at the time. We have now reexamined APC4, APC5, and APC6 protein expression using alternative antibodies over an infection time course in mock and AD169 infected cells. Interestingly, both APC4 and APC5 expression were significantly lower in the virus-infected samples by 8–10 h p.i. and remained at or below the limits of detection through the end of the time course, whereas no significant differences were observed for APC6 (Figure 3.3A). The expression pattern is also observed with Towne and the ΔUL97 deletion virus infections.

To discriminate between a defect at the protein or transcriptional level, total RNA from mock or HCMV infected cells was isolated over an infection time course and analyzed by qRT-PCR with primers and probe to APC4 and APC5. Values were normalized to G6PD, which served as an internal control for RNA input, and expressed as the fold induction from 0 h p.i. No significant changes in either APC5 or APC4 expression levels were observed from the time of infection for both mock and virus infected samples through the time course (Figure 3.3B), indicating that the decrease in expression is likely due to a destabilization at the protein level or a translational defect.

Proteasome inhibitors were used to address whether APC4 and APC5 are targeted for degradation during the infection. HFFs infected with Towne at an MOI of 2 or mock infected were treated with either the reversible proteasome inhibitor MG132 (2.5 μM) or irreversible inhibitor Sal A (100 nM) from 6–12 h p.i. Cells were harvested at the end of treatment or the drug was washed out with the cells cultured in fresh media for an additional 12 h before harvesting. As shown in Figure 3.4, addition of either proteasome inhibitor from 6–12 h p.i. prevented the loss of APC4 and APC5 expression. Degradation of both proteins continued upon washout of the MG132-treated cells, while expression levels remained stable in the Sal A treated cells as expected, further suggesting the loss of expression is proteasome-dependent. No change in APC8 expression was observed with the various treatments, indicating that this targeted degradation is specific to APC4 and APC5. p53 was analyzed as a control for proteasome inhibition and drug washout. As shown in the uninfected cells, p53 levels were stabilized with either inhibitor treatment from 6–12 h p.i. The level was reduced and comparable to that of the DMSO treated after washout of the MG132 but remained elevated in the Sal A treated cells as expected. While addition of proteasome inhibitors prevented further degradation of the APC4 and APC5 subunits, expression levels never recovered to that of the uninfected. APC4 and APC5 levels appear to be very stable and not readily turned over. Similar assays done with the E1 inhibitor PYR-41 also showed comparable results in preventing the loss of the APC subunits (data not shown), further supporting that this is a UPS-mediated event.

APC dissociation during HCMV infection is due to loss of APC 4 and APC5. If the loss of APC4 and APC5 is the root cause of the dissociation of the APC

during the infection, then preventing the degradation of the subunits may keep the complex intact. APC3 co-IP studies were done with mock or Towne infected HFFs that were treated with or without Sal A from 6–14 h p.i. Cells were harvested at 14 h p.i. and the coimmunoprecipitated proteins were analyzed by Western blot. As shown in Figure 3.5, APC3 and APC8 were equally pulled down from all the samples. No significant changes were seen with APC4, APC5, or APC1 in the IP lanes with or without inhibitor treatment in the uninfected cells. Treatment with Sal A appeared to have prevented the dissociation of the complex, as levels of APC4, APC5, and APC1 that coimmunoprecipitated with APC3 were increased compared to the untreated viral sample and only slightly lower than that observed in the uninfected samples. Some recovery of Cdh1 association with APC3 was also observed in the virus plus inhibitor treatment sample. This may be the result of the intact complex providing the necessary binding conformation for Cdh1 association, and/or UL97 expression and phosphorylation of Cdh1 may be delayed with the addition of Sal A. The remaining unassociated Cdh1 in the post-IP lane may be due to the UL97-mediated phosphorylation of Cdh1 at this point. GAPDH is further shown as a negative control. Together, these results support that the disassembly of the APC is associated with the loss of APC4 and APC5 expression.

Viral early gene expression is necessary to mediate the degradation of APC4 and APC5. Given the kinetics with which APC4 and APC5 protein are lost during the infection, the potential viral protein(s) involved are likely expressed at IE or early times of the infection or brought in with the viral tegument. To establish whether viral tegument proteins alone are sufficient, HFFs were infected with UV-inactived

virus and harvested over an infection time course, with protein expression assayed by Western blot. As shown in Figure 3.6, both APC4 and APC5 expression remained stable throughout the infection, suggesting that the viral tegument proteins themselves were insufficient to induce the expression loss. As controls, APC8 expression remained unchanged and no viral IE or UL44 expression were detected as expected. Cyclohexamide (CHX) was then used to inhibit viral early gene expression such that the requirement for IE expression could be examined. Mock or Towne infected HFFs were treated with CHX from 2–12 h p.i. and assayed for protein expression. As shown by Western blot, IE1 72 and IE2 86 were expressed but not the early protein UL44 (Figure 3.6). Again, no changes in APC subunit expression were observed, indicating that some viral early gene expression may be required.

A combination of CHX and ActD treatments were then used to further delineate the involvement of viral early gene expression in mediating the loss of APC4 and APC5 (Figure 3.7). First, mock or Towne infected HFFs were treated with CHX at the beginning of the infection from 0–6 h p.i. and then washed and released into fresh media. Cell samples were harvested at 6, 18, and 24 h p.i. This allowed for the accumulation of viral transcripts from 0–6 h p.i., which would all then be expressed upon release of the drug. If these viral transcripts were sufficient to effect the change, then a decrease in APC4 and/or APC5 expression would be expected in the cells harvested at 6 h p.i.; however, no significant changes were seen as compared to the untreated samples. Expression of both APC4 and APC5 were decreased at 18 and 24 h p.i., albeit not as significantly as in the infected cells treated with DMSO. This is likely due to the delay in viral gene expression. Alternatively, ActD was added at 6 h

p.i. to inhibit further transcription, and cells were then harvested at 18 and 24 h p.i. As evidenced by the presence of UL44, some early gene expression still occurred under these conditions. The treatment resulted in an intermediate decrease in APC4 and APC5 expression, indicating that the viral transcript(s) involved are likely expressed by 6 h p.i. To assess the effects of viral proteins expressed by 6 h p.i., CHX was added to the cells at 6 h p.i. and harvested at 18 and 24 h p.i. Again, a similar intermediate decrease in APC4 and APC5 expression levels were observed at both 18 and 24 h p.i. Taken together, these results suggest that the viral transcript(s) likely responsible for causing the degradation of APC4 and APC5 is expressed by 6 h p.i.; however, there may be insufficient amount of viral protein expressed by 6 h p.i. to efficiently target APC4 and APC5 or other viral protein(s) that are not expressed yet may also be required.

DISCUSSION

In continuing our studies into the inactivation of the APC during HCMV infection, we have further defined the mechanisms by which this occurs and have identified a key viral protein involved. As we have previously reported (175), multiple factors can be attributed to the inactivation of the APC, namely the phosphorylation of Cdh1 and the dissociation of the APC core complex. Although these two events occur with similar kinetics during the infection, we have further distinguished them to be the result of two independent mechanisms.

Increasing evidence have shown UL97 as a CDK mimic with several cellular targets, including Rb, thereby presenting itself as a likely candidate involved in the phosphorylation of Cdh1 during the infection. We have shown that Cdh1 becomes phosphorylated beginning 8–10 h p.i. during wild type HCMV infection; however, in the context of the ΔUL97 infection, Cdh1 appears to remain unphosphorylated through at least 24 h p.i., No apparent band migration shift was observed when whole cell lysates were analyzed by SDS-PAGE or after phosphatase treatment compared to wild type virus. Although minimal phosphorylations on Cdh1 could have been present that were beyond the detection sensitivity of the assay, the Cdh1 expressed from the two different viruses were noticeably different. The phosphorylation of Cdh1 by UL97 in vitro further supports Cdh1 as a direct substrate of UL97. Nevertheless, the dissociation of the APC, including Cdh1, and accumulation of APC substrates still occurred during the ΔUL97 infection with similar kinetics as in the wild type infection despite Cdh1 remaining unphosphorylated at that time and presumably still capable of

binding and activating the APC. Thus, the dissociation of the APC appears to occur through a mechanism independent of the UL97-mediated phosphorylation of Cdh1. Whether the UL97-mediated phosphorylation of Cdh1 represents a redundant pathway in ensuring the inactivation of the APC or is simply another cellular substrate of UL97 remains unclear. While the sufficiency of the UL97-mediated modification of Cdh1 in blocking its association and activation of the APC still needs to be verified, it is interesting to speculate whether the phosphorylation of Cdh1 serves another purpose in facilitating viral replication other than mediating the inactivation of the APC. The UL97-mediated phosphorylation of Cdh1 would, however, provide a small kinetic advantage in the wild type virus infection in allowing for the inactivation of the APC to occur slightly earlier and faster. Based on the time course analysis presented in Figure 3.8, the majority of the Cdh1 is dissociated in the AD169 infection by 12 h p.i. and completely dissociated by 14 h p.i., whereas some of the complex still remains intact.

The specific targeting of an individual subunit in disrupting APC activity appears to be a common strategy utilized by different viruses. Adenovirus E4orf4 targets PP2A to APC6 to inactivate the complex through dephosphorylation (73), chicken anemia virus has been shown to target APC1 through its apoptin protein (49, 148), and a recent report suggests that the PACR protein encoded by poxvirus acts as an APC11 mimic to inhibit APC activity (100). In this study, we have further shown that the dissociation of the APC during HCMV infection is mediated through the proteasome-dependent loss of APC5 protein expression, and perhaps to a lesser extent APC4 protein expression. Decreased expression of both proteins is observed

beginning at about 8 h p.i., followed by the dissociation of the APC. Addition of proteasome inhibitors prevented further loss of the subunits as well as APC dissociation. The effect of the proteasome inhibitors could be two-fold, however, in preventing the degradation of the subunits as well as inhibiting the viral infection itself and expression of viral early proteins that may be involved in targeting the APC subunits. It is unclear whether APC5 and APC4 are individually targeted or if the loss of APC4 is the result of losing APC5. The binding of APC8, APC4, APC5, and APC1 is interdependent, such that the loss of any one subunit greatly decreases the binding of the other three. While the loss of either APC5 or APC4 alone may not sufficiently dissociate the complex, the concerted loss of both subunits seems to ensure the complete untethering of the APC3/TPR subcomplex from APC1 and thereby the catalytic core containing APC2 and APC11 as well (Figure 3.8). This would account for the observed dissociation of the TPR subcomplex from APC1 during the infection.

ACKNOWLEDGEMENTS

We are grateful to Dr. Mark Prichard for the UL97 deletion virus RCΔ97.08, to Dr. Bradley Moore for the sample of Sal A, and to Jeremy Kamil and Don Coen for their help with the UL97/Cdh1 kinase assays. This work was supported by NIH grants CA73490 and CA34729 to D.H.S.

Figure 3.1 Expression of HCMV proteins and accumulation of APC substrates are slightly delayed in ΔUL97 infection compared to wild type. G_0-synchronized HFFs (by confluence) were either mock infected or infected with ΔUL97 (Δ) or AD169 (V) at an MOI of 3 after trypsinization and replating at lower densities to induce cell cycle progression, or the virus was added directly to the confluent monolayer as indicated. **A)** G_0-synchronized HFFs were released into G_1 as described in the Materials and Methods. Cells were harvested over an infection time course and analyzed by Western blot for IE2, IE1, UL57, UL44, UL99, and geminin expression. Actin is shown as a loading control. **B)** G_0-synchronized confluent monolayers were infected as described in the Materials and Methods. Cell samples were harvested at the times indicated and analyzed by Western blot for IE2, IE1, UL57, UL44, Cdh1, Cyclin B, Cdc6, geminin, and securin. Actin is shown as a loading control. **C)** HFFs were infected as cells were released into G_1 and harvested at 16 h p.i. Lysates were treated with or without lambda protein phosphatase (λpp) and analyzed by Western blot. Rb is shown as a positive control for the phosphatase assay, while actin is shown as a loading and negative control.

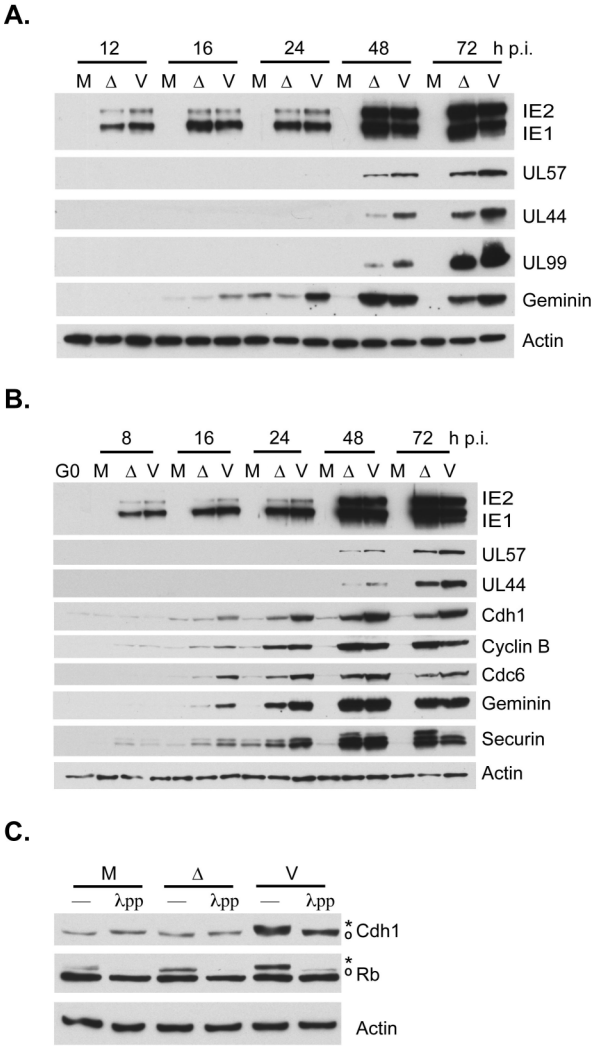
A.
12
16
24
48
72 h p.i.
M Δ V M Δ V M Δ V M Δ V M Δ V
IE2
IE1
UL57
UL44
UL99
Geminin
Actin
B.
8
16
24
48
72 h p.i.
G0 M Δ V M Δ V M Δ V M Δ V M Δ V
IE2
IE1
UL57
UL44
Cdh1
Cyclin B
Cdc6
Geminin
Securin
Actin
C.
M
Δ
V
— λpp — λpp — λpp
Cdh1
Rb
Actin

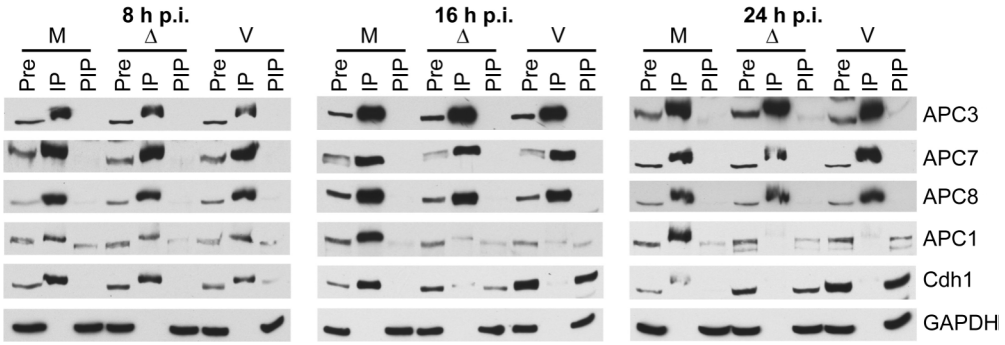

Figure 3.2 APC still dissociates with similar kinetics during ΔUL97 infection as wild-type virus. HFFs infected with ΔUL97 (Δ) or AD169 (V) at MOI 3 or mock-infected (M) were harvested at the times indicated. The APC was immunoprecipitated using an anti-APC3 antibody and coimmunoprecipitated proteins were assayed by Western blot with antibodies to APC3, APC8, APC4, APC5, APC1, and Cdh1. GAPDH is shown as a negative and loading control.

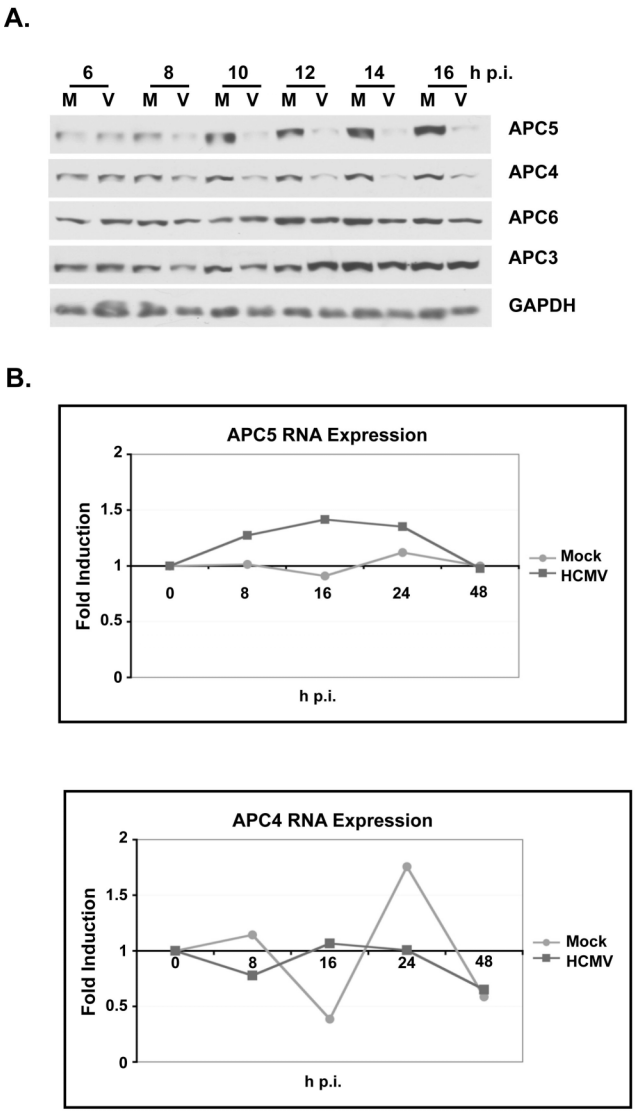

Figure 3.3 Loss of APC4 and APC5 protein expression during HCMV infection. **A)** APC5, APC4, APC6, and APC3 protein expression in mock (M) or HCMV-Towne (V) infected cells were assessed by Western blot. GAPDH is shown as a loading control. **B)** Total RNA was isolated from mock or HCMV-Towne infected cells and analyzed for APC4, APC5, and G6PD expression by qRT-PCR. APC4 and APC5 values were normalized to that of G6PD as a control for input RNA. Values are expressed as the fold induction over 0 h p.i.

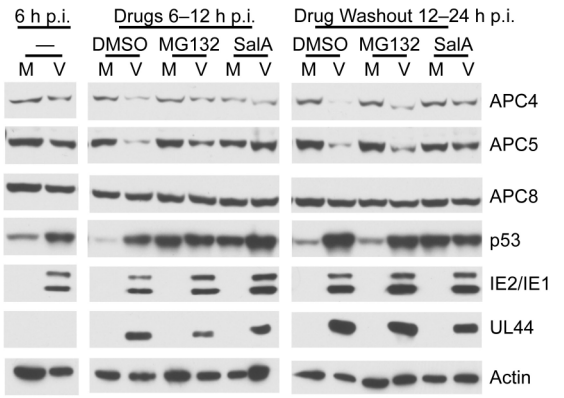

Figure 3.4 APC4 and APC5 are degraded by the proteasome during HCMV infection. HFFs infected with Towne (MOI 2) or mock infected were treated with proteasome inhibitors MG132 (2.5 μM, reversible) or Sal A (100 nM, irreversible) at 6 h p.i. Cells were harvested at 12 h p.i. or recovered in fresh media without drug and harvested at 24 h p.i. Samples were processed by Western blot for protein expression.

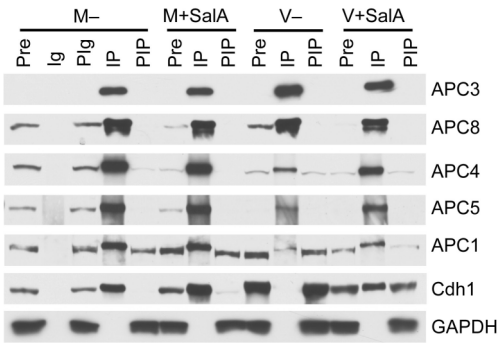

Figure 3.5 APC dissociation is prevented with proteasome inhibitors. Mock (M) or HCMV-infected HFFs (MOI 2) were treated with or without Sal A (100 nM) from 6–14 h p.i. Cells were harvested at 14 h p.i. and the APC immunoprecipitated as previously described. Presence of other APC subunits and Cdh1 were checked by Western blot. GAPDH is shown as a negative and loading control.

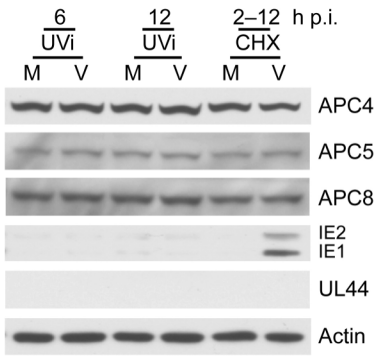

Figure 3.6 Viral tegument and immediate early protein expression is insufficient to cause the loss of APC4 and APC5 protein expression. HFFs were treated with UV-irradiated (UVi) mock (M) or viral (V) supernatants and harvested at 6 and 12 h p.i. To assess the requirement for IE expression, HFFs were infected with HCMV-Towne (MOI 2) and treated with 100 ug/ml CHX to prevent early gene expression. Samples were analyzed by Western blot.

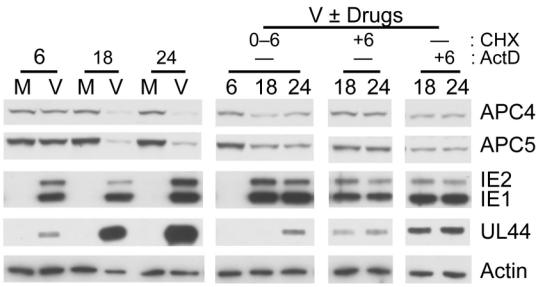

Figure 3.7 Viral early gene expression is required to mediate the degradation of APC4 and APC5. Mock (M) or virus (V) infected HFFs (MOI 2) were treated with CHX (100 ug/ml) from 0–6 h p.i. and harvested at 6 h p.i. or washed and released into fresh media and harvested at 18 and 24 h p.i. CHX or ActD (20 μM) was added at 6 h p.i. and harvested at 18 and 24 h pi.i. Lysates were analyzed by Western blot for APC4, APC5, IE, and UL44 expression. Actin is shown as a loading control.

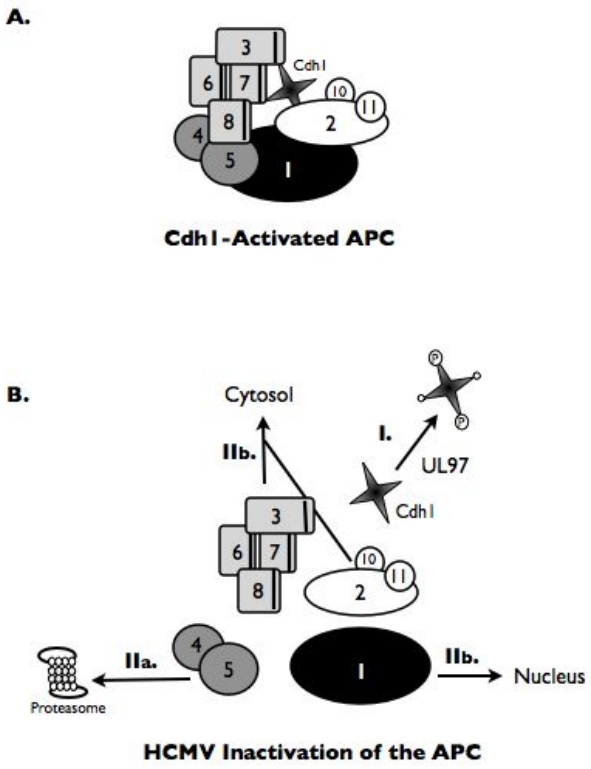

Figure 3.8 HCMV inactivation of the APC. A) Schematic diagram of Cdh1-activated APC. The essential APC core subunits are shown and numbered accordingly. **B)** Model illustrating the mechanisms by which the APC is disabled during HCMV infection. (I) Cdh1 is phosphorylated, mediated by UL97, and no longer associates with the complex. (IIa) APC5 and APC4 are targeted for degradation by the proteasome. (IIb) The loss of APC5 and APC4 causes the remaining subunits to dissociate, with the TPR subunits and APC10 localizing to the cytosol while APC1 remains nuclear.

CHAPTER 4

PROTEASOME SUBUNITS RELOCALIZE DURING HUMAN CYTOMEGALOVIRUS INFECTION AND PROTEASOME ACTIVITY IS NECESSARY FOR EFFICIENT VIRAL GENE TRANSCRIPTION AND DNA REPLICATION

ABSTRACT

We have continued studies to further understand the role of the ubiquitin-proteasome system (UPS) in human cytomegalovirus (HCMV) infection. With specific inhibitors of the proteasome, we show that ongoing proteasome activity is necessary for facilitating the various stages of the infection. IE2 expression is modestly reduced with addition of proteasome inhibitors at the onset of infection; however, both early and late gene expression are significantly delayed, even if the inhibitor is removed at 12 hours post infection. Adding the inhibitor at later times during the infection blocks the further accumulation of viral early and late gene products, the severity of which is dependent on when the proteasome is inhibited. This can be attributed primarily to a block in viral RNA transcription, although DNA synthesis is also partially inhibited. Proteasome activity and expression increase as the infection progresses, and this coincides with the relocalization of active proteasomes to the rim of the viral DNA replication center, which is the likely site of viral transcription. Interestingly, one 19S subunit, Rpn2, is specifically recruited into the

viral DNA replication center. The relocalization of the subunits requires viral DNA replication, but their maintenance around or within the replication center is not dependent on continued viral DNA synthesis or the proteolytic activity of the proteasome. These studies highlight the importance of the UPS at all stages of the HCMV infection and support further studies into this pathway as a potential antiviral target.

INTRODUCTION

The fundamental role of the ubiquitin-proteasome system (UPS), not only in general proteolysis but also in the regulation of several different cellular systems, has gained increasing attention in recent years. These processes include cell cycle regulation, signal transduction, apoptosis, and antigen presentation, among others (27) (33). Numerous studies have also linked the UPS to transcription regulation, DNA repair, and chromatin remodeling, at both a proteolytic and non-proteolytic level (24, 32, 72, 79, 99, 126). Thus, its potential role in disease pathogenesis has also been an area of great interest. Different viral strategies have evolved that either utilize or subvert the UPS in facilitating a productive infection (5, 8, 38, 138). Among these is human cytomegalovirus (HCMV), which is a ß-herpesvirus endemic within the human population that can cause serious disease in immunocompromised individuals and is also the leading infectious cause of birth defects.

In brief, the UPS utilizes a highly regulated process in which the proteasome selectively degrades proteins that have become ubiquitinated through a multi-step mechanism involving E1 (ubiquitin activating enzyme), E2 (ubiquitin conjugating enzyme), and E3 (ubiquitin ligase) enzymes (40). The mammalian 26S proteasome usually comprises one or two 19S regulatory subcomplexes on either end of the 20S catalytic core complex (115). The 19S is further subdivided into the base and lid. The base is composed of 6 AAA (ATPases associated with different cellular activities)

ATPase subunits (i.e. Rpt1–6), forming a hexameric base ring, plus 3 non-ATPase subunits (i.e. Rpn1, Rpn2, and Rpn10/S5a). The ATPase subunits are also collectively known as the APIS (AAA proteins independent of the 20S). The 19S lid is composed of nine non-ATPases (i.e. Rpn3, Rpn5, Rpn6, Rpn7, Rpn8, Rpn9, Rpn11, Rpn12, and Rpn15). Regulatory functions of the 19S include: polyubiquitin recognition, substrate binding, facilitation of deubiquitination, protein unfolding and translocation into the 20S for degradation (3). The 20S catalytic core is formed by four stacked rings of α (1–7), β (1–7), β (1–7), and α (121) subunits, and primarily functions in protein degradation via the catalytic ß1, ß2, and ß5 subunits, which contain caspase-like, trypsin-like, and chymotrypsin-like peptidase activities, respectively. The ß1, ß2, and ß5 subunits can also be substituted by the ß1i, ß2i, and ß5i subunits to form the immunoproteasomes upon interferon-γ stimulation. Other than the 19S, several non-ATPase complexes (i.e. PA28/11S REG, and Blm10/PA200,) can associate with the 20S and differentially alter its activity (124). Since these complexes do not bind polyubiquitin chains, they likely regulate ubiquitin-independent proteolytic activity.

One of the first indications that HCMV exploits the UPS was the discovery that the virus expresses two proteins, US2 and US11, that facilitate evasion of host immune surveillance by relocalizing MHC class I molecules from the endoplasmic reticulum to the cytoplasm for proteasome-mediated degradation (for review, see (151). Subsequently it was found that the input viral tegument protein pp71 interacts with ND10-associated Daxx and promotes its ubiquitin-independent and proteasome-mediated degradation, thus facilitating viral transcription (16, 55, 57, 60, 93, 129).

pp71 can also induce ubiquitin-independent proteasome-mediated degradation of unphosphorylated Rb, p107, and p130 (65, 66). HCMV has also been shown to inhibit the degradation of several cell cycle proteins by inactivating the anaphase-promoting complex, an E3 ubiquitin ligase (7, 152, 164, 167). In general, inhibition of the proteasome appears to impact negatively on viral replication (119, 128) (69). Productive viral infection requires that cells be infected in G_0/G_1 phase of the cell cycle. We previously showed that if cells are infected in S phase, there is no viral IE gene expression until cells return to G_1. Interestingly, this block to IE gene expression could be relieved by addition of a proteasome inhibitor (34).

We have continued our studies on the interplay between HCMV and the UPS, further delineating the molecular mechanisms involved in the suppression of HCMV replication by proteasome inhibitors. Viral early and late protein expression is greatly reduced upon proteasome inhibitor treatment. This appears to be due primarily to a defect in continued viral gene transcription as well as a decrease in viral DNA synthesis, both of which are facilitated by the early replication proteins. Not only is proteasome activity required for efficient viral gene expression, but the levels and activity of the proteasome also increase during the course of infection, correlating with times of viral early and late gene expression. By immunofluorescence assays (82), specific 19S subunits appear to be recruited to sites of viral replication. Interestingly, the 19S non-ATPase subunit Rpn2 accumulates in the viral DNA replication centers, whereas the other proteasome subunits analyzed are relocalized at the rim of the replication centers, where there is active RNA transcription.

MATERIALS AND METHODS

Cells and Virus. Human foreskin fibroblasts (HFFs), obtained from the University of California, San Diego, Medical Center, were cultured in minimum essential medium with Earle's salts supplemented with 10% heat-inactivated fetal bovine serum, 1.5 μg/ml amphotericin B, 2 mM L-glutamine, 200 U/ml penicillin, and 200 μg/ml streptomycin. All cell culture media were from Gibco-BRL. Cells were kept in incubators maintained at 37°C and 7% CO_2. The Towne strain of HCMV was obtained from the American Type Culture Collection (VR 977) and propagated as previously described (144).

Cell Synchronization and Infection. All experiments were performed under G_0 synchronization conditions (130). Cells were trypsinized 3 days after the monolayer reached confluency and then replated at a lower density to induce cell cycle progression. At the time of replating, cells were either infected with HCMV at the indicated multiplicity of infection (MOI) or mock infected with tissue culture supernatants as previously described (130). For proteasome inhibition assays, cell cultures were incubated with 2.5 μM MG132, 10 μM lactacystin, 100 nM salinosporamide A (Sal A), or DMSO as the vehicle control at the times indicated. MG132 and lactacystin were obtained from Calbiochem, while Sal A was a gift from Dr. Bradley Moore (Scripps Institute of Oceanography, University of California San Diego). The viral DNA inhibitors ganciclovir (GCV) and phosphonoacetic acid (PAA)

were obtained from Sigma and used at 20 μM and 360 μM, respectively. Cells were harvested at the indicated times post infection (p.i.) and processed as described for each experiment. All experiments were performed at least twice.

Western Blot Analysis. Cells were lysed in Laemmli reducing sample buffer (62.5 mM Tris pH 6.8, 2% SDS, 10% glycerol, 5% β-mercaptoethanol) supplemented with a protease inhibitor cocktail (Roche) and phosphatase inhibitors (50 mM sodium fluoride, 10 mM β-glycerophosphate, and 1 mM sodium orthovanadate), and the lysates were sonicated and boiled. Equal amounts of lysate (i.e. by cell number) were loaded onto SDS-polyacrylamide gels (SDS-PAGE) unless otherwise stated. Following electrophoresis, proteins were transferred to nitrocellulose (Schleicher & Schuell), and Western blot analyses were performed using appropriate antibodies. The Supersignal West pico and West femto chemiluminescent detection methods (Pierce) were used to visualize the proteins according to the manufacturer's instructions.

Quantitative real-time PCR. DNA from mock or HCMV-infected cells was isolated using a DNA Blood Mini Kit (Qiagen), and the concentration was determined by UV spectrophotometry. Quantitative real-time PCR (qPCR) was performed with the ABI Prism 7000 sequence detection system (Applied Biosystems) using TaqMan Universal PCR Master Mix (Applied Biosystems) along with oligonucleotide primers and TaqMan dual-labeled (5' 6-carboxyfluorescein, 3' black hole quencher-1) probes (Integrated DNA Technologies) with 40 ng DNA per reaction. Probes were targeted to an unspliced region of HCMV UL77, IE2 (UL122), and the GAPDH promoter, which was used for normalization of input DNA, as previously described (163). Standard

curves were generated using DNA isolated from cells harvested at 48 h p.i. The primers and probes used were as follows: UL77 forward (5'-CGTTGCCCGGGAACG-3'), UL77 reverse (5'-GGTGTGAAAGCGGATAAAGGG-3'), and UL77 probe (5'-ACCTAGCTACTTTGGAATCACGCAGAACGA-3'); IE2 forward (5'-GCG CAA TAT CAT GAA CGA-3'), IE2 reverse (5'-GAT TGG TGT TGC GGA ACA TG-3'), and IE2 probe (5'-TCG GCG GGG TCGC-3'); GAPDH promoter forward (5'-TTT CAT CCA AGC GTG TAA GGG-3'), reverse (5'-CAG GAC TGG ACT GTG GGC A-3'), and probe (5'-CCC CGT CCT TGA CTC CCT AGT GTC-3').

Northern Blot Analysis. All reagents and kits were obtained from Ambion. Total RNA from mock or HCMV-infected cells was isolated using the RNAqueous kit with concentrations measured by UV-spectrophotometry. Northern blots were done using the NorthernMax kit per the manufacturer's instructions. Briefly, 10 µg RNA was resolved in a 1% agarose formaldehyde gel and transferred to a BrightStar-Plus membrane. Biotinylated probes were generated using the BrightStar Psoralen-Biotin Kit with the following DNA fragments: UL44 (Afl II/Sac II), UL99 (Kpn I/Sac II), UL83 (Sac II), UL82 (Pvu I/Sac II), and GAPDH (582 bp Afl III). Membranes were hybridized to probes at 42º overnight, washed, developed using the BrightStar BioDetect kit, and exposed to film for autoradiography.

Immunofluorescence Assays. Cells were seeded onto glass coverslips at the time of infection and fixed with 2–4% paraformaldehyde for 20 min at the indicated times p.i. Cells were permeabilized with 0.2% Triton X-100 for 5 min and washed in

PBS prior to immunofluorescence staining. Normal goat serum (10% in PBS) (Jackson ImmunoResearch) was used as a blocking solution and antibody diluent. Mouse or rabbit IgG (Jackson ImmunoResearch) served as negative controls. Following primary antibody incubation and subsequent washes in PBS, coverslips were incubated with appropriate fluorescein isothiocyanate- or tetramethyl rhodamine isothiocyanate-conjugated secondary antibody (Jackson ImmunoResearch) plus Hoescht stain. Coverslips were treated with SlowFade Gold (Molecular Probes), an anti-photobleaching reagent, and mounted onto a slide for imaging. Costained samples were analyzed by a DeltaVision deconvolution microscopy system (Applied Precision) with SoftWoRx software (Applied Precision) on a Silicon Graphics O2 workstation. Images were taken at 0.2 μm increments along the z-axis by a Photometrics CCD camera mounted on the fluorescence/differential interference contrast microscope. The fluorescence data sets were deconvolved and analyzed by DeltaVision SoftWoRx programs. Adobe Photoshop was used to prepare images for the figures.

BrU and BrdU Pulse-labeling Assays. HFFs were infected with HCMV at a MOI of 2 or mock infected and seeded onto coverslips. At 36 h p.i., cells were rinsed in PBS and incubated with fresh media containing 1 mM BrU (Sigma) or 10 μM BrdU (Sigma). DMSO was used as a negative control. Cells were fixed at 20, 30, and 60 min post labeling and processed by IFA using an anti-BrdU antibody (Sigma), which detects both BrU and BrdU.

Microinjection. Nuclear microinjections (MI) of 250 ug/ml DQ ovalbumin (DQ-ova; Molecular Probes, Invitrogen) and blue dextran (injection control) were

done on HFFs infected with HCMV at MOI 2 or mock-infected at 40 h p.i. Coinjections with 150 nM Sal A were used to inhibit proteasome activity as a negative control. The cells, which were seeded onto coverslips, were transferred into serum free media 30-60 min prior to MI and further incubated for an additional 30 min after microinjection to allow for proteolytic degradation of the DQ-ova. Cells were then fixed with 3.7% formaldehyde and processed for IFA.

Antibodies. All antibodies to proteasome subunits were obtained from Biomol, except for 19S subunit Rpn1 (Calbiochem). Antibodies to HCMV proteins UL57, UL44, UL83 (CH12), UL99 (CH19), and IE1/IE2 (CH16.0) were from Virusys, while those to UL97, UL85, and UL86 were gifts from William Britt (University of Alabama, Birmingham). Other antibodies used include: actin (AC-15, Sigma), GAPDH (6c5, Fitzgerald), BrdU (Sigma), H3K4 (Upstate), ARNA3 (Chemicon), H14 and H5 (Covance), and p53 and wee1 (Santa Cruz Biotechnology).

RESULTS

Viral protein expression is delayed upon inhibition of proteasome activity. Previous studies assessing the impact of proteasome inhibitors on HCMV infection have shown a decrease in viral titer and an apparent defect at all stages of the infection, with significant reduction in viral protein expression (69, 119). These studies were done with the proteasome inhibitor added after viral adsorption and maintained in culture through the time course. Given the temporal kinetics of HCMV gene expression, it was not possible to determine from these studies whether the early and late stages of the infection were blocked differentially, independent of the inhibitory effects on the IE proteins. The block in IE protein expression was later shown to be MOI dependent (69, 128), while early and late protein expression remained significantly impaired at all MOIs tested (69), further indicating that the stages of viral gene expression may be differentially affected by proteasome inhibition. Another potential complication that needs to be considered when studying the effects of proteasome inhibitors on HCMV gene expression is the time in which the virus and inhibitor are added in relation to the cell cycle. Expression of IE proteins can be detected in cells infected in G_0/G_1 by 1–2 h p.i. (34, 59). Cells infected in S phase fail to express IE proteins until cells divide and cycle to the next G_1; however, addition of a proteasome inhibitor was able to relieve this block in IE gene expression (34, 130). To more accurately assess the role of the proteasome in each stage of viral replication, it was important to use cells that had been synchronized to enter the cell cycle at the time of infection. For the experiments presented here, cells were

synchronized in G_0 and released into G_1 at the time of infection as described in the Materials and Methods.

To further delineate the stage(s) of HCMV replication that are proteasome-dependent, G_0-synchronized HFFs were released into G_1 by trypsinization and replating at a lower density and infected at a MOI of 2 at the time of replating. Proteasome inhibitors were added at different times p.i., and viral protein expression, correlating to the different kinetic classes, was examined by Western blot. Three different proteasome inhibitors (i.e. MG132, lactacystin, or Sal A) were used to minimize the risk the results were due to off-target effects. MG132 is a reversible inhibitor of the chymotrypsin-like activity of the proteasome, lactacystin blocks both the chymotrypsin-like and trypsin-like activities, and Sal A inhibits all three chymotrypsin-like, trypsin-like, and caspase-like activities. The effects of all three inhibitors on the infection were essentially the same.

In Figure 4.1A, MG132 was added with the virus inoculums, which were then washed out at 12 h p.i. Fresh media was added and samples were harvested at 12, 24, 48, and 72 h p.i. Although the drug was added with the virus, no apparent constraints on viral entry were observed, as viral IE1-72 and IE2-86 protein expression remained comparable with the proteasome inhibitor at 12 h p.i.; however, IE2-86 expression appeared shortly delayed thereafter with decreased expression observed in the inhibitor treated samples at 24, 48 and 72 h p.i. A significant delay in early (i.e. UL57) and late (i.e. UL99) protein expression was also observed. These results are consistent with previous studies (69, 119, 128) in showing that the addition of proteasome inhibitors at the time of infection negatively impacts viral protein expression. The lack

of effect on IE1-72 expression is likely due to the MOI used in this assay (69). Interestingly, both UL57 and UL99 remained significantly suppressed even after the 60 h release from the drug, further underscoring the importance of proteasome activity at the early stages of the infection in facilitating viral replication and the switch to early and late gene expression. This may in part be attributed to the decrease observed in IE2-86 expression.

To further assess the impact of proteasome inhibition on the later stages of the infection, lactacystin was added to the infected cells at 24, 36, or 48 h p.i. After 12 h in the presence or absence of the drug, the cells were harvested and processed for Western blot analyses (Figure 4.1B). Decreased IE2-86 protein expression was still observed with the proteasome inhibitor added at these later times of infection. IE1-72 expression was slightly decreased with the drug present between 36 and 48 h p.i., and early protein expression (i.e. UL44 and UL57) was decreased when proteasome activity was inhibited from 24–36 h p.i or 36–48 h p.i., but little to no effect was seen for the 48–60 h p.i. treatment. Late protein expression (i.e. UL83, UL99, UL86) was also significantly reduced when the drug was present from 36–48 h p.i. or 48–60 h p.i., except for UL85 expression, for which only a slight decrease was observed with drug treatment at the different time periods. Interestingly, UL44 and UL57 levels after proteasome inhibition from 36–48 h p.i. were similar to that observed at 36 h p.i. with no treatment, and UL83 and UL99 levels after the 48–60 h p.i. drug treatment were comparable to those seen at 48 h p.i. with no drug. Similar results were also obtained with PYR-41, an inhibitor of the ubiquitin-activating enzyme, E1 (data not shown). These results suggested that proteasome inhibition prevented further accumulation of

the viral proteins, but we could not distinguish whether protein processing is stalled at the translational level or an earlier step (i.e. transcription or DNA replication) is inhibited. However, given that the protein expression is less affected after the prime expression period for each kinetic class (i.e. early proteins are not as affected when the inhibitor is added at late times of infection), the latter possibility seemed more likely.

Proteasome inhibitors prevent further accumulation of viral transcripts. To differentiate whether protein expression was affected at the RNA or protein level, Northern blots were used to assess RNA levels of representative early and late transcripts. HFFs were synchronized in G_0 and infected with HCMV at MOI 2 or mock infected at the time of release into G_1. Lactacystin (10 μM) was added from 24–36 h p.i. or 36–48 h p.i., the times during which the greatest effects on protein accumulation were observed, with total RNA isolated from cells at the end of treatment. GAPDH and 28S RNA levels were used as loading controls. The samples were first analyzed with a probe to the coding region of UL99, which allowed for the simultaneous detection and analysis of the 3' co-terminal transcripts from the UL93–UL99 coding region that are expressed with different temporal kinetics during the infection (169). As defined in the study by Wing et al. (169), kinetic class determination was based on whether transcript expression was dependent on viral DNA replication. UL97 transcript expression was independent of viral DNA replication and defined as early, whereas UL93 and UL94 were dependent and designated as late transcripts. UL95, UL96, and UL98 RNA levels were somewhat reduced after GCV treatment and were classified as early-late transcripts. Interestingly, UL96 and UL98 expression was also observed to be higher at 5 h p.i.

than at 72 h p.i. with GCV treatment, indicating that these genes may be under the control of multiple promoter elements and expressed in more than one kinetic class.

In our study, we found that UL95, UL96, and UL98 transcripts were expressed at high levels by 24 h p.i. (Figure 4.2). Addition of the proteasome inhibitor at 24–36 h p.i. or 36–48 h p.i. appeared to prevent further accumulation of UL95 as expression levels remained similar to when the drug was added, while levels continued to increase with no drug. Interestingly, both UL96 and UL98 RNA levels dropped below that seen at 24 h p.i. after each drug addition period, which may reflect a shorter half-life of these RNAs. The expression of the UL93, UL94, and UL99 transcripts was not readily detected until 36 or 48 h p.i., consistent with late kinetics, and was greatly reduced upon treatment with the proteasome inhibitor. The early UL97 transcript was not as readily detectable but showed no significant changes with the 36–48 h p.i. drug addition upon longer exposures of the blot (data not shown).

To ensure that the observed downregulation is not specific to the UL99 transcription unit, we also tested UL44 (early), UL83 (early-late), and UL82 (late) expression levels. As shown in Figure 4.2, UL44 expression was reduced in both treatment periods, although less of an effect was seen with the 36–48 h p.i. lactacystin addition. UL82 expression was also significantly decreased with the proteasome inhibitor at 36–48 h p.i. The effects on UL83 were more variable, as expression levels with the inhibitor added at 24–36 h p.i. showed little to no difference, while addition of the inhibitor at 36–48 h p.i. showed a modest decrease. In general, inhibition of the proteasome appears to prevent further expression or accumulation of the early transcripts (i.e. UL44 and UL95), while the early-late transcripts of UL96 and UL98

may have a shorter half-life. The significant reduction in the late transcripts (i.e. UL93, UL94, UL99, and UL82) may be due to a block in switching to late gene expression in the presence of the inhibitor.

Decreased viral late gene expression and viral yield has also been observed in HSV-1 infected cells treated with MG132 or lactacystin (25). The associated recovery of overall RNAP II levels, especially that of pSer2-RNAP II, which normally decreases during HSV-1 infection, led to the hypothesis that proteasome inhibitor treatment prevents the degradation of stalled RNAP II complexes at later times of infection (25, 37, 80). To determine whether this may also be the case with HCMV, RNAP II levels during HCMV infection were assessed with or without proteasome inhibition. Mock or HCMV infected cells were treated with lactacystin at 36–48 h p.i. or 48–60 h p.i. and harvested at the end of treatment for Western blot analyses using RNAP II phospho-specific antibodies. As reported previously (145), unlike HSV-1, an overall increase in RNAP II expression was observed during HCMV infection, as shown by both the ARNA3 (RNAP IIo/a) and H14 (pSer5-RNAP IIo) antibodies, while pSer2-RNAP II (H5) levels did not accumulate in the HCMV infected cells until later during the infection (Figure 4.3). Furthermore, no significant effect on the various forms of RNAP II was observed with lactacystin treatment in either mock or HCMV infected cells. Actin is shown as a loading control, while p53 and wee1 (131) served as positive controls for proteasome inhibition in mock or virus infected cells, respectively.

Viral DNA synthesis is modestly decreased upon proteasome inhibitor treatment. Previously, it was shown that the presence of the proteasome inhibitor

from the beginning of the infection inhibited viral DNA replication (69, 119), but this could have been the result of reduced expression of the viral early proteins necessary for viral DNA synthesis. To address this question more directly, HFFs were infected with HCMV at an MOI of 2 and were treated with MG132 during the intervals of 24–48 h p.i., 36–60 h p.i., or 48–72 h p.i. Cells were harvested at the end of each treatment period and analyzed for viral DNA accumulation by qPCR with primers and probe to the UL77 gene. A probe to the GAPDH promoter was used as a control for input DNA and normalization. Values are expressed as the fold inhibition of UL77 DNA accumulation in the MG132 treated as compared to DMSO during each treatment period (Figure 4.4). The accumulation of viral DNA decreased by ~3.5-fold with the 24–48 h p.i. treatment. Similar decreases were seen with the later treatments, with ~3-fold for 36–60 h p.i. and ~2-fold for 48–72 h p.i. Since UL77 is relatively close to the origin of viral DNA replication, we also used primers and probe to the IE2 (UL122) region of the genome, which is further from the origin, to determine whether there might be a greater decrease in apparent viral DNA synthesis due to preferential effects on the elongation step of DNA replication. No differences were observed, however, indicating that the inhibition is likely at the initiation step or just after conversion to the elongation step (data not shown).

Proteasome activity and expression increase at later times of the infection. Given the decrease in viral RNA expression upon proteasome inhibition and the many reports indicating a functional role of proteasomes in transcription, we hypothesized that the proteasome facilitates HCMV transcription. If this is the case, then proteasome activity or abundance might increase as the infection progresses. The 26S

proteasome is composed of two subcomplexes, the 19S regulatory complex and the 20S catalytic core. Although free 20S maintains some catalytic activity, the 26S complex is responsible for the major proteolytic activity in the cell. In-gel peptidase assays using a fluorogenic substrate were performed to measure the proteolytic activity of mock or HCMV-infected cells harvested at 12, 24, 48, and 85 h p.i. Increased peptidase activity was observed in the virus-infected samples beginning 24–48 h p.i. and remained at elevated levels throughout the time course, while levels were unchanged in the uninfected (Figure 4.5A). Separate gels were run for Western blot analyses. Alignment of blots probed for 19S subunit Rpn2 and 20S subunit α6 showed that the slower migrating activity bands correspond to the 26S proteasome complex (i.e. 19S + 20S), whereas the lower molecular weight band represents free 20S activity (Figure 4.5A).

Western blots were also used to screen the various proteasome subunits to determine whether the elevated activity correlated with an increase in proteasome abundance during HCMV infection. HFFs that were infected with HCMV (MOI 5) or mock infected were harvested over a 72 h time course. Expression of all 19S and 20S subunits have been examined in these experiments, except for the 19S lid subunits Rpn3, Rpn5, Rpn6, Rpn9, Rpn15, and Rpn11, as well as the 20S subunit α1. Representative subunits from each subcomplex are shown with actin as a loading control (Figure 4.5B). As with the peptidase assay, protein expression levels of most subunits were higher in the virus-infected cells beginning 24–48 h p.i. and continued to increase throughout the time course.

Proteasome subunits relocalize around viral replication sites. IFA was used to determine whether proteasomes localize to sites of viral replication. Intracellular distribution studies regarding proteasome localization have led to conflicting results, but in general, proteasomes appear to be abundantly distributed throughout the cytosol and nucleus (but excluded from the nucleoli) and have been found associated with intermediate filaments, ER membrane, and centrosomes (54). Mock or HCMV-infected (MOI 5) HFFs were fixed onto coverslips and stained at various times p.i. using antibodies targeted against different proteasome subunits. We were limited in this analysis to the use of antibodies that did not show a high level of accumulation at the golgi due to the presence of the viral-encoded Fc receptor. Subunits that have been tested include the 19S subunits Rpt1–Rpt6, Rpn1, Rpn2, Rpn10, and Rpn12 as well as the 20S subunits α2, α4, α5, α6, and ß1.

Mock-infected cells show a faint diffuse staining of the various proteasome subunits throughout the cytosol with more prominent staining in the nucleus. This same localization pattern is maintained throughout the 72-h time course. The 19S subunit Rpt6 and 20S subunit α6 are shown costained in a mock-infected cell at 48 h p.i. as a representative example (Figure 4.6A). The 20S α6 appears to be more diffusely expressed than 19S Rpt6, which shows more punctate staining. This is consistent with 20S also being free or associated with different regulatory complexes. In the infected cells, a general increase in staining was observed for the majority of the subunits at 48–72 h p.i. (data not shown), which corresponds to the increased protein expression seen by Western analysis. Cells were also costained with antibodies to viral replication proteins, UL57 or UL44, which serve as a marker for the viral

replication center, and analyzed by deconvolution microscopy to establish whether proteasomes localize to viral replication sites. Several 19S subunits (i.e. Rpt6, Rpt1, Rpt5, Rpn10, Rpn12), 11S subunit REGγ, and 20S α6 all exhibit some staining within the replication center and an enhanced accumulation at the rim of the replication center in infected cells beginning at ~36 h p.i. (Figure 4.6B and data not shown). As representative examples, the 19S subunits Rpn12, Rpn10, and Rpt6 are shown costained with UL57, while 11S REGγ is shown costained with 20S α6 in a mid cross sectional plane at 48 h p.i. (Figure 4.6B).

The relocalization of the proteasome subunits occurs after the onset of viral DNA synthesis. Since this relocalization of the proteasome subunits is first detected shortly after the onset of viral DNA replication, we wanted to determine whether the relocalization is dependent on viral DNA synthesis. HCMV DNA replication begins ~16 h p.i., requiring both viral and cellular proteins (for review, see (101). Six core viral replication proteins (i.e. UL44, UL57, UL54, UL70, UL102, and UL105) along with UL84, UL112-113, and UL114 are necessary for efficient viral DNA replication, as measured in transient expression assays. The UL112-113 phosphoproteins localize adjacent to PML-oncogenic domains (PODs) at sites of input viral genome accumulation and IE transcription of viral genes, where it then recruits the core replication proteins in forming the pre-replication centers (1, 112). These foci eventually coalesce into large replication centers as viral replication proceeds.

Mock or HCMV infected HFFs were treated with the viral DNA polymerase inhibitor PAA at 0–48 h p.i. or 36–48 h p.i. and then fixed at 48 h p.i. for IFA with antibodies to 19S subunits Rpt1, Rpt6, Rpn10, and 20S α6. As representative

examples, 19S Rpt6 and 20S α6 are shown costained with UL57 in Figure 4.7. The presence of the drug had no significant effect on the localization of 19S Rpt6 or 20S α6 in the mock infected cells with either the 0–48 h p.i. (Figure 4.7A, panels 8 and 16) or 36–48 h p.i. treatment (Figure 4.7B, panels 12 and 24). Addition of PAA at the onset of infection severely limited viral replication, as only pre-replication center foci were observed by UL57 staining (Figure 4.7A, panels 6 and 14), compared to the large replication centers in the untreated samples (Figure 4.7A, panels 2 and 10). Interestingly, both 19S Rpt6 and 20S α6 remain diffusely localized throughout the infected nuclei and are excluded from the pre-replication center foci in the presence of the inhibitor (Figure 4.7A, white arrows in panels 7 and 15 and adjacent magnified sections). This is consistent with the relocalization of the proteasome subunits occurring after the onset of viral DNA synthesis.

To address whether ongoing viral DNA replication is necessary to maintain the proteasome subunits at the rim of the replication center, PAA was added at 36 h p.i., which is after the initiation of viral DNA synthesis, and cells were analyzed by IFA at 48 h p.i. At 36 h p.i., some enhancement of both 19S Rpt6 and 20S α6 can be observed at the rim of the replication center, with some punctate foci observed for 20S α6 (Figure 4.7B, panels 1 and 13). The accumulation of the proteasome subunits at the periphery of the replication center continues with the addition of DMSO from 36–48 h p.i. (Figure 4.7B, panels 5–7 and 17–19). No significant differences were seen in the localization of 19S Rpt6 in the presence of PAA from 36–48 h p.i. (Figure 4.7B, panels 9–11), whereas the 20S α6 was slightly more diffusely localized within and around the replication centers with PAA (Figure 4.7B, panels 13–21). The drug

treatment had no effect on the localization of the proteasomes in mock-infected cells (Figure 4.7B, panels 12 and 24). Taken together, these data indicate that ongoing viral DNA replication is not required for the maintenance of the proteasome subunits at this site. Similar results were also obtained using GCV (data not shown).

Active proteasomes accumulate around the viral DNA replication center in regions of RNA synthesis. The same shift in localization to the rim of the replication center has previously been reported for the phosphorylated forms of RNAP II in HCMV infected cells (145), further suggesting that the proteasomes may be involved in transcriptional processes during the infection. To assess whether RNA synthesis is occurring at the border of the replication center, BrU pulse-labeling experiments were performed. HFFs infected with HCMV or mock infected were pulse-labeled with 1 mM BrU at 36 h p.i. for 20, 30, or 60 min. Cells were then fixed and processed by IFA. In the uninfected cells, BrU localized diffusely throughout the nucleus with signal intensities increasing with pulse length; a representative cell with a 30 min BrU pulse is shown costained with UL57 (Figure 4.8A, panel 3). In the HCMV-infected cells, the incorporated BrU located around the viral replication center, as marked by UL57 (Figure 4.8A, panels 1 and 2). As a complement, mock or virus infected cells were pulse-labeled with BrdU (60 min) and costained for UL57 (Figure 4.8A) to localize the area of DNA synthesis. Given the viral-mediated shutoff of cellular DNA synthesis, the BrdU would primarily be incorporated into replicating viral DNA. While the area of BrdU incorporation is diffusely spread through the nucleus in the uninfected cells (Figure 4.8A, panel 6), the BrdU in the infected cells localized specifically within the viral replication center as marked by UL57 (Figure

4.8A, panels 4 and 5). Taken together, these data indicate that ongoing RNA and DNA synthesis occurs in spatially distinct areas in the infected cell, with RNA synthesis occurring outside the viral replication center and viral DNA synthesis occurring inside the replication center, as marked by UL57.

Mock or virus infected cells were further examined by IFA to confirm whether the relocalization of the proteasome subunits during the infection correlate to areas of active transcription. In Figure 4.8B, cells pulsed with BrU for 30 min were assayed for BrU and 19S Rpt6 localization. Comparable staining patterns were observed with both BrU and Rpt6 localizing at the periphery of the viral replication center in the infected cell (Figure 4.8B). Other markers associated with active transcription were also analyzed, including histone H3 that is trimethylated at residue K4 (H3K4) and pSer2-RNAP II. Both H3K4 and pSer2-RNAP II also shifted from a diffusely nuclear localization in the uninfected cells to the peri-replication center region in the infected cells, as indicated by costains with 19S Rpt6 and UL57 in Figures 4.8C and 4.8D, respectively. These results further support that proteasomes localize to active transcription areas during the infection. If the localization of proteasomes to this peri-replication center region is pertinent to efficient viral transcription, then the decrease in viral transcript expression upon proteasome inhibition may be attributed to an altered positioning of the proteasomes during drug treatment. To address this, proteasome localization was also analyzed in cells treated with MG132 from 36–48 h p.i. The localization of proteasome subunits 19S Rpt1 and Rpt6, 20S α6, and 11S REGγ have been assessed, and Rpt6 is shown costained with UL57 as a representative example in Figure 4.8E. Rpt6 localization was not significantly altered with MG132,

as the shift to the peri-replication center region was still observed (Figure 4.8E). Together, these results indicate that ongoing transcriptional activity occurs outside the viral replication center at sites where proteasome subunits also locate during later times of the infection.

To determine if the proteasome is active at these peri-replication center sites, the nuclei of mock or virus-infected HFFs were microinjected with DQ-ova at 40 h p.i. DQ-ova is conjugated to BODIPY FL-dye, which is self quenching and exhibits low background signal but displays green fluorescence upon proteolytic degradation, allowing for the localization of proteolytic activity to be tracked. Cells were fixed 30 min post injection and processed by IFA. Coinjections with the proteasome inhibitor Sal A (150 nM) sufficiently blocked DQ-ova fluorescence, confirming that the observed fluorescence is proteasome dependent (data not shown). In the mock-infected cells, DQ-ova localized throughout the nucleus (Figure 4.9). In the virus-infected cells, however, the majority of the DQ-ova localized around the replication center, although faint staining within the center was still observed, as shown by costains with 19S Rpt6, 20S α6, or UL57 (Figure 4.9). Thus, this peri-replication center region supports both transcriptional and proteolytic activity during later times of the infection.

The 19S non-ATPase base subunit Rpn2 relocalizes to the viral DNA replication center. While several 19S, 20S, and 11S proteasome subunits relocalized around the replication center during the infection, a marked difference in localization pattern was observed for the 19S non-ATPase base subunit Rpn2. In mock-infected cells, Rpn2 appeared diffusely distributed throughout the cytosol and nucleus (Figure

10, parts B and C). However, in cells infected with HCMV at an MOI of 2, Rpn2 was observed within the viral replication center beginning at ~30 h p.i., and continued to accumulate there as the infection progressed (Figure 4.10 and data not shown). To better assess whether Rpn2 relocalization coincides with viral replication center formation, low MOI infections, which allowed for the closer observation of replication centers at various stages of development, were analyzed for Rpn2, UL44, and UL57 localization by IFA. Cells fixed on day 4 and stained for Rpn2 and UL57 are shown in Figure 4.10A as a representative example. As indicated by the white arrow in Figure 4.10A, UL57 is present at the pre-replication foci but not Rpn2. Rpn2 was not present at the replication centers until they were slightly more developed (Figure 4.10A, pink arrow) and continued to accumulate there as the replication centers grew and coalesced (Figure 4.10A, orange arrow). Thus, Rpn2 is not brought in with the core replication machinery and likely does not play a role in replication center formation.

Rpn2 localization was also assessed in the presence of PAA or GCV to determine whether the relocalization is dependent on viral DNA synthesis. With the addition of PAA at 0–48 h p.i., replication center foci containing UL57 are observed, but Rpn2 remains diffusely nuclear and cytoplasmic and does not accumulate in the foci with UL57 (Figure 4.10B). These data suggest that the Rpn2 relocalization also occurs after the onset of viral DNA synthesis. Similar results were also seen with GCV (data not shown). Addition of PAA at 36–48 h p.i. after the onset of viral DNA synthesis appeared to prevent further accumulation of Rpn2 in the viral replication center, as levels remained comparable to those seen at 36 h p.i. (Figure 4.10C). Further accumulation of Rpn2 into the replication center was similarly inhibited with the

addition of the proteasome inhibitor MG132 at 36–48 h p.i. (Figure 4.10C). These data indicate that the relocalization of Rpn2 to the replication center is dependent on the initiation of viral DNA synthesis. Further accumulation of the subunit, but not maintenance once relocalized, also requires ongoing viral DNA synthesis and proteasome proteolytic activity.

DISCUSSION

In this report, we extend the studies from our lab and others on the interactions between HCMV and the ubiquitin-proteasome degradation pathway (7, 16, 34, 55, 57, 60, 65, 69, 93, 119, 128, 129, 151, 152, 164, 167). Previous studies have shown HCMV infection to be negatively affected by inhibition of the proteasome (69, 119, 128), and in the experiments presented here, we have elucidated the temporal and molecular basis of this inhibition. We show that proteasome proteolytic activity is important for viral transcription, and that as the infection progresses, the proteasome subunits accumulate in regions of RNA synthesis at the periphery of the viral DNA replication center in the nucleus.

We found that proteasome inhibition during the initial 12 h p.i. had little effect on IE gene expression., though IE2-86 expression decreased thereafter either after release from the drug or when the inhibitor was added at later times during the infection (Figure 4.1). Previous studies reported a decrease in both IE1-72 and IE2-86 expression when the proteasome inhibitor was added at the onset of infection and maintained throughout the infection time course (69, 119, 128). This discrepancy, especially with regards to IE1-72 expression, may be attributed to a difference in the MOI (69) and/or cell lines (128) used in these assays. The recent study by Sadanari et al. (128) showed that the effect of proteasome inhibitors on IE gene expression can be cell-type specific, with inhibition in glioma and astrocytoma cell lines and activation in a neuroblastoma cell line. Although proteasome activity did not appear necessary to facilitate efficient viral entry or initial IE expression in the context of the experiments

presented in this study, the requirement may also vary depending on MOI and cell type. The effects on IE2-86 expression upon proteasome inhibition has been more consistently observed with decreased expression seen in multiple cell lines infected with HCMV at different MOIs, although little to no effect was seen at higher MOIs ((119), (69),(128), this study). The observed modest decrease in IE2-86 expression with the inhibitor present 0–12 h p.i. may in part account for the associated suppression of viral early and late protein expression, as there may not be sufficient transactivation of the viral early and late genes or cellular genes. Interestingly, early and late protein expression did not fully recover even after 60 h release from MG132. This suggests that the switch to early gene expression and/or viral DNA synthesis may be critically dependent on the proteasome-mediated events that occur during the first 12 h p.i. For instance, cellular factors that are normally degraded (e.g. Daxx, unphosphorylated Rb, etc.) to facilitate efficient viral replication would not be. Proteasome inhibition may also cause further cell cycle deregulation that is not conducive for viral replication.

The effect on viral early and late gene expression became less pronounced as the proteasome inhibitor was added later during the infection time course, such that addition at late times no longer affected early gene expression, while late gene expression was impacted to varying degrees. The proteasome inhibitors appeared to prevent further accumulation of both viral RNA and protein. If the inhibitor was added after expression had peaked, then gene expression was no longer affected. Although DNA synthesis decreased during intervals that the proteasome inhibitor was present, the effect was relatively modest (2 to 3-fold inhibition in accumulation over a 24 h

period). Whether this inhibition is due to a direct effect on DNA synthesis or decreased expression of the viral early genes, which encode the majority of the viral DNA replication proteins, remains to be determined.

While several studies have localized IE transcription to the viral transcriptosomes, which are subnuclear foci that contain the input viral genome as well as several cellular transcription factors, cyclin dependent kinases, and RNAP II that form adjacent to POD/ND10 structures (58, 59, 68, 145), the site of viral late gene transcription has not been established, although it has been hypothesized to occur around the replication center, given the localization of phosphorylated RNAP II there at the later times of infection (145). We have further identified H3K4 and newly labeled BrU transcripts to localize outside the viral replication center, further indicating the peri-replication center region to be transcriptionally active. Although we could not discriminate whether the BrU incorporated into viral or cellular transcripts in the BrU pulse-labeling assays, we provide further evidence that ongoing transcriptional activity is occurring outside the viral replication center at later times of the infection.

Interestingly, all of the proteasome subunits tested by IFA, except for Rpn2, showed enhanced localization around the replication center as the infection progressed into early-late times, when the majority of viral transcription occurs. In accord with this temporal relocalization, there was requirement for initiation of viral DNA synthesis. Taken together with the increase in both the activity and abundance of the proteasome and the effect of proteasome inhibitors, these results further suggest that proteasome activity is required to facilitate efficient viral transcription. This would be

consistent with the large body of evidence that the proteasome and its proteolytic activity play a major role in cellular transcription (24, 47, 99). At this time, we cannot exclude a non-proteolytic role for specific subunits, as the 19S subunits also possess chaperone activities and can aid in remodeling protein complexes during transcription, modifying histones, and recruiting cotransactivator complexes (24, 32, 47, 72, 78, 99). The HIV-1 promoter is a notable example of transcription regulation mediated by both proteolytic and nonproteolytic mechanisms (77, 104, 108, 139). A study with adenovirus reported on the selective and independent recruitment of the APIS (19S ATPase proteins independent of 20S) and 20S complexes to the adenovirus E1A transactivation domain CR3 (123) and their roles in transcription initiation and elongation. The authors further showed that treatment with proteasome inhibitors inhibited E1A transcription (123).

A role for the proteasome in HSV-1 replication has been suggested by the finding that viral transcription is associated with a decrease in RNAP II levels, particularly the Ser2-phosphorylated form of the large subunit, which is the active form during transcription elongation (25, 36, 37, 80). The addition of proteasome inhibitors resulted in reduced levels of HSV-1 late protein expression and viral titers, while the ubiquitin-mediated degradation of pSer2-RNAP II was prevented. This led to the hypothesis that proteasome degradation of stalled RNAP II complexes is necessary in times of robust HSV-1 early and late gene transcription (25, 80). Although the specific removal of RNAP II does not appear to be the case during HCMV infection, given that both Ser2- and Ser5-phosphorylated forms of RNAP II

increase during the infection (145, this study), proteasome proteolytic activity may be required for removal of other proteins involved in transcription.

The relocalization of the proteasome subunits to the HCMV replication center periphery is reminiscent of the enrichment of proteasomes in the VICE (virus-induced chaperone enriched) domains that develop adjacent to the replication center in HSV-1 infected cells. Along with proteasomes, the domains contain various cellular chaperone proteins (i.e. Hsp70, Hsp40, Hsp90, and Hsc70) and ubiquitin-conjugated substrates (14, 15, 25, 80, 84, 85). It is proposed that the VICE domains regulate and sequester misfolded or modified proteins to prevent innate immune responses (i.e. apoptosis or unfolded protein response) from being activated as well as facilitate the removal of stalled RNAP II complexes from HSV-1 templates when RNA synthesis is occurring at high levels.

The only proteasome subunit that appeared to accumulate within the HCMV DNA replication center was Rpn2. Interestingly, recent studies regarding 19S base assembly have shown that Rpn2/S1 is the only proteasome subunit that is not incorporated into a subcomplex prior to formation of the whole base complex, and thus it may exist as a free pool (67). It has been found that many cellular proteins, including p53, RPA, PCNA Nbs1, Rad50, Atrip, Chk1, cdk7, and MAT-1 accumulate in the viral replication center (28, 35, 90). Whether the accumulation of Rpn2 in the replication center is associated with a role in viral DNA synthesis or simply reflects its existence as a free pool is an important question to address.

While HCMV has developed multiple mechanisms to subvert and inhibit cellular functions to create an environment more conducive for viral replication, it is

dependent on host factors and machinery to facilitate a productive infection. Given the many cellular systems the ubiquitin-proteasome pathways regulate, it is a convenient target for the virus to modify and manipulate. In this report, we have shown yet another facet in which HCMV utilizes the UPS in enhancing viral replication. The importance of the UPS at all stages of the HCMV infection support further studies into this pathway as a potential antiviral target.

ACKNOWLEDGEMENTS

We are grateful to Dr. Bradley Moore for the sample of Sal A, to Dr. William Britt for the UL97, UL85, and UL86 antibodies, and to Dr. David Rose for his help with the microinjection assays. We appreciate the use of the microscopy resources at the UCSD School of Medicine Light Microscopy Facility. We would also like to thank the members of the Spector lab for their support and comments on the manuscript. This work was supported by NIH grants CA073490 and CA034729 to D.H.S.

The text of this chapter is from material submitted to the *Journal of Virology*, October 2009. Tran, K., J.A Mahr, and D.H. Spector. Proteasome subunits relocalized during human cytomegalovirus infection and proteasome activity is necessary for efficient viral gene transcription and DNA replication.

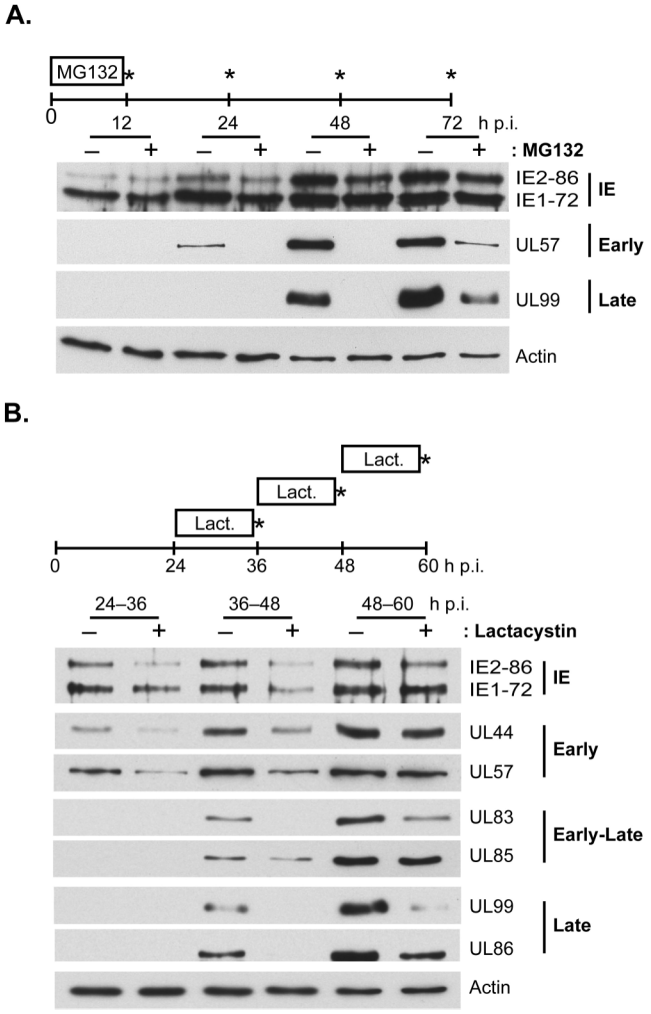

Figure 4.1 HCMV protein expression is delayed by proteasome inhibitor treatment. HFFs infected with HCMV at MOI 2 were treated with **A)** MG132 (2.5 μM) from 0–12 h p.i. with cells harvested at the times indicated or **B)** lactacystin (Lact, 10 μM) from 24–36, 36–48, or 48–60 h p.i. with cells harvested at the end of treatment and processed for Western blot analyses with antibodies to HCMV proteins IE2, IE1, UL44, UL57, UL99, UL83, UL85, and UL86. Actin is shown as a loading control.

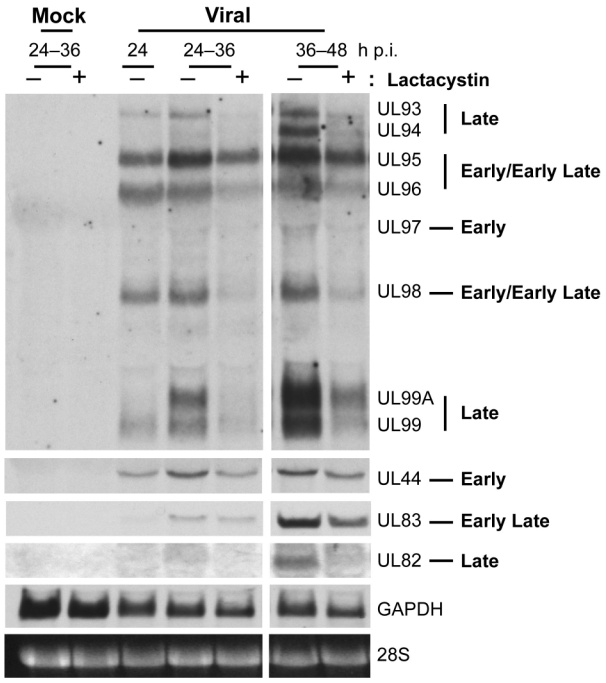

Figure 4.2 Proteasome inhibition prevents further accumulation of viral transcripts. HFFs infected with HCMV at MOI 2 or mock infected were treated with lactacystin (10 μM) at the times indicated and harvested at the end of treatment. Total RNA was isolated and processed for Northern blot analyses with probes to the 3' co-terminal region of UL92–UL99, UL44, UL83, and UL82. GAPDH mRNA and 28S rRNA are shown as loading controls.

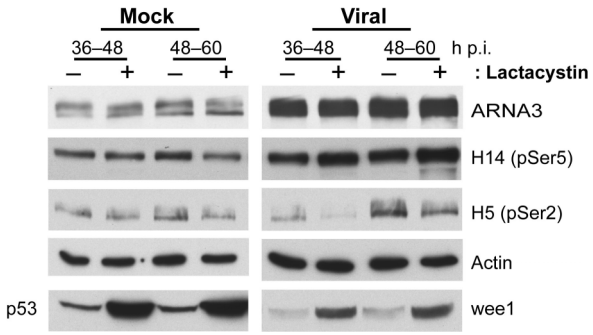

Figure 4.3 RNAP II expression is increased during HCMV infection but not affected upon proteasome inhibition. HFFs infected with HCMV at MOI 2 or mock infected were treated with lactacystin (10 μM) at the times indicated and harvested at the end of treatment for Western blot analyses with antibodies to RNAP IIo/a (ARNA3), pSer5-RNAP IIo (H14), pSer2-RNAP IIo (H5), p53, wee1, and actin.

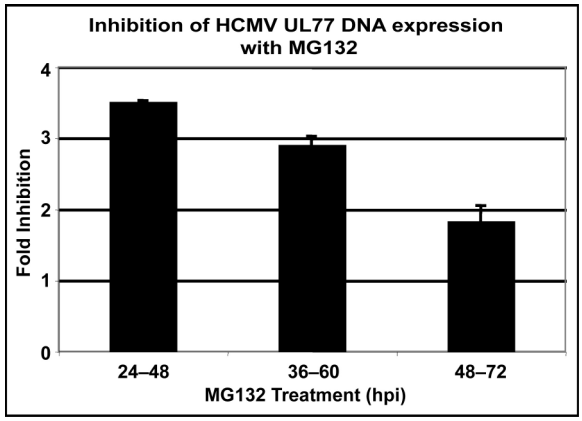

Figure 4.4 DNA synthesis is downregulated upon proteasome inhibitor treatment. Viral DNA accumulation was measured by qPCR (with primers and probe to the UL77 gene) using total DNA isolated from HCMV infected HFFs (MOI 2) treated with DMSO or MG132 (2.5 μM) for 24 h at the times indicated. Values were normalized to the GAPDH promoter and expressed as the fold inhibition of DNA accumulation in MG132-treated samples compared to DMSO control samples during the 24 h period. Mean values from two experiments are shown.

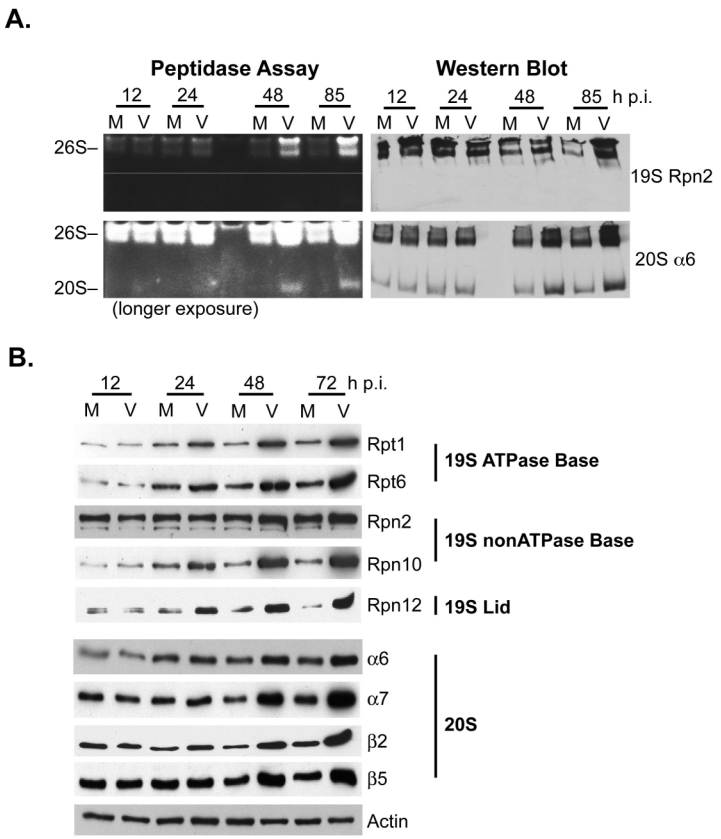

Figure 4.5 Proteasome activity and subunit expression increases during HCMV infection. A) Mock (M) or virus (V) infected HFFs were harvested at the times indicated. Cell lysates were processed by an in gel peptidase assay using a fluorigenic peptide to measure proteasome activity. Western blots for 19S Rpn2 and 20S α6 were done in parallel on separate gels to identify the 26S and 20S proteasome fractions. **B)** Western blot analyses of proteasome subunit expression in mock (M) or virus (V) infected HFFs over an infection time course. Representative subunits from each subcomplex are shown. Actin was used as a loading control.

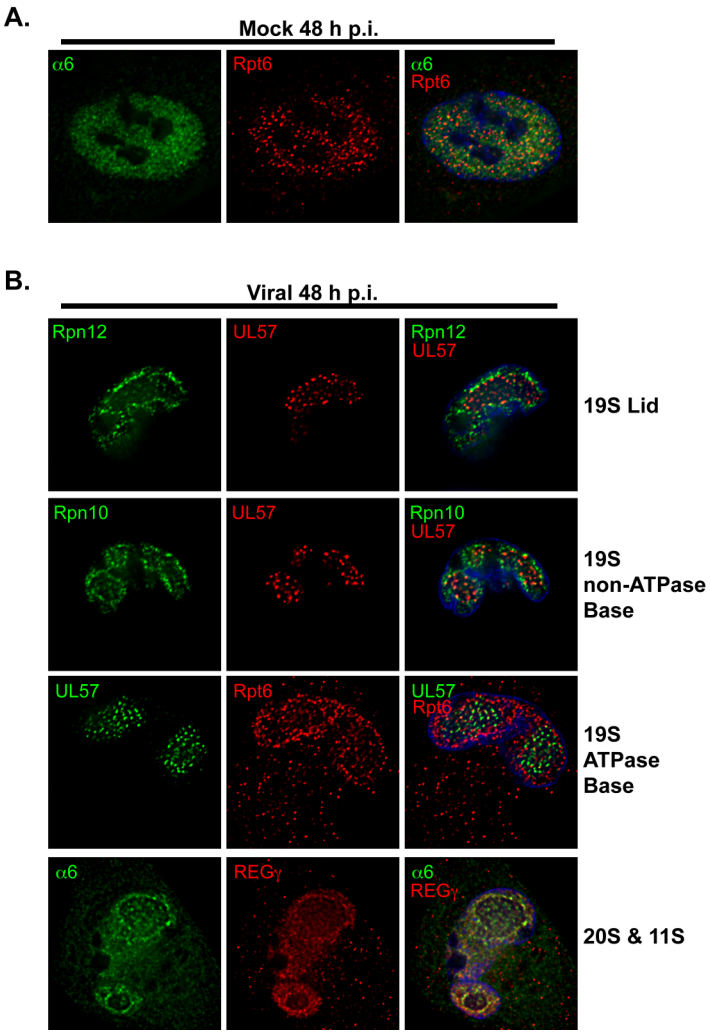

Figure 4.6 Proteasome subunits relocalize around the viral replication center during HCMV infection. Mock or virus-infected HFFs were fixed onto coverslips at 48 h p.i., processed for IFA, and imaged by deconvolution microscopy at 0.2-μm sections at a magnification of 1000X under oil immersion conditions. Mid-sectional planes of representative cells are shown. **A)** Mock-infected HFFs were fixed at 48 h p.i. and costained for 19S Rpt6 (red) and 20S α6 (green) with Hoescht stain in blue. **B)** HCMV-infected HFFs (MOI 5) were fixed at 48 h p.i. and costained with antibodies to: 19S Rpn12 (green) and UL57 (red), 19S Rpn10 (green) and UL57 (red), 19S Rpt6 (red) and UL57 (green), or 20S α6 (green) and 11S REGγ (red).

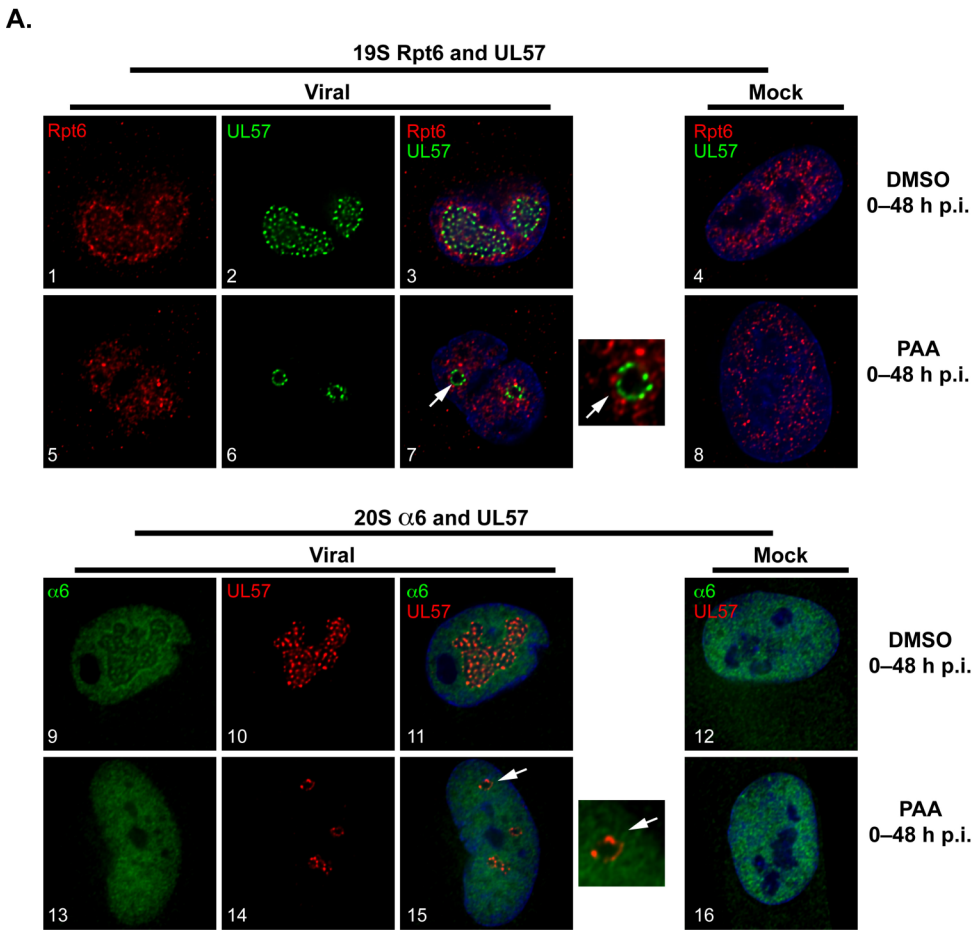

Figure 4.7 Relocation of proteasome subunits to the replication center periphery occurs after the onset of viral DNA replication. A) Mock or HCMV infected HFFs (MOI 2) were treated with DMSO or PAA at 0–48 h p.i. and fixed at 48 h p.i. for IFA with antibodies to 19S Rpt6, 20S α6, and UL57.

Figure 4.7 (Continued) Relocation of proteasome subunits to the replication center periphery occurs after the onset of viral DNA replication. B) DMSO or PAA was added at 36–48 h p.i. to inhibit viral DNA synthesis during this 12 h period. Cells were fixed at 36 h p.i. prior to treatment and at 48 h p.i. and processed for IFA with antibodies to 19S Rpt6, 20S α6, and UL57. Cells were imaged by deconvolution microscopy at 0.2-μm sections at a magnification of 1000X under oil immersion conditions. Mid-sectional planes of representative cells are shown merged with Hoescht stain (blue). Panels are numbered as indicated. Magnified images of the pre-replication foci (as indicated by the white arrow) are shown adjacent to panels 7 and 15 in panel A.

B.

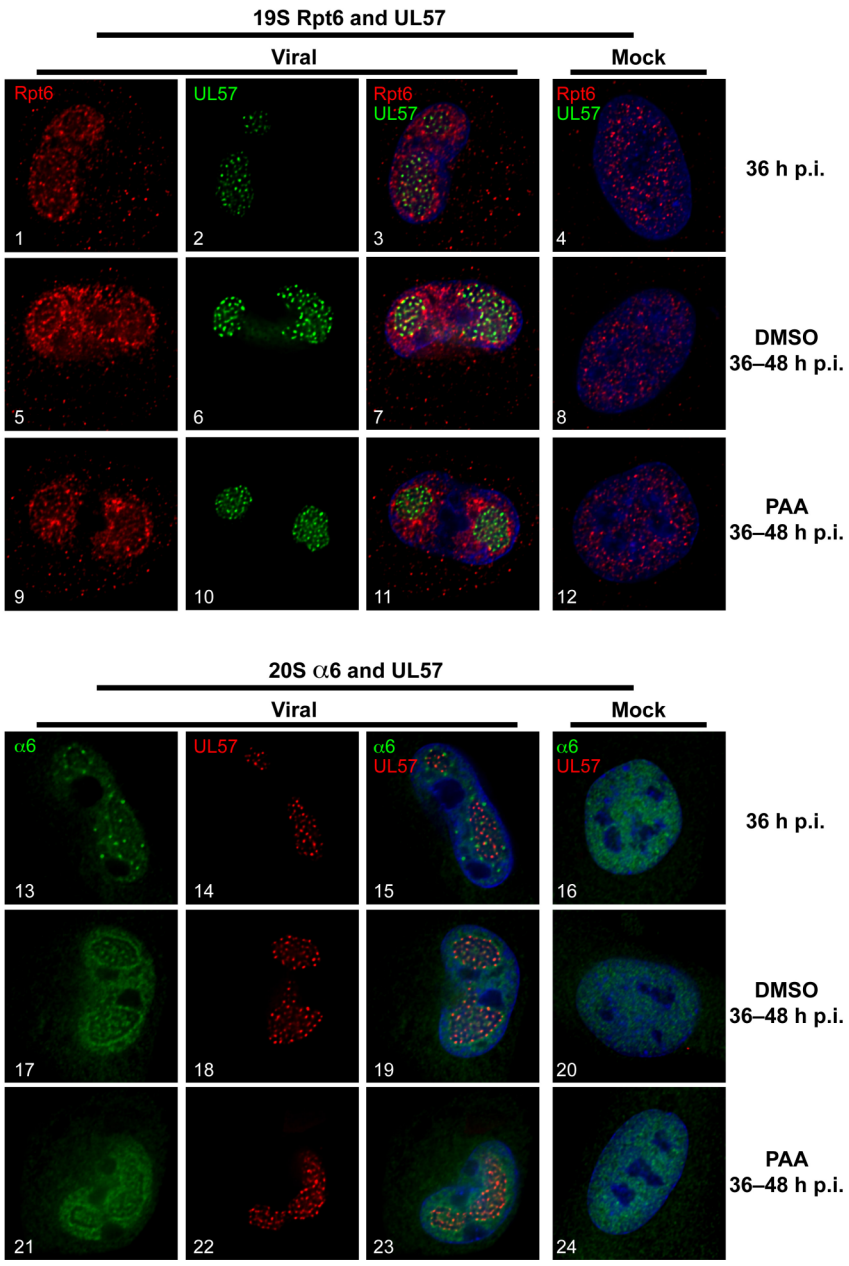
19S Rpt6 and UL57
Viral
Mock
Rpt6
UL57
Rpt6
UL57
Rpt6
UL57
1
2
3
4
36 h p.i.
5
6
7
8
DMSO
36–48 h p.i.
9
10
11
12
PAA
36–48 h p.i.
20S α6 and UL57
Viral
Mock
α6
UL57
α6
UL57
α6
UL57
13
14
15
16
36 h p.i.
17
18
19
20
DMSO
36–48 h p.i.
21
22
23
24
PAA
36–48 h p.i.

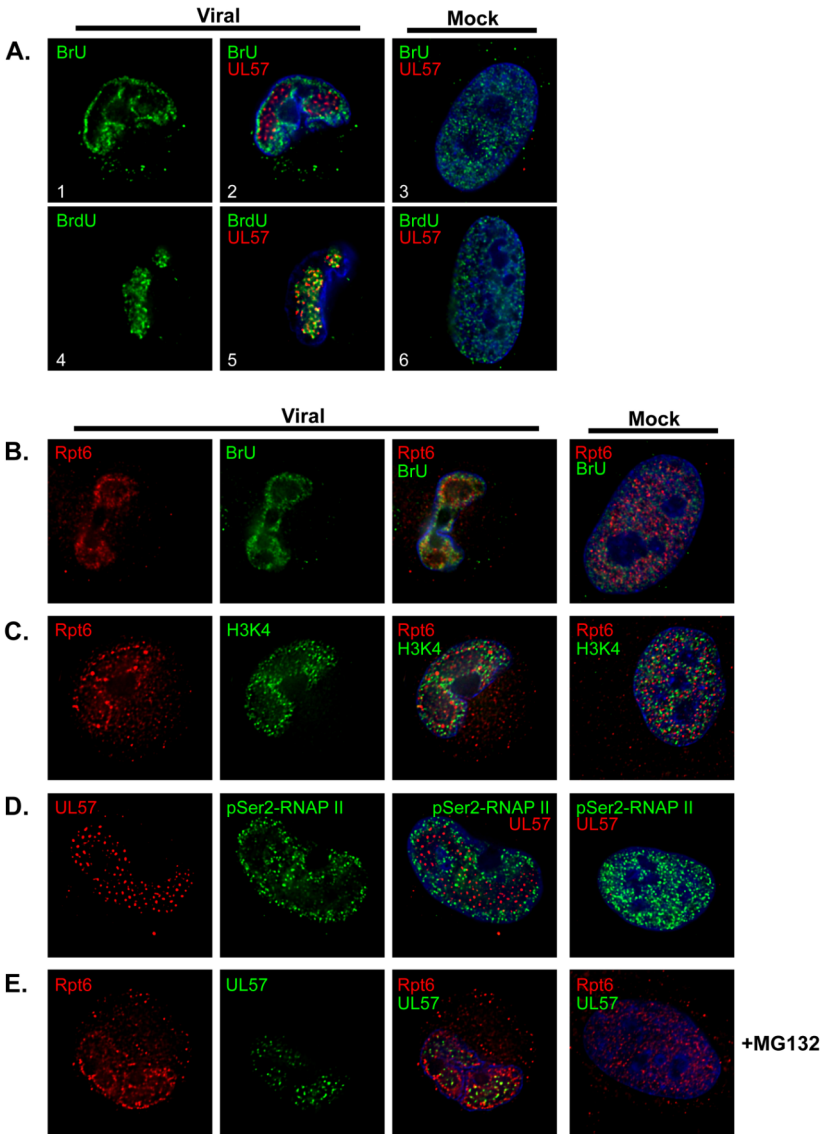

Figure 4.8 The peri-replication center region is transcriptionally active. Mock or virus infected HFFs (MOI 2) were treated as indicated and processed by IFA with Hoescht stain in blue. Mid-sectional planes of representative cells imaged by deconvolution microscopy at 0.2-µm sections at a magnification of 1000X under oil immersion conditions are shown with panels numbered as indicated. **A)** Cells were pulsed with BrU (30 min) or BrdU (60 min) at 36 h p.i. and then fixed for IFA. Incorporated BrU or BrdU are shown in green with UL57 in red. **B)** Cells were pulsed with BrU at 36 h p.i. for 30 min and stained for 19S Rpt6 (red) and incorporated BrU (green). **C)** Cells were fixed at 48 h p.i. and stained for 19S Rpt6 (red) and H3K4 (green) or **D)** UL57 (red) and pSer2-RNAP II by the H5 antibody (green). **E)** Cells were treated with MG132 from 36–48 h p.i. and then fixed. Cells stained for 19S Rpt6 (red) and UL57 (green) are shown.

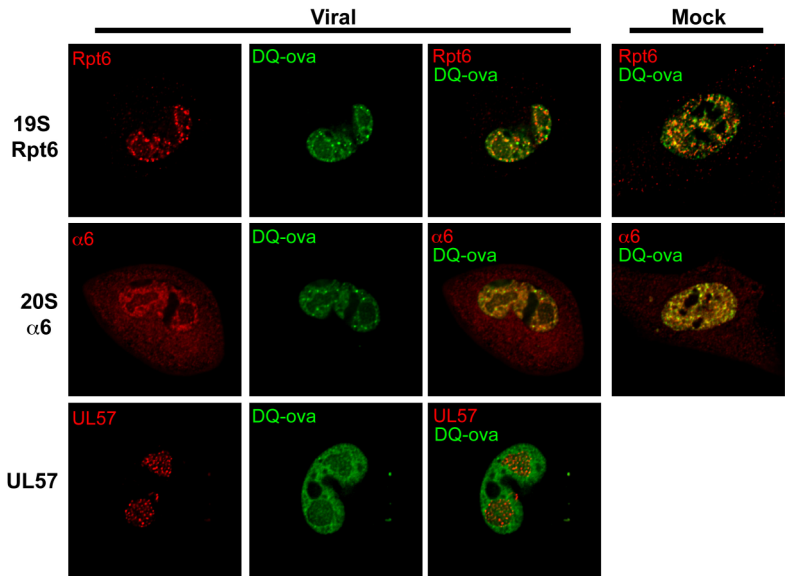

Figure 4.9 Enhanced proteolytic activity occurs in the peri-replication center region as HCMV infection progresses. HCMV or mock-infected HFFs were microinjected with DQ-ova (green) at 40 h p.i. Cells were fixed 30 min post injection and stained for 19S Rpt6, 20S α6, or UL57 (shown in red). Mid-sectional planes of representative cells imaged by deconvolution microscopy at 0.2-μm sections at a magnification of 600X under oil immersion conditions are shown.

Figure 4.10 Proteasome subunit 19S Rpn2 relocalizes to the viral replication center after the onset of viral DNA replication. Cells were fixed at the times indicated and stained for 19S Rpn2 (green), UL57 (red), and Hoescht (blue). Mid-sectional planes of representative cells imaged by deconvolution microscopy at 0.2-μm sections are shown. **A)** HFFs infected with HCMV (MOI 0.01) were fixed daily. Representative cells at different stages of infection from Day 4 are shown. Examples of pre-replication center foci (white arrow), mid-size replication centers (pink arrow), and a large coalesced replication center (orange arrow) are marked as indicated. Cells were imaged at a magnification of 400X under oil immersion conditions. **B)** Mock or virus infected HFFs (MOI 2) were treated with DMSO or PAA at the onset of infection and fixed at 48 h p.i. Cells were imaged at a magnification of 1000X under oil immersion conditions. **C)** Mock or virus infected HFFs (MOI 2) were treated with DMSO, PAA, or MG132 from 36–48 h p.i. Cells were fixed prior to treatment at 36 h p.i. and after treatment at 48 h p.i. Images were taken at a magnification of 1000X under oil immersion conditions.

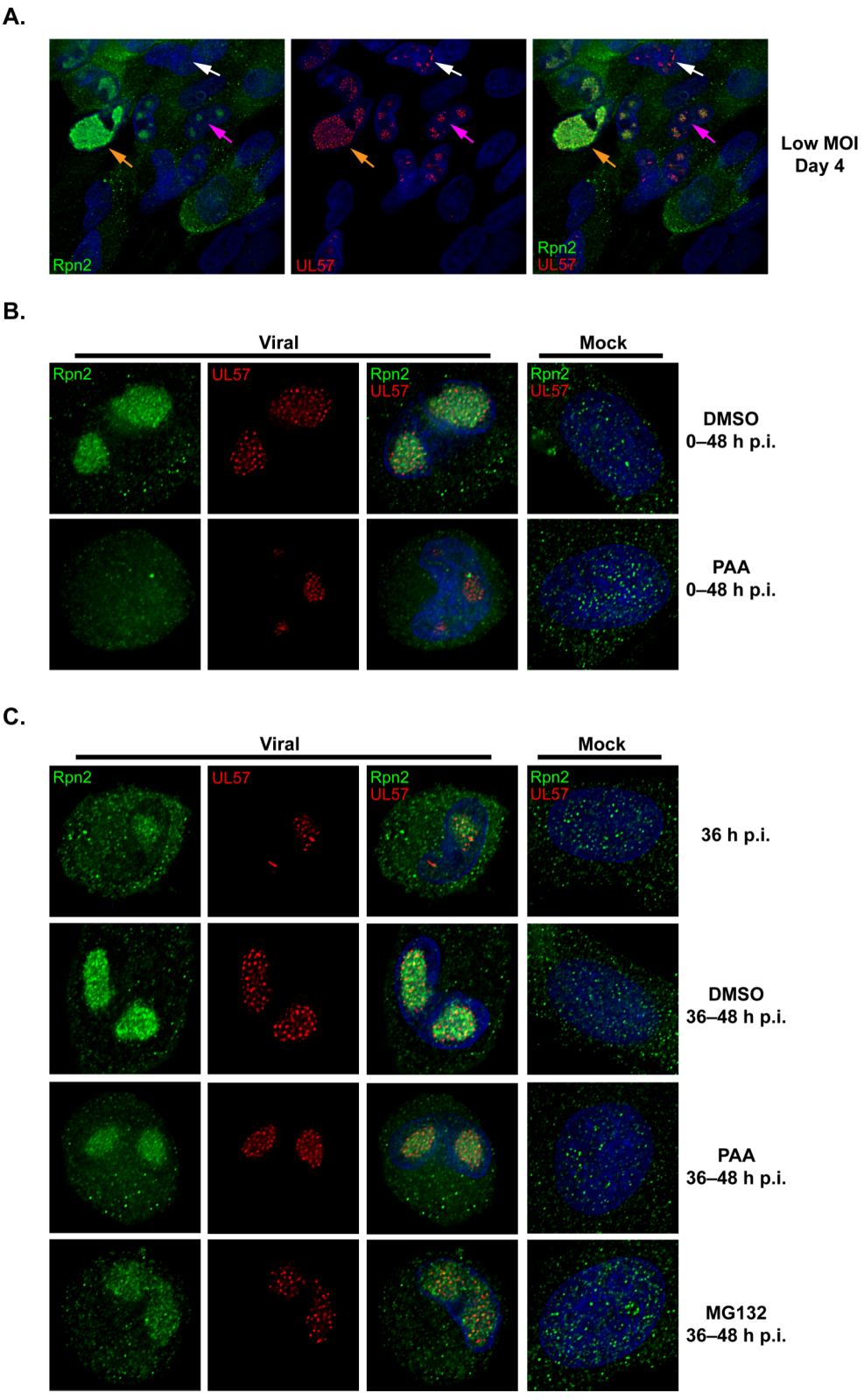
A.
Rpn2
UL57
Rpn2
UL57
Low MOI
Day 4
B.
Viral
Mock
Rpn2
UL57
Rpn2
UL57
Rpn2
UL57
DMSO
0–48 h p.i.
PAA
0–48 h p.i.
C.
Viral
Mock
Rpn2
UL57
Rpn2
UL57
Rpn2
UL57
36 h p.i.
DMSO
36–48 h p.i.
PAA
36–48 h p.i.
MG132
36–48 h p.i.

CHAPTER 5

DISCUSSION

A great appreciation for the UPS has developed over recent years as more and more studies have uncovered its many roles in regulating the cell cycle, cell division and mitotic exit, growth and differentiation, activation and silencing of transcription, signal transduction, immune and inflammatory responses, apoptosis, receptor mediated endocytosis, metabolic pathways, and general cell quality control in both a proteolytic and nonproteolytic fashion. This has also led to a greater insight into the pathogenesis of various viruses and diseases. Understandably, as a master regulator of the cell, a pathogen may utilize or subvert the UPS in rendering the cellular environment more suitable for its replication.

Inhibition of proteasome proteolytic activity appears to be detrimental to viral replication, as evidenced by HCMV (Chapter 4; (119), (69), (128)) as well as the many studies published in the past year characterizing the effects of proteasome inhibition on viral replication. In a study by Teale et al. (147), proteasome inhibition prevented formation of orthopoxvirus replication factories, DNA replication, and late gene expression, although early genes were still expressed. Proteasome inhibition also reduced avian reovirus transcription, protein translation, and replication (21) as well as vesicular stomatis virus (VSV) replication (105), whereas poliovirus replication was delayed (105). In vaccina virus, early gene expression occurred but was prolonged and viral DNA replication and subsequent intermediate and late gene expression were

inhibited upon proteasome inhibition, which is likely due to a defect in the onset of viral DNA synthesis (135). Similarly, HCMV replication was inhibited at all stages of the infection, with effects dependent on when the proteasome was inhibited (Chapter 4). Given the necessity to maintain proteasome proteolytic activity throughout the course of viral replication in the cell, it is not surprising viruses have evolved different strategies in targeting specific components of the UPS or encode proteins that would function as part of the UPS to subvert the pathway and deregulate cellular processes as needed (for review, see (122). This is especially true for HCMV, which must divert cellular resources for its own replication while evading host immune defense systems and maintaining cell viability during its relatively long replication cycle. A prime example of this is the targeting of the APC in manipulation of the cell cycle.

Extensive work has been done in the Spector lab and others in characterizing the cell cycle defects that occur during HCMV infection of quiescent cells, some of which include the deregulation of cyclin/Cdk expression, the untimely accumulation of various cell cycle regulators, and the inhibition of cellular DNA licensing complex formation, leading to cell cycle arrest (Chapter 1). The observation that many of these abnormally accumulated cell cycle proteins are substrates of the APC led to the hypothesis that the APC is inactivated during the infection (7). Initial studies done in the Spector lab (unpublished) and Wiebusch et al. (164) pointed toward a defect in the activation of the APC by its co-activator Cdh1, given its lack of association with APC3 despite elevated expression during the infection. As an extension of these studies, much of the work presented here sought to further delineate the mechanism by which HCMV disables the APC.

The complexity of the APC, both in structure and regulation, presents many potential mechanisms by which it can be disabled. The recent structural studies characterizing the APC (52, 94, 149) have been fundamental in aiding the analysis and elucidation of the mechanisms involved in its inactivation during HCMV infection. Briefly, the APC core can be separated into two main complexes: 1) the TPR subcomplex (i.e. the arc lamp) containing the TPR subunits (i.e. APC3, APC6, APC7, and APC8), which mediate activator and substrate binding, and 2) the catalytic core (i.e. the base) containing APC2 and APC11, forming the RING-cullin complex, which mediates the ubiquitination of the substrate. These two subcomplexes are bridged together through APC1, which serves as a scaffold. The TPR subcomplex is then tethered to APC1 through APC4 and APC5. As for the co-activators Cdh1 and Cdc20, at least two sequence motifs have been identified that mediate their binding to the APC. The Ile-Arg (IR) motif at the C-terminus of the activators binds the TPRs of APC3, while an as yet unidentified activator region binds the TPRs of APC8 (94). The APC binding site for the C-box, an eight-residue motif at the N-terminus of the activators, has also not been identified, but is thought to be in APC2, as removal of the subunit from the APC reduces activator binding (149). EM studies further suggest the activators to be situated between the TPR subcomplex and APC2 (52, 149).

With the interaction between Cdh1 and the APC as the focus, it was essential to first further characterize the Cdh1 and APC expressed in the infected cells, as a modification in either could potentially disrupt binding (Chapter 2). Initial analysis of Cdh1 showed it to be phosphorylated by a Cdk-independent mechanism beginning 8–12 h p.i. Phosphorylation of Cdh1 by cyclin A/Cdk2 at the end of G1 has been shown

to inhibit its binding to the APC (74, 142) as well as cause it to localize to the cytoplasm (176). Interestingly, addition of roscovitine, which inhibits Cdk1, 2, 5, 7, and 9, had no apparent effect on Cdh1 phosphorylation during the infection. This suggested that the phosphorylation might be mediated by other kinase(s), which may or may not be on Cdk phosphorylation sites. Mass spectrophotometry analysis of yeast Cdh1 has identified 19 in vivo phosphorylation sites, many of which are non-Cdk sites (42). Interestingly, mutation of the Cdk phosphorylation sites diminished phosphorylation at several of the non-Cdk sites, while mutation of the non-Cdk sites had no apparent effect on the phosphorylation of the Cdk residues (42). While mutation of the Cdk phosphorylation sites results in constitutive activation of the APC (174), mutation of the non-Cdk sites did not, which suggest that phosphorylation of Cdh1 at these sights may differentially regulate its function (42).

Recent studies characterizing the viral protein kinase UL97 as a Cdk mimic with similar cellular substrates (e.g. Rb, lamins) as well as structural similarity to Cdk2 (95), led to the hypothesis that it was also responsible for phosphorylating Cdh1 during the infection. Indeed, Cdh1 phosphorylation was not observed in experiments utilizing a UL97 deletion virus (Chapter 3). In vitro kinase assays further suggested Cdh1 to be a direct substrate of UL97. Thus, the viral mediated phosphorylation of Cdh1 can potentially inhibit its binding to the APC or may act to sequester it from the APC and/or substrates. Once the UL97 phosphorylation sites on Cdh1 are identified, it will be interesting to see whether they are sufficient to prevent binding to the APC and/or serve to regulate Cdh1 by other means.

While the UL97-mediated phosphorylation of Cdh1 may prevent its binding and/or activation of the APC, in vitro binding studies using APC isolated from mock or HCMV-infected cells at different points during the infection showed decreased binding affinity to exogenous Cdh1 at later times of the infection, while no changes were observed with the uninfected cells (Chapter 2). This experiment was important in indicating that the viral-mediated modification of Cdh1 alone may not be sufficient to account for the decreased binding of Cdh1 to the APC during the infection and suggested that the APC may also be modified during the infection.

The APC and its individual subunits were further analyzed for potential modifications that would also account for the disrupted binding to Cdh1 or its inactivation (Chapter 2 and 3). An initial question that was addressed was whether the APC core complex remained intact during the infection. To this end, APC3 co-immunoprecipitation assays using an antibody targeted against APC3 were performed over an infection time course. Surprisingly, APC1 dissociated from APC3 with similar kinetics as Cdh1, although APC7 and APC8 remained bound (Chapter 2). APC3, APC7, and APC8 are part of the TPR subcomplex, while APC1 serves as the scaffold bridging the TPR subunits with the catalytic core of APC2 and APC11. Therefore, the detachment of APC1 from the TPR subunits indicates that the APC becomes destabilized and disassembles during the infection. This loss in structural integrity may also account for the dissociation of Cdh1, as the interaction may no longer be sufficiently supported. Although Cdh1 has been shown to interact directly with APC3, APC2 has also been shown to facilitate its binding. This would also account for the inability of APC complexes isolated from infected cells to bind Cdh1 synthesized

in vitro (Chapter 2) or to Cdc20 (164). Interestingly, the spatial distribution of the TPR proteins was also altered upon virus infection, as they became more cytoplasmic while APC1 remained nuclear during the course of infection, with the same kinetics as the dissociation of the complex (Chapter 2). This brought to question whether the separation of the TPR subcomplex is the cause or result of the complex dissociation. One or more of the TPR subunits could be modified or targeted, causing it to relocate to the cytoplasm, reminiscent to the phosphorylation-induced relocalization of Cdh1 to the cytoplasm.

The key to addressing this question came from the structural studies of the APC, which has shown that the TPR subcomplex is tethered to APC1 via APC4 and APC5 (149). Moreover, the interaction between APC1, APC4, APC5, and APC8 is interdependent with the loss of any one subunit severely diminishing binding of the other three (149). Examination of APC4 and APC5 expression during an infection time course revealed a significant loss of both proteins beginning 6–8 h p.i. (Chapter 3). This was an interesting result given that all other subunits that have been examined have shown comparable, if not elevated, expression levels compared to mock-infected cells (Chapter 2 and 3, (164)). Further assays using proteasome inhibitors and qRT-PCR analysis indicated that the loss of APC5 and APC4 protein expression is due to proteasome-mediated degradation and not a lack of transcript expression (Chapter 3). Addition of proteasome inhibitors also appeared to retain APC1 association with APC3, further supporting that the dissociation of the complex is mediated through the loss of APC5 and APC4. Cdh1 binding to APC3 was also recovered to some extent, although this could be due in part to decreased UL97 expression upon proteasome

inhibition. Use of the UL97 deletion virus in these experiments may help clarify this result. Whether the degradation of APC5 is ubiquitin-mediated has yet to be verified, although experiments using the E1 inhibitor, PYR-41, also prevented the loss of APC5 and APC4 expression. A strong candidate for inducing ubiquitin-independent degradation of the subunits is the viral tegument protein pp71 since it has been shown to target the ubiquitin-independent degradation of Daxx and unphosphorylated Rb, p130, and p107. However, initial studies using UV-inactivated virus indicated that the viral tegument proteins alone are insufficient to mediate the degradation and that some viral early protein expression is required (Chapter 3).

Based on the experimental conditions of these studies, the critical time window for the viral-mediated inactivation of the APC appears to be 6–8 h p.i. At this time, there is sufficient viral gene and protein expression to mediate the phosphorylation of Cdh1 and the proteasome-dependent degradation of APC5 and APC4, followed by the dissociation of the complex and accumulation of substrates. Whether the UL97-mediated phosphorylation of Cdh1 and the targeted degradation of APC5 and APC4 are redundant mechanisms in ensuring the inactivation of the APC has not been resolved. It is possible that the phosphorylation of Cdh1 may facilitate replication of the virus by other means, or Cdh1 may simply be another cellular protein with phosphorylation sites recognized by UL97. It is clear, however, that Cdh1 phosphorylation and APC subunit degradation occur via independent pathways, as APC5 and APC4 are still degraded and APC dissociation still occurs in the ΔUL97 infection with the same kinetics as wild type virus (Chapter 3).

Whether APC inactivation is essential to the infection remains unresolved. Disabling of the APC appears to be a common strategy adopted by different viruses to arrest the cell cycle. Adenovirus E4orf4 and chicken anemia virus' apoptin have been shown to target the APC to induce G_2/M arrest (73, 148). A recent report suggests poxvirus PACR acts as an APC11 mimic to inhibit APC activity, and deletion of PACR significantly impaired viral growth (100). APC inactivation may also be required to allow HCMV replication proteins to be stably expressed since several of them have potential KEN and/or D boxes. Bovine papillomavirus replicative helicase E1 has been identified as an APC target; addition of APC inhibitor Emi1 or disruption of E1's KEN and D-box motifs stabilized the protein and increased viral DNA replication (97). The targeted degradation of APC5 also brings to question whether the destabilization of the APC is simply the result of the loss of APC5 and whether the inhibition of APC5 in particular is necessary for efficient viral replication. In the context of the APC, APC5 mostly functions in a structural capacity in tethering the TPR subunits to the rest of the complex. APC5 and APC7 have also been shown to interact and stimulate the activities of CBP and p300, universal coactivators (154). The inhibition of APC5 may facilitate the downregulation of CBP and in turn its downstream targets (e.g. p53).

Whether or not the destabilization of the APC is necessary for viral replication, the ramifications of its inactivation may contribute to the clinical complications caused by the infection. While numerous studies have characterized the role of the APC in regulating the cell cycle, several recent studies have also highlighted its importance in regulating neurobiology, differentiation, and tumor suppression. Congenital HCMV

infection may lead to birth defects (i.e. mental retardation, hearing loss, and vision loss), which may be present at birth or may not develop until a later age. Impaired brain development is likely linked to HCMV infection and subsequent deregulation of neuronal cells. HCMV readily infects neuronal precursor cells (NPCs) as well as neurons and astroglia differentiated from NPCs (20, 21, 107). NPC differentiation into neurons is attenuated upon HCMV infection, and higher apoptosis rates have been observed in infected cells following differentiation (107). The neuronal defects caused by the infection may be associated with the inactivation of the APC. APC^{Cdh1} is involved in regulating axon growth and patterning, synapse development, and neuronal survival (for review see reference, (71)). A recent study has also shown its importance in preventing glycolysis-associated oxidative stress and cell death in neurons (50). Pfkfb3, which mediates the downstream activation of glycolysis, is maintained at low levels through APC^{Cdh1}-mediated degradation in neurons. Upregulation of Pfkfb3 in neurons, either through the inhibition of Cdh1 or overexpression of Pfkfb3, led to the activation of glycolysis, along with decreased oxidation of glucose, oxidative stress, and apoptotic death (50). Therefore, inactivation of the APC may cause deleterious effects on neurons or neuronal development. Deregulation of APC^{Cdh1} can also contribute to genomic instability and tumorigenesis (for review see reference, (162)). Thus, understanding the mechanisms involved in the inactivation of the APC not only provides further insight into the molecular pathology of the infection but also to the clinical manifestations.

REFERENCES

1. **Ahn, J.-H., W.-J. Jang, and G. S. Hayward.** 1999. The human cytomegalovirus IE2 and UL112-113 proteins accumulate in viral DNA replication compartments that initiate from the periphery of promyelocytic leukemia protein-associated nuclear bodies (PODs or ND10). J. Virol. **73:**10458-10471.

2. **Baek, M.-C., P. M. Krosky, A. Pearson, and D. M. Coen.** 2004. Phosphorylation of the RNA polymerase II carboxyl-terminal domain in human cytomegalovirus-infected cells and in vitro by the viral UL97 protein kinase. Virol. **324:**184-193.

3. **Bajorek, M., and M. H. Glickman.** 2004. Keepers at the final gates: regulatory complexes and gating of the proteasome channel. Cell. Mol. Life Sci. **61:**1579-88.

4. **Baldick, C., Jr., A. Marchini, C. E. Patterson, and T. Shenk.** 1997. Human cytomegalovirus tegument protein pp71 (ppUL82) enhances the infectivity of viral DNA and accelerates the infectious cycle. J. Virol. **71:**4400-4408.

5. **Banks, L., D. Pim, and M. Thomas.** 2003. Viruses and the 26S proteasome: hacking into destruction. Trends Biochem Sci **28:**452-9.

6. **Biron, K. K., R. J. Harvey, S. C. Chamberlain, S. S. Good, A. A. Smith, M. G. Davis, C. L. Talarico, W. H. Miller, R. Ferris, R. E. Dornsife, S. C. Stanat, J. C. Drach, L. B. Townsend, and G. W. Koszalka.** 2002. Potent and selective inhibition of human cytomegalovirus replication by 1263W94, a benzimidazole L-riboside with a unique mode of action. Antimicrob Agents Chemother **46:**2365-72.

7. **Biswas, N., V. Sanchez, and D. H. Spector.** 2003. Human cytomegalovirus infection leads to accumulation of geminin and inhibition of the licensing of cellular DNA replication. J. Virol. **77:**2369-2376.

8. **Blanchette, P., and P. E. Branton.** 2009. Manipulation of the ubiquitin-proteasome pathway by small DNA tumor viruses. Virology **384:**317-23.

9. **Borissenko, L., and M. Groll.** 2007. 20S proteasome and its inhibitors: crystallographic knowledge for drug development. Chem Rev **107:**687-717.

10. **Bresnahan, W. A., I. Boldogh, E. A. Thompson, and T. Albrecht.** 1996. Human cytomegalovirus inhibits cellular DNA synthesis and arrests productively infected cells in late G1. Virology **224:**156-160.

11. **Bresnahan, W. A., and T. E. Shenk.** 2000. UL82 virion protein activates expression of immediate early viral genes in human cytomegalovirus-infected cells. Proc. Natl. Acad. Sci. U.S.A. **97:**14506-11.

12. **Bresnahan, W. A., E. A. Thompson, and T. Albrecht.** 1997. Human cytomegalovirus infection results in altered Cdk2 subcellular localization. J. Gen. Virol. **78:**1993-1997.

13. **Britt, W.** 2008. Manifestations of human cytomegalovirus infection: proposed mechanisms of acute and chronic disease. Current Topics in Microbiology and Immunology **325:**417.

14. **Burch, A. D., and S. K. Weller.** 2005. Herpes simplex virus type 1 DNA polymerase requires the mammalian chaperone hsp90 for proper localization to the nucleus. J Virol **79:**10740-9.

15. **Burch, A. D., and S. K. Weller.** 2004. Nuclear sequestration of cellular chaperone and proteasomal machinery during herpes simplex virus type 1 infection. J. Virol. **78:**7175-7185.

16. **Cantrell, S. R., and W. A. Bresnahan.** 2005. Interaction between the human cytomegalovirus UL82 gene product (pp71) and hDaxx regulates immediate-early gene expression and viral replication. J. Virol. **79:**7792-7802.

17. **Castillo, J. P., and T. M. Kowalik.** 2002. Human cytomegalovirus immediate early proteins and cell growth control. Gene **290:**19-34.

18. **Castro, A., C. Bernis, S. Vigneron, J. C. Labbe, and T. Lorca.** 2005. The anaphase-promoting complex: a key factor in the regulation of cell cycle. Oncogene **24:**314-325.

19. **Challacombe, J. F., A. Rechtsteiner, R. Gottardo, L. M. Rocha, E. P. Browne, T. Shenk, M. R. Altherr, and T. S. Brettin.** 2004. Evaluation of the host transcriptional response to human cytomegalovirus infection. Physiol. Genomics **18:**51-62.

20. **Cheeran, M., S. Hu, H. Ni, W. Sheng, J. Palmquist, P. Peterson, and J. Lokensgard.** 2005. Neural precursor cell susceptibility to human cytomegalovirs diverges along glial or neuronal differentiation pathways. J Neurosci Res **82:**839–50.

21. **Chen, G., Y. Luo, X. Wang, Z. Zhao, H. Liu, H. Zhang, and Z. Li.** 2009. A relatively simple and economical protocol for proteomic analyses of human 20S proteasome: Compatible with both scaled-up and scaled-down purifications. Electrophoresis **30:**2422-2430.

22. **Chen, Z., E. Knutson, A. Kurosky, and T. Albrecht.** 2001. Degradation of p21cip1 in cells productively infected with human cytomegalovirus. J. Virol. **75:**3613-3625.

23. **Ciechanover, A.** 1994. The ubiquitin-proteasome proteolytic pathway. Cell **79:**13-21.

24. **Collins, G. A., and W. P. Tansey.** 2006. The proteasome: a utility tool for transcription? Curr. Opin. Genet. Dev. **16:**197-202.

25. **Dai-Ju, J. Q., L. Li, L. A. Johnson, and R. M. Sandri-Goldin.** 2006. ICP27 interacts with the C-terminal domain of RNA polymerase II and facilitates its recruitment to herpes simplex virus 1 transcription sites, where it undergoes proteasomal degradation during infection. J. Virol. **80:**3567-3581.

26. **De Azevedo, W. F., S. Leclerc, L. Meijer, L. Havlicek, M. Strnad, and S. H. Kim.** 1997. Inhibition of cyclin-dependent kinases by purine analogues: crystal structure of human cdk2 complexed with roscovitine. Eur. J. Biochem. **243:**518-526.

27. **Demartino, G. N., and T. G. Gillette.** 2007. Proteasomes: machines for all reasons. Cell **129:**659-62.

28. **Dittmer, D., and E. S. Mocarski.** 1997. Human cytomegalovirus infection inhibits G1/S transition. J. Virol. **71:**1629-1634.

29. **Dube, P., F. Herzog, C. Gieffers, B. Sander, D. Riedel, S. A. Muller, A. Engel, J. M. Peters, and H. Stark.** 2005. Localization of the coactivator Cdh1 and the cullin subunit Apc2 in a cryo-electron microscopy model of vertebrate APC/C. Mol. Cell **20:**867-879.

30. **Dyson, N.** 1998. The regulation of E2F by pRB-family proteins. Genes Dev. **12:**2245-2262.

31. **Edamatsu, H., C. L. Gau, T. Nemoto, L. Guo, and F. Tamanoi.** 2000. Cdk inhibitors, roscovitine and olomoucine, synergize with farnesyltransferase inhibitor (FTI) to induce efficient apoptosis of human cancer cell lines. Oncogene **19:**3059-3068.

32. **Ezhkova, E., and W. P. Tansey.** 2004. Proteasomal ATPases link ubiquitylation of histone H2B to methylation of histone H3. Mol. Cell **13:**435-442.

33. **Finley, D.** 2009. Recognition and Processing of Ubiquitin-Protein Conjugates by the Proteasome. Annu. Rev. Biochem. **78:**477-513.

34. **Fortunato, E. A., V. Sanchez, J. Y. Yen, and D. H. Spector.** 2002. Infection of cells with human cytomegalovirus during S phase results in a blockade to immediate-early gene expression that can be overcome by inhibition of the proteasome. J. Virol. **76:**5369-5379.

35. **Fortunato, E. A., and D. H. Spector.** 1998. p53 and RPA are sequestered in viral replication centers in the nuclei of cells infected with human cytomegalovirus. J. Virol. **72:**2033-2039.

36. **Fraser, K. A., and S. A. Rice.** 2007. Herpes simplex virus immediate-early protein ICP22 triggers loss of serine 2-phosphorylated RNA polymerase II. J. Virol. **81:**5091-5101.

37. **Fraser, K. A., and S. A. Rice.** 2005. Herpes simplex virus type 1 infection leads to loss of serine-2 phosphorylation on the carboxyl-terminal domain of RNA polymerase II. J. Virol. **79:**11323-11334.

38. **Gao, G., and H. Luo.** 2006. The ubiquitin-proteasome pathway in viral infections. Can. J. Physiol. Pharmacol. **84:**5-14.

39. **Gieffers, C., P. Dube, J. R. Harris, H. Stark, and J. M. Peters.** 2001. Three-dimensional structure of the anaphase-promoting complex. Mol. Cell **7:**907-913.

40. **Glickman, M. H., and A. Ciechanover.** 2002. The ubiquitin-proteasome proteolytic pathway: destruction for the sake of construction. Physiol. Rev. **82:**373-428.

41. **Glickman, M. H., and D. Raveh.** 2005. Proteasome plasticity. FEBS Lett. **579:**3214-3223.

42. **Hall, M. C., E. N. Warren, and C. H. Borchers.** 2004. Multi-kinase phosphorylation of the APC/C activator Cdh1 revealed by mass spectrometry. Cell Cycle **3:**1278-84.

43. **Hamazaki, J., S. Iemura, T. Natsume, H. Yashiroda, K. Tanaka, and S. Muratua.** 2006. A novel proteasome interacting protein recruits the deubiquitinating enzyme UCH37 to 26S proteasomes. EMBO J. **25:**4524-4536.

44. **Hamirally, S., J. Kamil, Y. Ndassa-Colday, A. Lin, W. Jahng, M. Baek, S. Noton, L. Silva, M. Simpson-Holley, and D. Knipe.** 2009. Viral mimicry of Cdc2/cyclin-dependent kinase 1 mediates disruption of nuclear lamina during human cytomegalovirus nuclear egress. PLoS Pathogens **5**.

45. **Harel, N. Y., and J. C. Alwine.** 1998. Phosphorylation of the human cytomegalovirus 86-kilodalton immediate-early protein IE2. J. Virol. **72:**5481-5492.

46. **Hassink, G. C., M. T. Barel, S. B. Van Voorden, M. Kikkert, and E. J. Wiertz.** 2006. Ubiquitination of MHC class I heavy chains is essential for dislocation by human cytomegalovirus-encoded US2 but not US11. J Biol Chem **281:**30063-71.

47. **Hegde, A. N., and S. C. Upadhya.** 2006. Proteasome and transcription: a destroyer goes into construction. Bioessays **28:**235-9.

48. **Heilman, D. W., M. R. Green, and J. G. Teodoro.** 2005. The anaphase promoting complex: a critical target for viral proteins and anti-cancer drugs. Cell Cycle **4:**560-563.

49. **Heilman, D. W., J. G. Teodoro, and M. R. Green.** 2006. Apoptin nucleocytoplasmic shuttling is required for cell type-specific localization, apoptosis, and recruitment of the anaphase-promoting complex/cyclosome to PML bodies. J. Virol. **80:**7535-7545.

50. **Herrero-Mendez, A., A. Almeida, E. Fernández, C. Maestre, S. Moncada, and J. P. Bolaños.** 2009. The bioenergetic and antioxidant status of neurons is controlled by continuous degradation of a key glycolytic enzyme by APC/C-Cdh1. Nat Cell Biol **11:**747-52.

51. **Hertel, L., and E. S. Mocarski.** 2004. Global analysis of host cell gene expression late during cytomegalovirus infection reveals extensive dysregulation of cell cycle gene expression and induction of pseudomitosis independent of US28 function. J. Virol. **78:**11988-12011.

52. **Herzog, F., I. Primorac, P. Dube, P. Lenart, B. Sander, K. Mechtler, H. Stark, and J.-M. Peters.** 2009. Structure of the anaphase-promoting

complex/cyclosome interacting with a mitotic checkpoint complex. Science **323:**1477-81.

53. **Hicke, L.** 2001. Protein regulation by monoubiquitin. Nature Reviews Molecular Cell Biology **2:**195-201.

54. **Hirsch, C., and H. Ploegh.** 2000. Intracellular targeting of the proteasome. Trends Cell Biol **10:**268–72.

55. **Hofmann, H., H. Sindre, and T. Stamminger.** 2002. Functional interaction between the pp71 protein of human cytomegalovirus and the PML-interacting protein human Daxx. J. Virol. **76:**5769-5783.

56. **Hume, A. J., J. S. Finkel, J. P. Kamil, D. M. Coen, M. R. Culbertson, and R. F. Kalejta.** 2008. Phosphorylation of retinoblastoma protein by viral protein with cyclin-dependent kinase function. Science **320:**797-799.

57. **Hwang, J., and R. F. Kalejta.** 2007. Proteasome-dependent, ubiquitin-independent degradation of Daxx by the viral pp71 protein in human cytomegalovirus-infected cells. Virology **367:**334-8.

58. **Ishov, A. M., and G. G. Maul.** 1996. The periphery of nuclear domain 10 (ND10) as site of DNA virus deposition. J. Cell Biol. **134:**815-826.

59. **Ishov, A. M., R. M. Stenberg, and G. G. Maul.** 1997. Human cytomegalovirus immediate early interaction with host nuclear structures: Definition of an immediate transcript environment. J. Cell Biol. **138:**5-16.

60. **Ishov, A. M., O. V. Vladimirova, and G. G. Maul.** 2002. Daxx-mediated accumulation of human cytomegalovirus tegument protein pp71 at ND10 facilitates initiation of viral infection at these nuclear domains. J. Virol. **76:**7705-7712.

61. **Jault, F. M., J.-M. Jault, F. Ruchti, E. A. Fortunato, C. Clark, J. Corbeil, D. D. Richman, and D. H. Spector.** 1995. Cytomegalovirus infection induces high levels of cyclins, phosphorylated RB, and p53, leading to cell cycle arrest. J. Virol. **69:**6697-6704.

62. **Johnson, D. C., and N. R. Hegde.** 2002. Inhibition of the MHC class II antigen presentation pathway by human cytomegalovirus. Curr Top Microbiol Immunol **269:**101-15.

63. **Jørgensen, J. P., A.-M. Lauridsen, P. Kristensen, K. Dissing, A. H. Johnsen, K. B. Hendil, and R. Hartmann-Petersen.** 2006. Adrm1, a putative

cell adhesion regulating protein, is a novel proteasome-associated factor. Journal of molecular biology **360:**1043-52.

64. **Kalejta, R.** 2008. Functions of Human Cytomegalovirus Tegument Proteins Prior to Immediate Early Gene Expression. Curr. Top. Microbiol. Immunol.

65. **Kalejta, R. F., J. T. Bechtel, and T. Shenk.** 2003. Human cytomegalovirus pp71 stimulates cell cycle progression by inducing the proteasome-dependent degradation of the retinoblastoma family of tumor suppressors. Mol. Cell. Biol. **23:**1885-1895.

66. **Kalejta, R. F., and T. Shenk.** 2003. Proteasome-dependent, ubiquitin-independent degradation of the Rb family of tumor suppressors by the human cytomegalovirus pp71 protein. Proc. Natl. Acad. Sci. U.S.A. **100:**3263-3268.

67. **Kaneko, T., J. Hamazaki, S.-i. Iemura, K. Sasaki, K. Furuyama, T. Natsume, K. Tanaka, and S. Murata.** 2009. Assembly Pathway of the Mammalian Proteasome Base Subcomplex Is Mediated by Multiple Specific Chaperones. Cell **137:**914-925.

68. **Kapasi, A. J., and D. H. Spector.** 2008. Inhibition of the cyclin-dependent kinases at the beginning of the human cytomegalovirus infection specifically alters the levels and localization of the RNA polymerase II carboxyl-terminal domain kinases cdk9 and cdk7 at the viral transcriptosome. J. Virol. **82:**394-407.

69. **Kaspari, M., N. Tavalai, T. Stamminger, A. Zimmermann, R. Schilf, and E. Bogner.** 2008. Proteasome inhibitor MG132 blocks viral DNA replication and assembly of human cytomegalovirus. FEBS Lett **582:**666-72.

70. **Kawaguchi, Y., T. Matsumura, B. Roizman, and K. Hirai.** 1999. Cellular elongation factor 1delta is modified in cells infected with representative alpha-, beta-, or gammaherpesviruses. J. Virol. **73:**4456-60.

71. **Kim, A. H., and A. Bonni.** 2007. Thinking within the D box: initial identification of Cdh1-APC substrates in the nervous system. Mol Cell Neurosci **34:**281-7.

72. **Kinyamu, H. K., W. N. Jefferson, and T. K. Archer.** 2008. Intersection of nuclear receptors and the proteasome on the epigenetic landscapr. Environmental and Molecular Mutagenesis **49:**83–95.

73. **Kornitzer, D., R. Sharf, and T. Kleinberger.** 2001. Adenovirus E4orf4 protein induces PP2A-dependent growth arrest in Saccharomyces cerevisiae

and interacts with the anaphase-promoting complex/cyclosome. J. Cell Bio. **154:**331-344.

74. **Kramer, E. R., N. Scheuringer, A. V. Podtelejnikov, M. Mann, and J.-M. Peters.** 2000. Mitotic regulation of the APC activator proteins CDC20 and CDH1. Mol. Biol. Cell **11:**1555-1569.

75. **Krosky, P. M., M.-C. Baek, and D. M. Coen.** 2003. The human cytomegalovirus UL97 protein kinase, an antiviral drug target, is required at the stage of nuclear egress. J. Virol. **77:**905-14.

76. **Landolfo, S., M. Gariglio, G. Gribaudo, and D. Lembo.** 2003. The human cytomegalovirus. Pharmacol Ther **98:**269-97.

77. **Lassot, I., D. Latreille, E. Rousset, M. Sourisseau, L. K. Linares, C. Chable-Bessia, O. Coux, M. Benkirane, and R. E. Kiernan.** 2007. The Proteasome Regulates HIV-1 Transcription by Both Proteolytic and Nonproteolytic Mechanisms. Mol. Cell **25:**369-383.

78. **Lee, D., E. Ezhkova, B. Li, S. G. Pattenden, W. P. Tansey, and J. L. Workman.** 2005. The proteasome regulatory particle alters the SAGA coactivator to enhance its interactions with transcriptional activators. Cell **123:**423-36.

79. **Lee, S.-O., S. Hwang, J. Park, B. Park, B.-S. Jin, S. Lee, E. Kim, S. Cho, Y. Kim, K. Cho, J. Shin, and K. Ahn.** 2005. Functional dissection of HCMV US11 in mediating the degradation of MHC class I molecules. Biochem Biophys Res Commun **330:**1262-7.

80. **Li, L., L. A. Johnson, J. Q. Dai-Ju, and R. M. Sandri-Goldin.** 2008. Hsc70 focus formation at the periphery of HSV-1 transcription sites requires ICP27. PLoS ONE **3:**e1491.

81. **Lim, H. H., P. Y. Goh, and U. Surana.** 1998. Cdc20 is essential for the cyclosome-mediated proteolysis of both Pds1 and Clb2 during M phase in budding yeast. Curr. Biol. **8:**231-234.

82. **Listovsky, T., Y. S. Oren, Y. Yudkovsky, H. M. Mahbubani, A. M. Weiss, M. Lebendiker, and M. Brandeis.** 2004. Mammalian Cdh1/Fzr mediates its own degradation. EMBO J. **23:**1619-26.

83. **Listovsky, T., A. Zor, A. Laronne, and M. Brandeis.** 2000. Cdk1 is essential for mammalian cyclosome/APC regulation. Experimental Cell Research **255:**184-191.

84. **Livingston, C. M., N. A. Deluca, D. E. Wilkinson, and S. K. Weller.** 2008. Oligomerization of ICP4 and Rearrangement of Heat Shock Proteins May Be Important for Herpes Simplex Virus Type 1 Prereplicative Site Formation. Journal of Virology **82:**6324-6336.

85. **Livingston, C. M., M. F. Ifrim, A. E. Cowan, and S. K. Weller.** 2009. Virus-Induced Chaperone-Enriched (VICE) domains function as nuclear protein quality control centers during HSV-1 infection. PLoS Pathogens **5:**e1000619.

86. **Loureiro, J., and H. L. Ploegh.** 2006. Antigen presentation and the ubiquitin-proteasome system in host-pathogen interactions. Adv Immunol **92:**225-305.

87. **Lu, M., and T. Shenk.** 1996. Human cytomegalovirus infection inhibits cell cycle progression at multiple points, including the transition from G1 to S. J. Virol. **70:**8850-8857.

88. **Ludlow, J. W., J. Shon, J. M. Pipas, D. M. Livingston, and J. A. DeCaprio.** 1990. The retinoblastoma susceptibility gene product undergoes cell cycle-dependent dephosphorylation and binding to and release from SV40 large T. Cell **60:**387-396.

89. **Lukas, C., C. S. Sorensen, E. Kramer, E. Santoni-Rugiu, C. Lindeneg, J.-M. Peters, J. Bartek, and J. Lukas.** 1999. Accumulation of cyclin B1 requires E2F and cyclin-A-dependent rearrangement of the anaphase-promoting complex. Nature **401:**815-818.

90. **Luo, M. H., K. Rosenke, K. Czornak, and E. A. Fortunato.** 2007. Human cytomegalovirus disrupts both ataxia telangiectasia mutated protein (ATM)-and ATM-Rad3-related kinase-mediated DNA damage responses during lytic infection. J. Virol. **81:**1934-1950.

91. **Maiorano, D., J. Moreau, and M. Mechali.** 2000. XCDT1 is required for the assembly of pre-replicative complexes in *Xenopus laevis.* Nature **404:**622-625.

92. **Marschall, M., M. Freitag, P. Suchy, D. Romaker, R. Kupfer, M. Hanke, and T. Stamminger.** 2003. The protein kinase pUL97 of human cytomegalovirs interacts with and phosphorylates the DNA polymerase processivity factor pUL44. Virology **311:**60–71.

93. **Marshall, K. R., K. V. Rowley, A. Rinaldi, I. P. Nicholson, A. M. Ishov, G. G. Maul, and C. M. Preston.** 2002. Activity and intracellular localization of the human cytomegalovirus protein pp71. J. Gen. Virol. **83:**1601-1612.

94. **Matyskiela, M., M. Rodrigo-Brenni, and D. Morgan.** 2009. Mechanisms of ubiquitin transfer by the anaphase-promoting complex. J Biol **8:**92.

95. **Maurer, S. Auerochs, A. Marzi, H. Sticht, and M. Marschall.** 2006. Analysis of the Structure-Activity Relationship of Four Herpesviral UL97 Subfamily Protein Kinases …. J. Med. Chem.

96. **McElroy, A. K., R. S. Dwarakanath, and D. H. Spector.** 2000. Dysregulation of cyclin E gene expression in human cytomegalovirus-infected cells requires viral early gene expression and is associated with changes in the Rb-related protein p130. J. Virol. **74:**4192-4206.

97. **Mechali, F., C.-Y. Hsu, A. Castro, T. Lorca, and C. Bonne-Andrea.** 2004. Bovine papillomavirus replicative helicase E1 is a target of the ubiquitin ligase APC. J. Virol. **78:**2615-9.

98. **Meijer, L., A. Borgne, O. Mulner, J. P. J. Chong, J. J. Blow, N. Inagaki, M. Inagaki, J. G. Delcros, and J. P. Molinoux.** 1997. Biochemical and cellular effects of roscovitine, a potent and selective inhibitor of the cyclin-dependent kinases cdc2, cdk2 and cdk5. Eur. J. Biochem. **243:**527-536.

99. **Mittenberg, A., T. Moiseeva, and N. Barlev.** 2008. Role of proteasomes in transcription and their regulation by covalent modifications. Frontiers in bioscience: a journal and virtual library **13:**7184.

100. **Mo, M., S. Fleming, and A. Mercer.** 2009. Cell cycle deregulation by a poxvirus partial mimic of anaphase-promoting complex subunit 11. Proc Natl Acad Sci USA.

101. **Mocarski, E. S., T. Shenk, and R. F. Pass.** 2007. Cytomegaloviruses. *In* D. M. Knipe and P. M. Howley (ed.), Fields' Virology, Fifth ed, vol. 2. Wolters Kluwer Health/Lippincott Williams & Wilkins, Philadelphia.

102. **Muganda, P., O. Mendoza, J. Hernandez, and Q. Qian.** 1994. Human cytomegalovirus elevates levels of the cellular protein p53 in infected fibroblasts. J. Virol. **68:**8028-8034.

103. **Murphy, E., and T. Shenk.** 2008. Human cytomegalovirus genome. Current Topics in Microbiology and Immunology **325:**1-20.

104. **Nelbock, P., P. J. Dillon, A. Perkins, and C. A. Rosen.** 1990. A cDNA for a protein that interacts with the human immunodeficiency virus tat transactivator. Science **248:**1650-1653.

105. **Neznanov, N., E. M. Dragunsky, K. M. Chumakov, L. Neznanova, R. C. Wek, A. V. Gudkov, and A. K. Banerjee.** 2008. Different effect of proteasome inhibition on vesicular stomatitis virus and poliovirus replication. PLoS ONE **3:**e1887.

106. **Nishitani, H., Z. Lygerou, T. Nishimoto, and P. Nurse.** 2000. The Cdt1 protein is required to license DNA for replication in fission yeast. Nature **404:**625-628.

107. **Odeberg, J., N. Wolmer, S. Falci, M. Westgren, A. Seiger, and C. Söderberg-Nauclér.** 2006. Human cytomegalovirus inhibits neuronal differentiation and induces apoptosis in human neural precursor cells. J Virol **80:**8929-39.

108. **Ohana, B., P. A. Moore, S. M. Ruben, C. D. Southgate, M. R. Green, and C. A. Rosen.** 1993. The type 1 human immunodeficiency virus Tat binding protein is a transcriptional activator belonging to an additional family of evolutionary conserved genes. Proceedings of the National Academy of Sciences USA **90:**138-142.

109. **Pass, R. F.** 2001. Cytomegalovirus, p. 2675-2705. *In* D. M. Knipe and P. M. Howley (ed.), Fields Virology, 4th ed, vol. 2. Lippincott Williams & Wilkins, Philadelphia.

110. **Pass, R. F., A. M. Duliegè, S. Boppana, R. Sekulovich, S. Percell, W. Britt, and R. L. Burke.** 1999. A subunit cytomegalovirus vaccine based on recombinant envelope glycoprotein B and a new adjuvant. Journal of Infectious Diseases **180:**970-5.

111. **Passmore, L. A., C. R. Booth, C. Venien-Bryan, S. J. Ludtke, C. Fioretto, L. N. Johnson, W. Chiu, and D. Barford.** 2005. Structural analysis of the anaphase-promoting complex reveals multiple active sites and insights into polyubiquitylation. Mol. Cell **20:**855-866.

112. **Penfold, M. E., and E. S. Mocarski.** 1997. Formation of cytomegalovirus DNA replication compartments defined by localization of viral proteins and DNA synthesis. Virology **239:**46-61.

113. **Peters, J.-M.** 2006. The anaphase promoting complex/cyclosome: a machine designed to destroy. Nat. Rev. Mol. Cell Biol. **7:**644-56.

114. **Pickart, C. M.** 2001. Mechanisms underlying ubiquitination. Annu Rev Biochem **70:**503-33.

115. **Pickart, C. M., and R. E. Cohen.** 2004. Proteasomes and their kin: proteases in the machine age. Nat. Rev. Mol. Cell Biol. **5:**177-187.

116. **Powers, C., V. DeFilippis, D. Malouli, and K. Fruh.** 2008. Cytomegalovirus immune evasion. Current Topics in Microbiology and Immunology **325:**333-360.

117. **Prichard, M. N., N. Gao, S. Jairath, G. Mulamba, P. Krosky, D. M. Coen, B. O. Parker, and G. S. Pari.** 1999. A recombinant human cytomegalovirus with a large deletion in UL97 has a severe replication deficiency. J Virol **73:**5663-5670.

118. **Prichard, M. N., E. Sztul, S. L. Daily, A. L. Perry, S. L. Frederick, R. B. Gill, C. B. Hartline, D. N. Streblow, S. M. Varnum, R. D. Smith, and E. R. Kern.** 2008. Human cytomegalovirus UL97 kinase activity is required for the hyperphosphorylation of retinoblastoma protein and inhibits the formation of nuclear aggresomes. J. Virol. **82:**5054-5067.

119. **Prösch, S., C. Priemer, C. Höflich, C. Liebenthaf, N. Babel, D. H. Krüger, and H.-D. Volk.** 2003. Proteasome inhibitors: a novel tool to suppress human cytomegalovirus replication and virus-induced immune modulation. Antivir Ther (Lond) **8:**555-67.

120. **Qiu, X.-B., S.-Y. Ouyang, C.-J. Li, S. Miao, L. Wang, and A. L. Goldberg.** 2006. hRpn13/ADRM1/GP110 is a novel proteasome subunit that binds the deubiquitinating enzyme, UCH37. EMBO J. **25:**5742-5753.

121. **Radkov, S. A., P. Kellam, C. B. Oct, and 6(10):1121-7.** 2000. The latent nuclear antigen of Kaposi sarcoma-associated herpesvirus targets the retinoblastoma-E2F pathway and with the oncogene Hras transforms primary rat cells. Nat. Med. **6:**1121-1127.

122. **Randow, F., and P. J. Lehner.** 2009. Viral avoidance and exploitation of the ubiquitin system. Nat Cell Biol **11:**527-34.

123. **Rasti, M., R. J. A. Grand, A. F. Yousef, M. Shuen, J. S. Mymryk, P. H. Gallimore, and A. S. Turnell.** 2006. Roles for APIS and the 20S proteasome in adenovirus E1A-dependent transcription. EMBO J. **25:**2710-22.

124. **Rechsteiner, M., and C. P. Hill.** 2005. Mobilizing the proteolytic machine: cell biological roles of proteasome activators and inhibitors. Trends Cell Biol **15:**27–33.

125. **Reddehase, M. J., M. Balthesen, M. Rapp, S. Jonji*c, I. Pavi*c, and U. H. Koszinowski.** 1994. The conditions of primary infection define the load of latent viral genome in organs and the risk of recurrent cytomegalovirus disease. Journal of Experimental Medicine **179:**185-93.

126. **Reed, S. H., and T. G. Gillette.** 2007. Nucleotide excision repair and the ubiquitin proteasome pathway--do all roads lead to Rome? DNA Repair (Amst) **6:**149-56.

127. **Rialland, M., F. Sola, and C. Santocanale.** 2002. Essential role of human CDT1 in DNA replication and chromatin licensing. J. Cell Sci. **115:**1435-1440.

128. **Sadanari, H., J. Tanaka, Z. Li, R. Yamada, K. Matsubara, and T. Murayama.** 2009. Proteasome inhibitor differentially regulates expression of the major immediate early genes of human cytomegalovirus in human central nervous system-derived cell lines. Virus Res **142:**68-77.

129. **Saffert, R. T., and R. F. Kalejta.** 2006. Inactivating a cellular intrinsic immune defense mediated by Daxx is the mechanism through which the human cytomegalovirus pp71 protein stimulates viral immediate-early gene expression. J. Virol. **80:**3863-3871.

130. **Salvant, B. S., E. A. Fortunato, and D. H. Spector.** 1998. Cell cycle dysregulation by human cytomegalovirus: Influence of the cell cycle phase at the time of infection and effects on cyclin transcription. J. Virol. **72:**3729-3741.

131. **Sanchez, V., A. K. McElroy, and D. H. Spector.** 2003. Mechanisms governing maintenance of cdk1/cyclin B1 kinase activity in cells infected with human cytomegalovirus. J. Virol. **77:**13214-13224.

132. **Sanchez, V., A. K. McElroy, J. Yen, S. Tamrakar, C. L. Clark, R. A. Schwartz, and D. H. Spector.** 2004. Cyclin-dependent kinase activity is required at early times for accurate processing and accumulation of the human cytomegalovirus UL122-123 and UL37 immediate-early transcripts and at later times for virus production. J. Virol. **78:**11219-11232.

133. **Sanchez, V., and D. Spector.** 2008. Subversion of cell cycle regulatory pathways. Current Topics in Microbiology and Immunology **325:**243-262.

134. **Sanchez, V., and D. H. Spector.** 2006. Cyclin-dependent kinase activity is required for efficient expression and posttranslational modification of human

cytomegalovirus proteins and for production of extracellular particles. J. Virol. **80:**5886-5896.

135. **Satheshkumar, P. S., L. C. Anton, P. Sanz, and B. Moss.** 2009. Inhibition of the Ubiquitin-Proteasome System Prevents Vaccinia Virus DNA Replication and Expression of Intermediate and Late Genes. Journal of Virology **83:**2469-2479.

136. **Schang, L. M., A. Bantly, M. Knockaert, F. Shaheen, L. Meijer, M. H. Malim, N. S. Gray, and P. A. Schaffer.** 2002. Pharmacological cyclin-dependent kinase inhibitors inhibit replication of wild-type and drug-resistant strains of herpes simplex virus and human immunodeficiency virus type 1 by targeting cellular, not viral, proteins. J. Virol. **76:**7874-7882.

137. **Schwartz, P., and M. Ciechanover.** 1999. The ubiquitin-proteasome pathway and pathogenesis of human diseases. Annual review of medicine **50:**57-74.

138. **Shackelford, J., and J. S. Pagano.** 2005. Targeting of host-cell ubiquitin pathways by viruses. Essays Biochem **41:**139-56.

139. **Shibuya, H., K. Irie, J. Ninomiya-Tsuji, M. Goebl, T. Taniguchi, and K. Matsumoto.** 1992. A new human gene encoding a positive modulator of HIV Tat-mediated transactivation. Nature **357:**700-702.

140. **Shirayama, M., A. Toth, M. Galova, and K. Nasmyth.** 1999. APC(Cdc20) promotes exit from mitosis by destroying the anaphase inhibitor Pds1 and cyclin Clb5. Nature **402:**203-207.

141. **Shteinberg, M., Y. Protopopov, T. Listovsky, M. Brandeis, and A. Hershko.** 1999. Phosphorylation of the cyclosome is required for its stimulation by Fizzy/cdc20. Biochem. Biophys. Res. Commun. **260:**193-198.

142. **Sørensen, C. S., C. Lukas, E. R. Kramer, J. M. Peters, J. Bartek, and J. Lukas.** 2001. A conserved cyclin-binding domain determines functional interplay between anaphase-promoting complex-Cdh1 and cyclin A-Cdk2 during cell cycle progression. Mol Cell Biol **21:**3692-703.

143. **Talarico, C. L., T. C. Burnette, W. H. Miller, S. L. Smith, M. G. Davis, S. C. Stanat, T. I. Ng, Z. He, D. M. Coen, B. Roizman, and K. K. Biron.** 1999. Acyclovir is phosphorylated by the human cytomegalovirus UL97 protein. Antimicrob Agents Chemother **43:**1941-6.

144. **Tamashiro, J. C., L. J. Hock, and D. H. Spector.** 1982. Construction of a cloned library of the *Eco*RI fragments from the human cytomegalovirus genome (strain AD169). J. Virol. **42:**547-557.

145. **Tamrakar, S., A. J. Kapasi, and D. H. Spector.** 2005. Human cytomegalovirus infection induces specific hyperphosphorylation of the carboxyl-terminal domain of the large subunit of RNA polymerase II that is associated with changes in the abundance, activity, and localization of cdk9 and cdk7. J. Virol. **79:**15477-15493.

146. **Tanahashi, N., Y. Murakami, Y. Minami, N. Shimbara, K. B. Hendil, and K. Tanaka.** 2000. Hybrid proteasomes. Induction by interferon-gamma and contribution to ATP-dependent proteolysis. J Biol Chem **275:**14336-45.

147. **Teale, A., S. Campbell, N. Van Buuren, W. C. Magee, K. Watmough, B. Couturier, R. Shipclark, and M. Barry.** 2009. Orthopoxviruses Require a Functional Ubiquitin-Proteasome System for Productive Replication. Journal of Virology **83:**2099-2108.

148. **Teodoro, J. G., D. W. Heilman, A. E. Parker, and M. R. Green.** 2004. The viral protein Apoptin associates with the anaphase-promoting complex to induce G2/M arrest and apoptosis in the absence of p53. Genes Dev. **18:**1952-1957.

149. **Thornton, B. R., T. M. Ng, M. E. Matyskiela, C. W. Carroll, D. O. Morgan, and D. P. Toczyski.** 2006. An architectural map of the anaphase-promoting complex. Genes Dev. **20:**449-460.

150. **Thornton, B. R., and D. P. Toczyski.** 2006. Precise destruction: an emerging picture of the APC. Genes Dev. **20:**3069-3078.

151. **Tortorella, D., B. Gewurz, D. Schust, M. Furman, and H. Ploegh.** 2000. Down-regulation of MHC class I antigen presentation by HCMV; lessons for tumor immunology. Immunol Invest **29:**97-100.

152. **Tran, K., J. A. Mahr, J. Choi, J. G. Teodoro, M. R. Green, and D. H. Spector.** 2008. Accumulation of Substrates of the Anaphase-Promoting Complex (APC) During Human Cytomegalovirus Infection is Associated with the Phosphorylation of Cdh1 and the Dissociation and Relocalization of the APC Subunits. J. Virol. **82:**529-537.

153. **Trgovcich, J., C. Cebulla, P. Zimmerman, and D. D. Sedmak.** 2006. Human cytomegalovirus protein pp71 disrupts major histocompatibility complex class I cell surface expression. J Virol **80:**951-63.

154. **Turnell, A., G. Stewart, R. Grand, S. Rookes, A. Martin, H. Yamano, S. Elledge, and P. Gallimore.** 2005. The APC/C and CBP/p300 cooperate to regulate transcription and cell-cycle progression. Nature **438:**690-695.

155. **van Leuken, R., L. Clijsters, and R. Wolthuis.** 2008. To cell cycle, swing the APC/C. Biochim. Biophys. Acta **1786:**49-59.

156. **Varnum, S. M., D. N. Streblow, M. E. Monroe, P. Smith, K. J. Auberry, L. Pasa-Tolic, D. Wang, D. G. Camp, K. Rodland, S. Wiley, W. Britt, T. Shenk, R. D. Smith, and J. A. Nelson.** 2004. Identification of proteins in human cytomegalovirus (HCMV) particles: the HCMV proteome. Journal of Virology **78:**10960-6.

157. **Vodermaier, H. C., C. Gieffers, S. Maurer-Stroh, F. Eisenhaber, and J. M. Peters.** 2003. TPR subunits of the anaphase-promoting complex mediate binding to the activator protein CDH1. Curr. Biol. **13:**1459-1468.

158. **Voges, D., P. Zwickl, and W. Baumeister.** 2000. The 26S proteasome: a molecular machine designed for controlled proteolysis. Annu. Rev. Biochem. **68:**1015-68.

159. **Wang, D., C. de la Fuente, L. Deng, L. Wang, I. Zilberman, C. Eadie, M. Healey, D. Stein, T. Denny, L. E. Harrison, L. Meijer, and F. Kashanchi.** 2001. Inhibition of human immunodeficiency virus type 1 transcription by chemical cyclin-dependent kinase inhibitors. J. Virol. **75:**7266-7279.

160. **Wang, J., A. N. Loveland, L. M. Kattenhorn, H. L. Ploegh, and W. Gibson.** 2006. High-Molecular-Weight Protein (pUL48) of Human Cytomegalovirus Is a Competent Deubiquitinating Protease: Mutant Viruses Altered in Its Active-Site Cysteine or Histidine Are Viable. Journal of Virology **80:**6003-6012.

161. **Wang, X., and L. Huang.** 2008. Identifying Dynamic Interactors of Protein Complexes by Quantitative Mass Spectrometry. Molecular & Cellular Proteomics **7:**46.

162. **Wäsch, R., J. A. Robbins, and F. R. Cross.** 2009. The emerging role of APC/Cdh1 in controlling differentiation, genomic stability and tumor suppression. Oncogene **28:**1-10.

163. **White, E. A., C. L. Clark, V. Sanchez, and D. H. Spector.** 2004. Small internal deletions in the human cytomegalovirus IE2 gene result in non-viable

recombinant viruses with differential defects in viral gene expression. J. Virol. **78:**1817-1830.

164. **Wiebusch, L., M. Bach, R. Uecker, and C. Hagemeier.** 2005. Human cytomegalovirus inactivates the G0/G1-APC/C ubiquitin ligase by Cdh1 dissociation. Cell Cycle **4:**1435-1439.

165. **Wiebusch, L., and C. Hagemeier.** 1999. Human cytomegalovirus 86-kilodalton IE2 protein blocks cell cycle progression in G(1). J. Virol. **73:**9274-83.

166. **Wiebusch, L., and C. Hagemeier.** 2001. The human cytomegalovirus immediate early 2 protein dissociates cellular DNA synthesis from cyclin dependent kinase activation. EMBO J. **20:**1086-1098.

167. **Wiebusch, L., R. Uecker, and C. Hagemeier.** 2003. Human cytomegalovirus prevents replication licensing by inhibiting MCM loading onto chromatin. EMBO Rep. **4:**42-6.

168. **Wiertz, E., T. Jones, L. Sun, M. Bogyo, H. Geuze, and H. Ploegh.** 1996. The human cytomegalovirus US11 gene product dislocates MHC class I heavy chains from the endoplasmic reticulum to the cytosol. Cell **84:**769-779.

169. **Wing, B. A., and E. S. Huang.** 1995. Analysis and mapping of a family of 3'-coterminal transcripts containing coding sequences for human cytomegalovirus open reading frames UL93 through UL99. J. Virol. **69:**1521-1531.

170. **Wolf, D., C. Courcelle, M. Prichard, and E. Mocarski.** 2001. Distinct and separate roles for herpesvirus-conserved UL97 kinase in cytomegalovirus DNA synthesis …. Proceedings of the National Academy of Sciences.

171. **Yao, T., L. Song, G. N. DeMartino, L. Florens, S. K. Swanson, M. P. Washburn, R. C. Conaway, J. W. Conaway, and R. E. Cohen.** 2006. Proteasome recruitment and activation of the Uch37 deubiquitinating enzyme by Adrm1. Nat. Cell Biol. **8:**994-1002.

172. **Yeong, F. M., H. H. Lim, C. G. Padmashree, and U. Surana.** 2000. Exit from mitosis in budding yeast: biphasic inactivation of the Cdc28-Clb2 mitotic kinase and the role of Cdc20. Mol. Cell **5:**501-511.

173. **Yudkovsky, Y., M. Shteinberg, T. Listovsky, M. Brandeis, and A. Hershko.** 2000. Phosphorylation of Cdc20/fizzy negatively regulates the mammalian cyclosome/APC in the mitotic checkpoint. Biochem. Biophys. Res. Commun. **271:**299-304.

174. **Zachariae, W., M. Schwab, K. Nasmyth, and W. Seufert.** 1998. Control of cyclin ubiquitination by CDK-regulated binding of Hct1 to the anaphase promoting complex. Science **282:**1721-1724.

175. **Zhang, H., H. O. al-Barazi, and A. M. Colberg-Poley.** 1996. The acidic domain of the human cytomegalovirus UL37 immediate early glycoprotein is dispensable for its transactivating activity and localization but is not for its synergism. Virology **223:**292-302.

176. **Zhou, Y., Y.-P. Ching, A. C. S. Chun, and D.-Y. Jin.** 2003. Nuclear localization of the cell cycle regulator CDH1 and its regulation by phosphorylation. J Biol Chem **278:**12530-6.